



聖若瑟大學  
UNIVERSITY OF  
SAINT JOSEPH



UNIVERSIDADE  
**NOVA**  
DE LISBOA

AIR QUALITY MANAGEMENT IN MACAO – ASSESSMENT, DEVELOPMENT  
OF AN OPERATIONAL FORECAST, AND FUTURE PERSPECTIVES

A Thesis

Presented to

The Academic Faculty

By

**Lei Man Tat, Thomas**

Thesis supervised by:

Francisco Cardoso Ferreira

David Manuel Flores Gonçalves

In Partial Fulfillment of the Requirements for the Degree of PhD in Science in the  
Institute of Science and Environment of the University of Saint Joseph, Macao and  
the Degree of PhD in Environment and Sustainability in the Faculdade de Ciências e

Tecnologia da Universidade NOVA de Lisboa, Portugal

December 2020

## ENDORSEMENT

I certify that this report is solely my work, and that it has never been previously submitted to any other higher education institutions for any academic award.



---

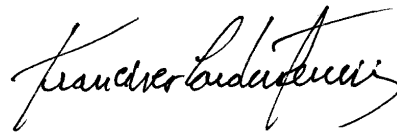
Lei Man Tat

We, the supervisors, believe that this Thesis is ready for assessment and reaches the accepted standard for the degree of PhD in Science in the Institute of Science and Environment of the University of Saint Joseph, Macao, and the degree of PhD in Environment and Sustainability in the Faculdade de Ciências e Tecnologia da Universidade NOVA de Lisboa, Portugal.



---

David Manuel Flores Gonçalves



---

Francisco Cardoso Ferreira



## **Acknowledgements**

I have to say thank you to my supervisors, Professor Francisco Ferreira and Professor David Gonçalves for their supervision throughout the doctoral thesis. They have played an important role, providing valuable comments and supports, and spending their valuable time on my supervision. At the same time, they are one of the nicest people that I have encountered.

I have to say thank you to the air quality research team in FCT NOVA, in particular of Joana Monjardino, Luisa Mendes, Paulo Pereira, and Hugo Tente. They have been very welcoming and supportive during my stay in Portugal and we have produced some good research together in our work, as shown in the journal publication. I hope to have a chance to continue working with the research group in the future.

I have to say thank you for the support of Macao Meteorological and Geophysical Bureau (SMG), in particular of Frankie Tam, for providing the necessary data and communication during our collaboration.

I have to say thank you to my family, in particular of my parents, my wife, and my son, who has encouraged me throughout my doctoral studies. Also, I have to say

thank you to my friends who has helped me throughout my doctoral studies.

I have been very fortunate to receive supports from all of those individuals mentioned above, and once again, I have to say thank you to all of you.

The work developed was supported by The Macao Meteorological and Geophysical Bureau (SMG). The research work of CENSE is financed by Fundação para a Ciência e Tecnologia, I.P., Portugal (UID/AMB/04085/2019).

## Abstract

A combination of assessment, operational forecast, and future perspective was thoroughly explored to provide an overview of the existing air quality problems in Macao. The levels of air pollution in Macao often exceed those recommended by the World Health Organization (WHO). In order for the population to take precautionary measures and avoid further health risks during high pollution episodes, it is important to develop a reliable air quality forecast. Statistical models based on linear multiple regression (MLR) and classification and regression trees (CART) analysis were successfully developed for Macao, to predict the next day concentrations of NO<sub>2</sub>, PM<sub>10</sub>, PM<sub>2.5</sub>, and O<sub>3</sub>.

Meteorological variables were selected from an extensive list of possible variables, including geopotential height, relative humidity, atmospheric stability, and air temperature at different vertical levels. Air quality variables translate the resilience of the recent past concentrations of each pollutant and usually are maximum and/or the average of latest 24-hour levels. The models were applied in forecasting the next day average daily concentrations for NO<sub>2</sub> and PM and maximum hourly O<sub>3</sub> levels for five air quality monitoring stations. The results are expected to support an operational air

quality forecast for Macao.

The work involved two phases. On a first phase, the models utilized meteorological and air quality variables based on five years of historical data, from 2013 to 2017. Data from 2013 to 2016 were used to develop the statistical models and data from 2017 was used for validation purposes. All the developed models were statistically significantly valid with a 95% confidence level with high coefficients of determination (from 0.78 to 0.93) for all pollutants. On a second phase, these models were used with 2019 validation data, while a new set of models based on a more extended historical data series, from 2013 to 2018, were also validated with 2019 data. There were no significant differences in the coefficients of determination ( $R^2$ ) and minor improvements in root mean square errors (RMSE), mean absolute errors (MAE) and biases (BIAS) between the 2013 to 2016 and the 2013 to 2018 data models. In addition, for one air quality monitoring station (Taipa Ambient), the 2013 to 2018 model was applied for two days ahead (D2) forecast and the coefficient of determination ( $R^2$ ) was considerably less accurate to the one day ahead (D1) forecast, but still able to provide a reliable air quality forecast for Macao.

To understand if the prediction model was robust to extreme variations in

pollutants concentration, a test was performed under the circumstances of a high pollution episode for PM<sub>2.5</sub> and O<sub>3</sub> during 2019, and a low pollution episode during 2020. Regarding the high pollution episode, the period of the Chinese National Holiday of 2019 was selected, in which high concentration levels were identified for PM<sub>2.5</sub> and O<sub>3</sub>, with peaks of daily concentration for PM<sub>2.5</sub> levels exceeding 55 µg/m<sup>3</sup> and the maximum hourly concentration for O<sub>3</sub> levels exceeding 400 µg/m<sup>3</sup>. For the low pollution episode, the 2020 period of implementation of the preventive measures for COVID-19 pandemic was selected, with a low record of daily concentration for PM<sub>2.5</sub> levels at 2 µg/m<sup>3</sup> and maximum hourly concentration for O<sub>3</sub> levels at 50 µg/m<sup>3</sup>.

The 2013 to 2018 model successfully predicted the high pollution episode with high coefficients of determination (0.92 for PM<sub>2.5</sub> and 0.82 for O<sub>3</sub>). Likewise, the low pollution episode was also correctly predicted with high coefficients of determination (0.86 and 0.84 for PM<sub>2.5</sub> and O<sub>3</sub>, respectively). Overall, the results demonstrate that the statistical forecast model is robust and able to correctly reproduce extreme air pollution events of both high and low concentration levels.

Machine learning methods maybe adopted to provide significant improvements in combination of multiple linear regression (MLR) and classification and regression



tree (CART) to further improve the accuracy of the statistical forecast. The developed air pollution forecasting model may be combined with other measures to mitigate the impact of air pollution in Macao. These may include the establishment of low emission zones (LEZ), as enforced in some European cities, license plate restrictions and lottery policy, as used in some Asian, tax exemptions on electric vehicles (EVs) and exclusive corridors for public transportations.

**Keywords:** Air pollution; Particulate Matter; Ozone; Macao; Statistical air quality

forecast; Pollution episodes; Chinese national holiday; COVID-19.

## Resumo

A complementaridade de uma avaliação, do desenvolvimento de uma previsão operacional, em conjunto com uma reflexão sobre perspetivas futuras, permitiu desenvolver uma visão integrada dos problemas de qualidade do ar de Macau. Os níveis de poluição do ar em Macau muitas vezes excedem os níveis recomendados pela Organização Mundial de Saúde (OMS). Para que a população tome precauções e evite maiores riscos à saúde em caso de elevada exposição a poluentes, é importante desenvolver uma previsão confiável da qualidade do ar. Modelos estatísticos baseados em regressão linear múltipla (MLR) e análise de árvores de classificação e regressão (CART) foram desenvolvidos com sucesso para Macau para prever as concentrações de  $\text{NO}_2$ ,  $\text{PM}_{10}$ ,  $\text{PM}_{2.5}$  e  $\text{O}_3$  no dia seguinte.

Um conjunto de variáveis meteorológicas foram selecionadas a partir de uma extensa lista de variáveis possíveis, incluindo altura de geopotencial, humidade relativa, estabilidade atmosférica e temperatura do ar em diferentes níveis verticais. As variáveis de qualidade do ar traduzem a resiliência das concentrações passadas recentes de cada poluente e geralmente são considerados os valores máximos e/ou a média dos níveis das últimas 24 horas. Os modelos foram aplicados na previsão das

concentrações médias diárias de NO<sub>2</sub> e PM no dia seguinte e dos níveis máximos horários de O<sub>3</sub> para cinco estações de monitorização da qualidade do ar. Espera-se que os resultados venham a ser utilizados numa previsão operacional da qualidade do ar para Macau.

O trabalho envolveu duas fases. Todos os modelos desenvolvidos foram estatisticamente significativamente válidos com um nível de confiança de 95% com altos coeficientes de determinação (de 0.78 a 0.93) para todos os poluentes. Os modelos utilizaram variáveis meteorológicas e de qualidade do ar baseadas em cinco anos de dados históricos, de 2013 a 2019.

Numa primeira fase, os modelos utilizaram variáveis meteorológicas e de qualidade do ar com base em cinco anos de dados históricos, de 2013 a 2017. Os dados de 2013 a 2016 foram usados para desenvolver os modelos estatísticos e os dados de 2017 foram usados para fins de validação. Todos os modelos desenvolvidos foram estatisticamente significativos e válidos para um nível de confiança de 95% com elevados coeficientes de determinação (de 0,78 a 0,93) para todos os poluentes. Numa segunda fase esses modelos foram usados com dados de validação de 2019, enquanto um novo conjunto de modelos baseado numa série de dados históricos mais extensa, de 2013 a 2018, foi

também validado com dados de 2019. Não houve diferenças significativas nos coeficientes de determinação ( $R^2$ ) e obtiveram-se pequenas melhorias na raiz dos erros quadráticos médios (RMSE), erros médios absolutos (MAE) e vieses (BIAS) entre o modelo com dados de 2013 a 2016 e o modelo com dados de 2013 a 2018. Adicionalmente, para uma estação de monitorização de qualidade do ar (Taipa Ambient), o modelo 2013-2018 foi aplicado para uma previsão com dois dias de antecedência (D2) e o coeficiente de determinação ( $R^2$ ) obtido foi consideravelmente menos preciso do que a previsão do dia seguinte (D1), mas ainda assim capaz de prever a qualidade do ar para Macau.

Para avaliar se o modelo de previsão era robusto em situações extremas de concentração de poluentes foi realizado um teste para um episódio de elevada poluição de  $PM_{2.5}$  e  $O_3$  durante 2019 e para um episódio de poluição reduzida durante 2020. Em relação ao episódio de elevada poluição, foi selecionado o período do Feriado Nacional Chinês de 2019, no qual foram identificados elevados níveis de concentração de  $PM_{2.5}$  e  $O_3$ , com picos de concentração diária para níveis de  $PM_{2.5}$  superiores a  $55 \mu\text{g}/\text{m}^3$  e concentrações máximas horárias de  $O_3$  superiores a  $400 \mu\text{g}/\text{m}^3$ . O episódio de reduzida poluição para  $PM_{2.5}$  e  $O_3$  foi identificado durante o

período pandémico de COVID-19 de 2020, com um registo de baixas concentrações diárias de  $PM_{2.5}$  de  $2 \mu\text{g}/\text{m}^3$  e concentração máxima horária de  $O_3$  a  $50 \mu\text{g}/\text{m}^3$ .

O modelo de 2013 a 2018 previu com sucesso o episódio de alta poluição com elevados coeficientes de determinação (de 0.92 para  $PM_{2.5}$  e 0.82 para  $O_3$ ). De igual modo, o modelo de 2013 a 2018 previu com sucesso o episódio de poluição reduzida com um elevado coeficiente de determinação (0.86 e 0.84 para  $PM_{2.5}$  e  $O_3$ , respetivamente). No geral, os resultados demonstram que o modelo de previsão estatística é robusto e capaz de reproduzir corretamente eventos extremos de poluição do ar em níveis altos e baixos de concentração.

Refira-se ainda que podem ser adotados métodos de aprendizagem automática para fornecer melhorias significativas na combinação de regressão linear múltipla (MLR) e árvore de classificação e regressão (CART) para aperfeiçoar ainda mais a precisão da previsão estatística. O modelo desenvolvido poderá ser combinado com outras medidas para mitigar o impacto da poluição atmosférica em Macau. Estas poderão incluir a implementação de uma Zona de Emissões Reduzidas (ZER), tal como estabelecido em algumas cidades europeias, a restrição de circulação dependente da matrícula do veículo ou uma política de sorteio de matrículas, como

tem lugar em algumas cidades asiáticas, a isenção de impostos sobre veículos elétricos (VE), bem como a marcação de corredores exclusivos para transportes públicos.

**Palavras-chave:** Poluição do ar; Matéria particulada; Ozono; Macau; Previsão estatística de qualidade do ar; Episódios de poluição; Feriado nacional chinês; COVID-19.

## Publications arising from this thesis

### Journal Articles

Lei, M. T., Monjardino, J., Mendes, L., Gonçalves, D., & Ferreira, F. (2020).

Statistical Forecast of Pollution Episodes in Macao during National Holiday and

COVID-19. *International Journal of Environmental Research and Public*

*Health*, 17(14), 5124. <https://doi.org/10.3390/ijerph17145124>

Lei, M. T., Monjardino, J., Mendes, L., Gonçalves, D., & Ferreira, F. (2019). Macao

air quality forecast using statistical methods. *Air Quality, Atmosphere and*

*Health*, 12(9), 1049–1057. <https://doi.org/10.1007/s11869-019-00721-9>

Lei, M. T., Monjardino, J., Mendes, L., & Ferreira, F. (2019). Macao air quality

forecast using statistical methods. *International Journal of Environmental*

*Impacts: Management, Mitigation and Recovery*, 2(3), 249–258.

<https://doi.org/10.2495/ei-v2-n3-249-258>

## Conference Articles

Lei, M. T., Monjardino, J., Mendes, L., & Ferreira, F. (2019). Macao air quality forecast using statistical methods. *International Journal of Environmental Impacts: Management, Mitigation and Recovery*. 27th International Conference on Modelling, Monitoring and Management of Air Pollution in Aveiro, Portugal.

## Conference Abstracts

Lei, M. T., Monjardino, J., Mendes, L., Gonçalves, D., & Ferreira, F. (2020).

Statistical Forecast Applied to Two Macao Air Monitoring Stations. *IOP*

*Conference Series: Earth and Environmental Science*, 489.

<https://doi.org/10.1088/1755-1315/489/1/012018>

Lei, M. T., Monjardino, J., Mendes, L., Gonçalves, D., & Ferreira, F. (2020). The Use

of Statistical Methods to Forecast Air Quality in Taipa Island of Macao.

Submitted to *Air Pollution Modeling and its Application* vol. XXVII, published

by Springer.



## **Conference Attended**

### **Oral Presentations**

Lei, M. T., Monjardino, J., Mendes, L., Gonçalves, D., & Ferreira, F. (2019).

Statistical Forecast Applied to Two Macao Air Monitoring Stations, ASAAQ15,

15th International Conference on Atmospheric Sciences and Applications to Air

Quality, 28 – 30 October 2019, Kuala Lumpur, Malaysia

Lei, M. T., Monjardino, J., Mendes, L., Gonçalves, D., & Ferreira, F. (2019). Macao

air quality forecast using statistical methods. Air Pollution 2019, 27th

International Conference on Modelling, Monitoring, and Management of Air

Pollution, 26 – 28 June 2019, Aveiro, Portugal

### **Poster Presentations**

Lei, M. T., Monjardino, J., Mendes, L., Gonçalves, D., & Ferreira, F. (2019). The Use

of Statistical Methods to Forecast Air Quality in Taipa Island of Macao. ITM

2019 – 37th International Technical Meeting on Air Pollution Modelling and its

Application, 23 – 27 September 2019, Hamburg, Germany

# TABLE OF CONTENTS

<b>ACKNOWLEDGEMENTS .....</b>	<b>I</b>
<b>ABSTRACT.....</b>	<b>III</b>
<b>RESUMO .....</b>	<b>VII</b>
<b>PUBLICATIONS ARISING FROM THIS THESIS .....</b>	<b>XII</b>
<b>TABLE OF CONTENTS.....</b>	<b>XV</b>
<b>LIST OF FIGURES .....</b>	<b>XIX</b>
<b>LIST OF TABLES.....</b>	<b>XXVI</b>
<b>GLOSSARY OF ACRONYMS AND ABBREVIATIONS.....</b>	<b>XXVIII</b>
<b>CHAPTER 1:INTRODUCTION .....</b>	<b>1</b>
1.1. BACKGROUND.....	2
1.2. RESEARCH QUESTIONS AND OBJECTIVES .....	4
1.3. STRUCTURE OF THE THESIS .....	6

<b>CHAPTER 2:LITERATURE REVIEW.....</b>	<b>9</b>
2.1 AIR QUALITY IN DENSELY POPULATED AREAS .....	10
2.2 HEALTH IMPACT OF AIR POLLUTION .....	11
2.3 SOURCE OF AIR POLLUTANTS .....	18
2.4 AIR QUALITY GUIDELINES .....	23
2.5 FORECASTING MODELS.....	28
2.5.1 <i>Deterministic Methods</i> .....	30
2.5.2 <i>Statistical Methods</i> .....	33
2.5.3 <i>Machine Learning Techniques</i> .....	34
<b>CHAPTER 3:BACKGROUND AND METHODOLOGY.....</b>	<b>37</b>
3.1 CASE STUDY OF MACAO .....	38
3.2 AIR QUALITY IN MACAO.....	40
3.3 METEOROLOGICAL CHARACTERISTICS OF MACAO .....	56
3.3.1 <i>Key Meteorological Variables</i> .....	58
3.3.2 <i>Meteorological Seasonal Variation in Macao</i> .....	66
3.4 DEVELOPMENT OF AIR QUALITY FORECAST USING STATISTICAL METHODS.	72

**CHAPTER 4:RESULT AND DISCUSSION .....85**

4.1 AIR QUALITY FORECAST USING 2013 TO 2016 DATA (VALIDATED WITH 2017 DATA) .....86

4.2 AIR QUALITY FORECAST USING 2013 TO 2018 DATA (VALIDATED WITH 2019 DATA) .....97

4.3 AIR QUALITY FORECAST USING 2013 TO 2018 DATA, FOR TWO DAYS AHEAD (D2) ..... 104

4.4 AIR QUALITY FORECAST DURING A HIGH POLLUTION EPISODE..... 106

4.5 AIR QUALITY FORECAST DURING A LOW POLLUTION EPISODE ..... 112

**CHAPTER 5:FUTURE MEASURES THAT COULD BE IMPLEMENTED TO IMPROVE AIR QUALITY IN MACAO.....123**

5.1 LOW EMISSION ZONE (LEZ) .....125

5.2 LICENSE PLATE RESTRICTION POLICY..... 130

5.3 INCENTIVES ON ELECTRIC VEHICLES (EV) .....133

**CHAPTER 6:CONCLUSIONS AND FUTURE DEVELOPMENT.....137**

6.1 AIR QUALITY FORECAST USING STATISTICAL METHODS ..... 138

6.2 AIR QUALITY FORECAST UNDER HIGH AND LOW POLLUTION EPISODES .... 140

6.3	ANSWERS TO RESEARCH QUESTIONS .....	141
6.4	MAIN CONSTRAINTS AND SUGGESTIONS TO FUTURE WORKS .....	144
<b>CHAPTER 7: REFERENCES.....</b>		<b>147</b>

## List of Figures

<b>Figure 2.1.</b> The path of air pollutants from emission to exposure (EEA, 2016).....	11
<b>Figure 2.2.</b> Regions affected by air pollution (WHO, 2020). .....	12
<b>Figure 2.3.</b> Health effects pyramids to exposure of air pollutants (EEA, 2014).....	13
<b>Figure 2.4.</b> Cause of death from air pollution (WHO, 2020).....	14
<b>Figure 2.5.</b> Diagrammatic representation of inhaled particulate matter of variable sizes and PM-linked respiratory, cardiovascular, and neurological diseases (Zaheer et al., 2018). .....	16
<b>Figure 2.6.</b> Health impacts of air pollution (EEA, 2020).....	17
<b>Figure 2.7.</b> Source of air pollution (WHO, 2020).....	19
<b>Figure 2.8.</b> Size comparison of PM particles (EPA, 2020). .....	21
<b>Figure 2.9.</b> Schematic representation of the photochemical formation of ozone in the presence of VOCs and NO <sub>x</sub> . (WHO Europe, 2008).....	22
<b>Figure 2.10.</b> Comparison of air quality standards for PM <sub>10</sub> .....	26
<b>Figure 2.11.</b> Comparison of air quality standards for PM <sub>2.5</sub> . .....	26
<b>Figure 2.12.</b> Comparison of air quality standards for nitrogen dioxide (NO <sub>2</sub> ). .....	27

<b>Figure 2.13.</b> Comparison of air quality standards for 8-hour average ozone (O <sub>3</sub> ).....	27
<b>Figure 2.14.</b> Air quality forecasting model using deterministic methods (Guttikunda et al., 2011).....	32
<b>Figure 2.15.</b> Different grids in deterministic models (Guttikunda et al., 2011).....	33
<b>Figure 2.16.</b> Steps of model development for an air quality forecast using statistical methods.....	34
<b>Figure 3.1.</b> Guangdong-Hong Kong-Macao regional air quality monitoring information system (SMG, 2020). ....	41
<b>Figure 3.2.</b> Settings of a Macao ambient station (SMG, 2020). ....	42
<b>Figure 3.3.</b> Settings of a Macao roadside station (SMG, 2020).....	42
<b>Figure 3.4.</b> Map of Macao air quality monitoring stations network. Adapted from SMG (2019). ....	44
<b>Figure 3.5.</b> Daily air quality index in Macao (SMG, 2020).....	45
<b>Figure 3.6.</b> Yearly average levels of PM <sub>10</sub> in the Macao air quality monitoring stations (2013 to 2019).....	47
<b>Figure 3.7.</b> Yearly average levels of PM <sub>2.5</sub> in the Macao air quality monitoring stations (2013 to 2019).....	47

<b>Figure 3.8.</b> Yearly average levels of NO <sub>2</sub> in the Macao air quality monitoring stations (2013 to 2019).....	48
<b>Figure 3.9.</b> Yearly average levels of O <sub>3</sub> in the Macao air quality monitoring stations (2013 to 2019).....	49
<b>Figure 3.10.</b> Monthly average levels of PM <sub>10</sub> in the Macao air quality monitoring stations (2013 to 2019).....	50
<b>Figure 3.11.</b> Monthly average levels of PM <sub>2.5</sub> in the Macao air quality monitoring stations (2013 to 2019).....	50
<b>Figure 3.12.</b> Monthly average levels of NO <sub>2</sub> in the Macao air quality monitoring stations (2013 to 2019).....	51
<b>Figure 3.13.</b> Monthly average levels of O <sub>3</sub> in the Macao air quality monitoring stations (2013 to 2019).....	52
<b>Figure 3.14.</b> Hourly average levels of PM <sub>10</sub> in the Macao air quality monitoring stations (2013 to 2019).....	53
<b>Figure 3.15.</b> Hourly average levels of PM <sub>2.5</sub> in the Macao air quality monitoring stations (2013 to 2019).....	54
<b>Figure 3.16.</b> Hourly average levels of NO <sub>2</sub> in the Macao air quality monitoring	



stations (2013 to 2019).....	55
<b>Figure 3.17.</b> Hourly average levels of O <sub>3</sub> in the Macao air quality monitoring stations (2013 to 2019).....	56
<b>Figure 3.18.</b> Wind rose of Macao from 2013 to 2019 (hourly counts). ....	58
<b>Figure 3.19.</b> Wind speed (m/s) of Macao from 2013 to 2019.....	59
<b>Figure 3.20.</b> Pollution rose of PM <sub>10</sub> (µg/m <sup>3</sup> ) from 2013 to 2019.....	60
<b>Figure 3.21.</b> Pollution rose of PM <sub>2.5</sub> (µg/m <sup>3</sup> ) from 2013 to 2019.....	60
<b>Figure 3.22.</b> Pollution rose of NO <sub>2</sub> (µg/m <sup>3</sup> ) from 2013 to 2019. ....	61
<b>Figure 3.23.</b> Pollution rose of O <sub>3</sub> (µg/m <sup>3</sup> ) from 2013 to 2019. ....	62
<b>Figure 3.24.</b> Yearly average temperature in Macao from 2013 to 2019. ....	62
<b>Figure 3.25.</b> Yearly total precipitation in Macao from 2013 to 2019.....	63
<b>Figure 3.26.</b> Monthly average temperature in Macao from 2013 to 2019.....	64
<b>Figure 3.27.</b> Monthly average wind speed in Macao from 2013 to 2019. ....	64
<b>Figure 3.28.</b> Monthly total precipitation in Macao from 2013 to 2019. ....	65
<b>Figure 3.29.</b> Hourly average temperature in Macao from 2013 to 2019. ....	66
<b>Figure 3.30.</b> Wind rose of Macao in winter season from 2013 to 2019 (hourly counts). .....	67

<b>Figure 3.31.</b> Pollution rose of PM <sub>2.5</sub> (µg/m <sup>3</sup> ) in winter season from 2013 to 2019.....	68
<b>Figure 3.32.</b> Pollution rose of O <sub>3</sub> (µg/m <sup>3</sup> ) in winter season from 2013 to 2019. ....	68
<b>Figure 3.33.</b> Typical winter meteorological surface chart of Macao (HKO, 2020). ...	69
<b>Figure 3.34.</b> Wind rose of Macao in summer season from 2013 to 2019 (hourly counts).....	70
<b>Figure 3.35.</b> Pollution rose of PM <sub>2.5</sub> (µg/m <sup>3</sup> ) in summer season from 2013 to 2019..	70
<b>Figure 3.36.</b> Pollution rose of O <sub>3</sub> (µg/m <sup>3</sup> ) in summer season from 2013 to 2019. ....	71
<b>Figure 3.37.</b> Typical summer meteorological surface chart in Macao (HKO, 2020)..	71
<b>Figure 3.38.</b> Flowchart for model development of air quality forecast by statistical methods. ....	82
<b>Figure 4.1.</b> CART tree obtained for O <sub>3</sub> MAX prediction at Taipa Ambient station. ....	87
<b>Figure 4.2.</b> Observed and predicted PM <sub>10</sub> concentrations for Coloane Ambient in 2017.....	94
<b>Figure 4.3.</b> Observed and predicted O <sub>3</sub> MAX concentrations for Coloane Ambient in 2017.....	94
<b>Figure 4.4.</b> PM <sub>2.5</sub> concentrations for Taipa Ambient highlighting a pollution episode immediately before, and during, the Chinese National Holiday of 2018 and 2019	

(September to November)..... 107

**Figure 4.5.** O<sub>3</sub> MAX concentrations for Taipa Ambient highlighting a pollution episode immediately before, and during, the Chinese National Holiday of 2018 and 2019

(September to November)..... 108

**Figure 4.6.** Observed and predicted PM<sub>2.5</sub> concentrations for Taipa Ambient during Chinese National Holiday (from September to November 2019). ..... 111

**Figure 4.7.** Observed and predicted O<sub>3</sub> MAX concentrations for Taipa Ambient during Chinese National Holiday (from September to November 2019). ..... 112

**Figure 4.8.** Comparison of PM<sub>2.5</sub> concentrations for Taipa Ambient during the previous year of 2019 and COVID-19 pandemic in 2020 (January to March). ..... 115

**Figure 4.9.** Comparison of O<sub>3</sub> MAX concentrations for Taipa Ambient during the previous year of 2019 and COVID-19 pandemic in 2020 (January to March). ..... 116

**Figure 4.10.** Monthly mean PM<sub>2.5</sub> concentrations for Taipa Ambient during the previous year of 2019 and COVID-19 pandemic in 2020 (January to March). ..... 117

**Figure 4.11.** Monthly mean O<sub>3</sub> MAX concentrations for Taipa Ambient during the previous year of 2019 and COVID-19 pandemic in 2020 (January to March). ..... 118

**Figure 4.12.** Observed and predicted PM<sub>2.5</sub> concentrations for Taipa Ambient during

preventive measures of COVID-19 pandemic (from January to March 2020). ..... 119

**Figure 4.13.** Observed and predicted  $O_3_{MAX}$  concentrations for Taipa Ambient during

preventive measures of COVID-19 pandemic (from January to March 2020). ..... 120

**Figure 5.1.** Low emission zone of Lisbon, Portugal (Santos, Gómez-Losada, & Pires,

2019). ..... 127

**Figure 5.2.** Total proposed EV charging stations in public parking lots of Macao... 135

## List of Tables

<b>Table 2-1.</b> Description of air pollutants. Adapted from (EEA, 2020). .....	18
<b>Table 2-2.</b> Air quality standards set at different countries and/or by different institutions. Adapted from (MEE, 2012; SMG, 2019; WHO Europe, 2006).....	25
<b>Table 3-1.</b> Air quality index (AQI) of Macao (SMG, 2019). .....	45
<b>Table 3-2.</b> Variables considered as predictors in the multiple linear regression (MLR) and classification and regression tree (CART) models in all of the air quality forecast models. ....	76
<b>Table 4-1.</b> Variables and model equations for each pollutant per air quality monitoring station for 2013-2016 model.....	87
<b>Table 4-2.</b> Model performance indicators for the 2013 to 2016 model validation with 2017 data.....	92
<b>Table 4-3.</b> CART model performance indicators for 2013 to 2016 model.....	96
<b>Table 4-4.</b> Model performance indicators for the 2013 to 2016 model and the 2013 to 2018 model, validation with 2019 data.....	98

**Table 4-5.** Variables and model equations for each pollutant per air quality monitoring station in the 2013 to 2018 model..... 100

**Table 4-6.** Model performance indicators for the 2013 to 2018 model validation with 2019 data, for two days ahead (D2) and one day ahead (D1)..... 105

## **Glossary of acronyms and abbreviations**

The following acronyms and abbreviations are used throughout the thesis:

ANN – Artificial neural network

AQG – Air Quality Guideline

AQI – Air Quality Index

AWS – Automatic Weather Stations

CART – Classification and regression tree

COVID-19 – Coronavirus disease

CTM – Chemical Transport Model

DSEC – Macao Statistics and Census Service

DSPA – Macao Environmental Protection Bureau

ECMWF – European Centre for Medium-Range Weather Forecast

EV – Electric vehicle

HKO – Hong Kong Observatory

HZMB – Hong Kong-Zhuhai-Macao Bridge

IT-1 – Interim-target 1

LUR – Land Use Regression

LEZ – Low Emission Zone

MAE – Mean absolute error

MEE – China Ministry of Ecology and Environment

ML – Machine learning

MLR – Multiple linear regression

NAQPMS – Nested Air Quality Prediction Modeling System

OSPM – Operational Street Pollution Model

PRD – Pearl River Delta

$R^2$  – Coefficient of Determination

RMSE – Root mean square error

SMG – Macao Meteorological and Geophysical Bureau

VOC – Volatile organic compound

WHO – World Health Organization

WRF-ARW model – Advanced Research Weather Research and Forecasting model

WRF model – Weather Research and Forecast model

UNESCO – United Nations Educational, Scientific and Cultural Organizations





## **Chapter 1: Introduction**

---

## **1.1. Background**

Air pollution is becoming epidemic in urban settings of many world regions. With growing urbanization and consumption, it is predicted that this problem will become aggravated during the coming decades, particularly in certain growing urban areas in developing countries. Similarly to weather forecast, being able to anticipate air pollution levels is extremely valuable as proper mitigation and safety measures can be preventively put in place. However, the variables influencing air pollution levels are multiple and regionally specific, increasing the difficulty of developing accurate models, and further investigation is needed.

Air pollution is also a serious local problem in Macao, affecting the health and quality of life of local citizens. The region of Macao has a serious air quality problem, which is extremely worrisome for the local authorities. Nevertheless, the Macao Meteorological and Geophysical Bureau (SMG) did not have the tools to forecast air quality, in particular because the implementation of a numerical model implies access to an updated and sufficiently detailed emission inventory, not available in Macao.

Besides understanding the air quality levels and trends and their relationship with

the meteorological conditions, the development of a forecast model for local air quality in Macao would be a helpful management instrument. Therefore, while several types of air quality models are available, under complex situations such as the one in Macao, a statistical forecast model can be an important tool to better understand the air pollution in Macao, providing at the same time a reliable and needed forecast. The results of such a forecast model can be used to issue warnings and advise the population to restrict from outdoor activities when the air quality is expected to be poor.

Macao is located in Southern China, in the Pearl River Delta (PRD) region. The levels of nitrogen dioxide (NO<sub>2</sub>), particulate matter (PM), particulate matter with an average aerodynamic diameter below 10 µm and 2.5 µm (PM<sub>10</sub> and PM<sub>2.5</sub>, respectively), and ozone (O<sub>3</sub>) in Macao are high, and often exceed the established limit values recommended by WHO's air quality guidelines (AQG). Since 2010, the worst air quality index classes in Macao have been due to PM<sub>10</sub> and PM<sub>2.5</sub> (SMG, 2019). Macao was listed as the number one most densely populated region in the world (Sheng & Tang, 2013), with a population density of about 20,000 inhabitants/km<sup>2</sup>. A significant proportion of Macao urban population is being exposed to air pollutants concentrations

above the limit or target values. In this context, it is relevant to develop a reliable methodology to forecast the concentration of air pollutants, which can provide an alert for health hazards in advance, in a way that the population can take precautionary actions to avoid exposure.

## **1.2. Research Questions and Objectives**

The main objective of this thesis is to identify the key parameters that influence air quality in Macao and to develop a statistical air quality forecast model for the daily or maximum hourly concentration (in the case of ozone) of air pollutants for the next day in Macao and converted into an AQI Index to provide warnings to the public. The sources of air pollution will be studied to better understand the air quality trend in Macao. We will explore the relationships between the meteorological parameters and the pollutants in Macao to develop a statistical model to forecast the air quality of within the next couple of days, based on meteorological parameters and the pollutants concentrations.. There are no available forecast modeling tools to predict the air quality for the region, which is necessary for Macao to keep up with the international information preventive practices, included the ones at neighboring regions. In this context, the research questions are the following:

1. What is the trend of the different air pollutant concentrations measured in the Macao air quality monitoring stations and the reason for those variations in the recent years?
2. Is it possible to develop a statistical model to accurately forecast the next day concentrations of air pollutant in the Macao region?
  - a. What are the key meteorological and air quality variables that are necessary to develop the statistical model?
  - b. Do additional years of meteorological and air quality historical data affect the performance of the statistical forecast?
  - c. How does the statistical forecast perform under extreme situations, such as during extremely high or low pollution episodes?

To answer these research questions, the following tasks were performed:

- Collecting the meteorological and air quality historical data from the past years;
- Analyzing the collected data and identifying the variations for levels of concentration amongst different years;
- Using the collected data to develop a statistical model to forecast the next day

concentration of air pollutants;

- Testing the developed statistical model against the observed data, including during high and low pollution episodes.

### **1.3. Structure of the Thesis**

This thesis is divided into five chapters as follows:

- Chapter 1 – Introduction
  - To introduce the background, research questions, and the objectives of the thesis.
- Chapter 2 – Literature Review
  - To review the past literature and related work on the topic of air quality
- Chapter 3 – Background and Methodology.
  - To show the background information of Macao and the methodology used to develop the air quality forecast.
- Chapter 4 – Results and Discussion
  - To show the results and discussion of the air quality forecast using different years of historical data and performance under pollution episodes.

- Chapter 5 – Future measures that could be implemented to improve air quality in Macao
  - To explore the potential measures that could be implemented to improve air quality in Macao, such as low emission zone (LEZ) and license plate restriction policy.
  
- Chapter 6 – Conclusion
  - To conclude the research findings of this thesis, answer to the research questions and discuss the limitations and suggestions for future works.

The work developed in this dissertation resulted in three journal articles, one conference article, two conference abstracts, and two oral presentations and one poster presentation in international conferences, summarized in “Publications arising from this thesis”.





## **Chapter 2: Literature Review**

---

## 2.1 Air Quality in Densely Populated Areas

According to the European Environment Agency (EEA), road transportation has contributed to about 23% of the total emissions of carbon dioxide (CO<sub>2</sub>), more than 30% of nitrogen oxides (NO<sub>x</sub>), and around 12% of primary PM<sub>2.5</sub> emissions in the European Union (EEA, 2016). In addition, as reported by the Hong Kong Environmental Protection Department (HKEPD), road transport was a major emission source of NO<sub>x</sub>, VOC, and CO, accounting for 20%, 19% and 53% of the total emissions in 2017, respectively in Hong Kong (HKEPD, 2020).

Figure 2.1 shows the path of air pollutants from emissions to exposures, which can be from man-made and natural sources, depending on the different pollutants, and lead to different impacts to the people and the environment.

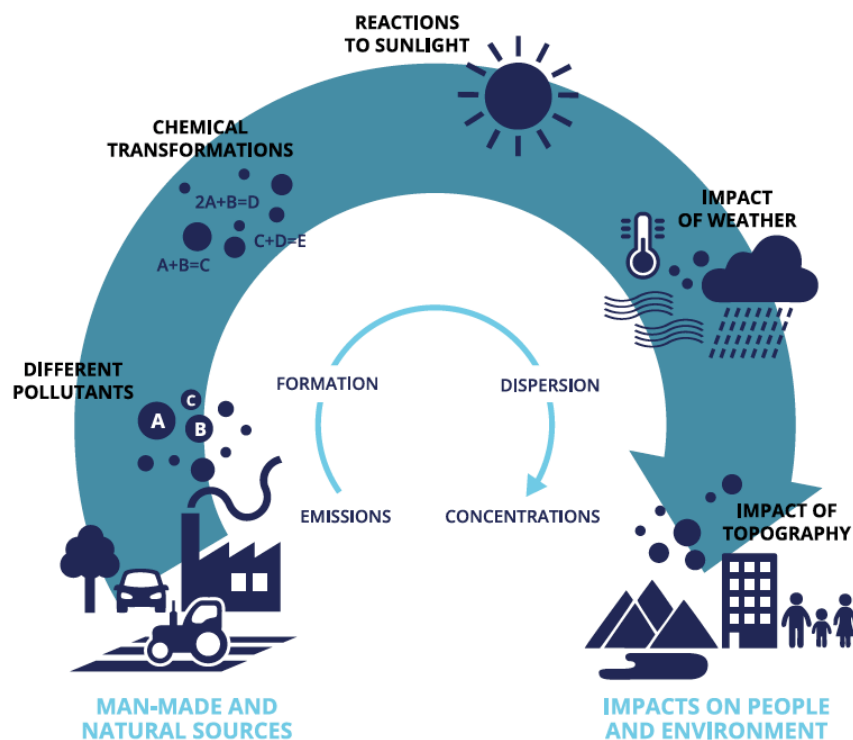


**Figure 2.1.** The path of air pollutants from emission to exposure (EEA, 2016).

## 2.2 Health Impact of Air Pollution

Seven million people die every year from the effects of air pollution. More than 90% of such deaths are in developing countries (WHO, 2019). Across southern Asia, levels of fine particulate matter (PM<sub>2.5</sub>) and surface ozone (O<sub>3</sub>) exceed the World Health Organization (WHO) limits for much of the year (Kumar et al., 2018).

As shown in Figure 2.2, air pollution has killed on an annual basis over 2 million people in both South-East Asian and Western Pacific Region, over 1 million people in African region, about 500,000 people in both Eastern Mediterranean and European region, and more than 300,000 people in the American region (WHO, 2020).

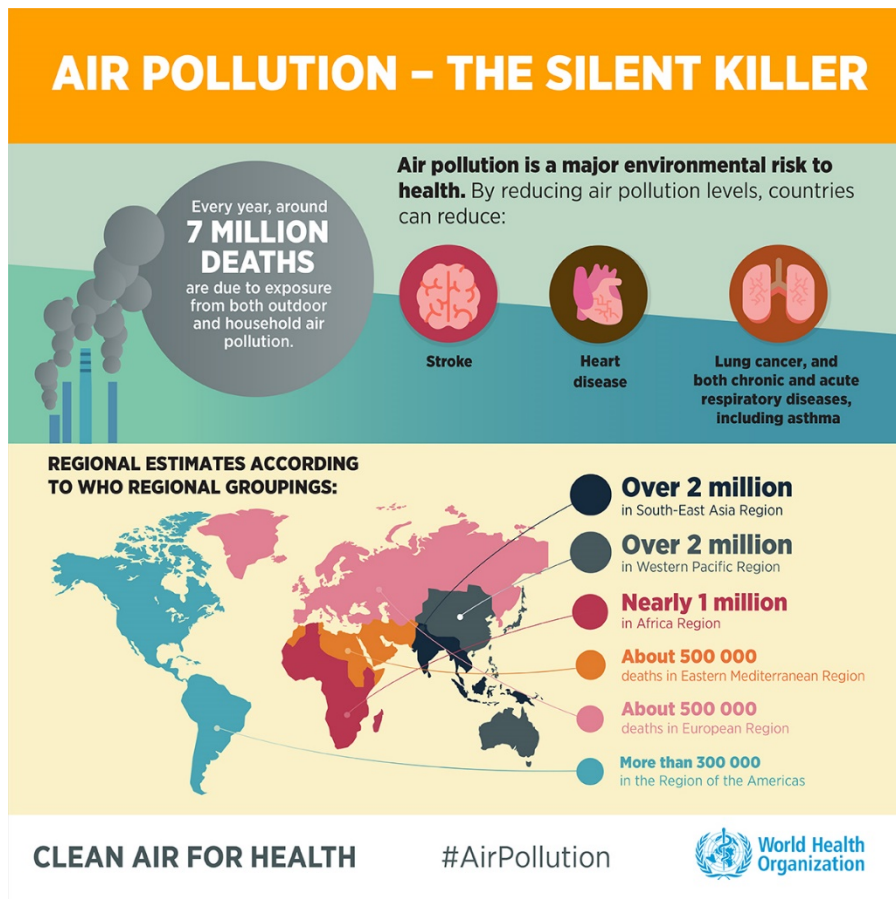


**Figure 2.2.** Regions affected by air pollution (WHO, 2020).

Total suspended particles (TSP) are primary contributors to premature death worldwide, with over four million premature deaths being recorded due to exposure to high levels of ambient PM<sub>2.5</sub> (Brauer et al., 2016; GBD 2015 Risk Factors Collaborators, 2016; Wendt et al., 2019). PM<sub>2.5</sub> can penetrate deep into the lungs when being inhaled, which leads to both acute and chronic health issues (Pope & Dockery, 2006; Wendt et al., 2019). NO<sub>2</sub> and TSP are responsible for 412,000 and 71,000 premature death per year, respectively, in the European Union (EEA, 2019; RCP, 2016).

Figure 2.3 shows the health effects pyramid to exposure of air pollutants, in regard to the seriousness of effects and number of people affected.

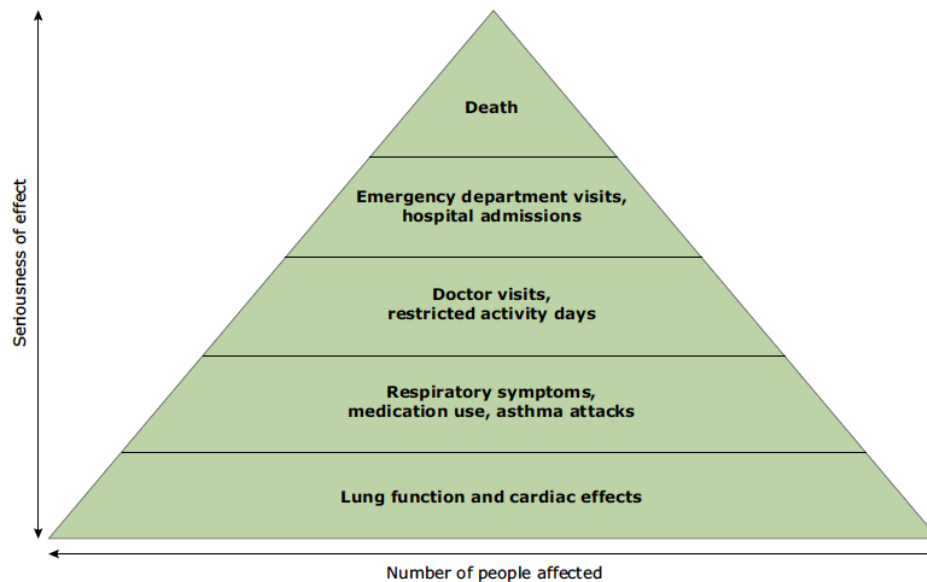


**Figure 2.3.** Health effects pyramids to exposure of air pollutants (EEA, 2014).

Moreover, previous studies show a strong correlation between short-term exposure to  $\text{NO}_2$  and both the number of hospital outpatients with eye and adnexa diseases (EADs) (Song et al., 2019) and the number of hospital admission due to cardiovascular diseases (CVD) (Jevtić et al., 2014).

The exposure to air pollutants such as  $\text{NO}_2$ , PM, and  $\text{O}_3$  increase the chance of hospital admissions for cardiovascular and respiratory disease and mortality in the world (Liu & Peng, 2018; WHO, 2018).

Exposure to  $\text{PM}_{10}$  and  $\text{PM}_{2.5}$  can affect the cardiovascular system. Numerous

studies showed that exposure to PM<sub>10</sub> and PM<sub>2.5</sub> has increased hospital admissions and emergency room visits and leading even to death from heart or lung diseases (US EPA, 2003). The exposure to PM<sub>10</sub> and PM<sub>2.5</sub> increases the chance of hospital admissions for cardiovascular and respiratory disease and mortality in the world (WHO, 2003).

Figure 2.4 shows the cause of deaths from air pollution, which demonstrated 21% due to pneumonia, 20% from stroke, 34% from ischemic heart disease, 19% from chronic obstructive pulmonary disease (COPD) and 7% from lung cancer (WHO, 2020).

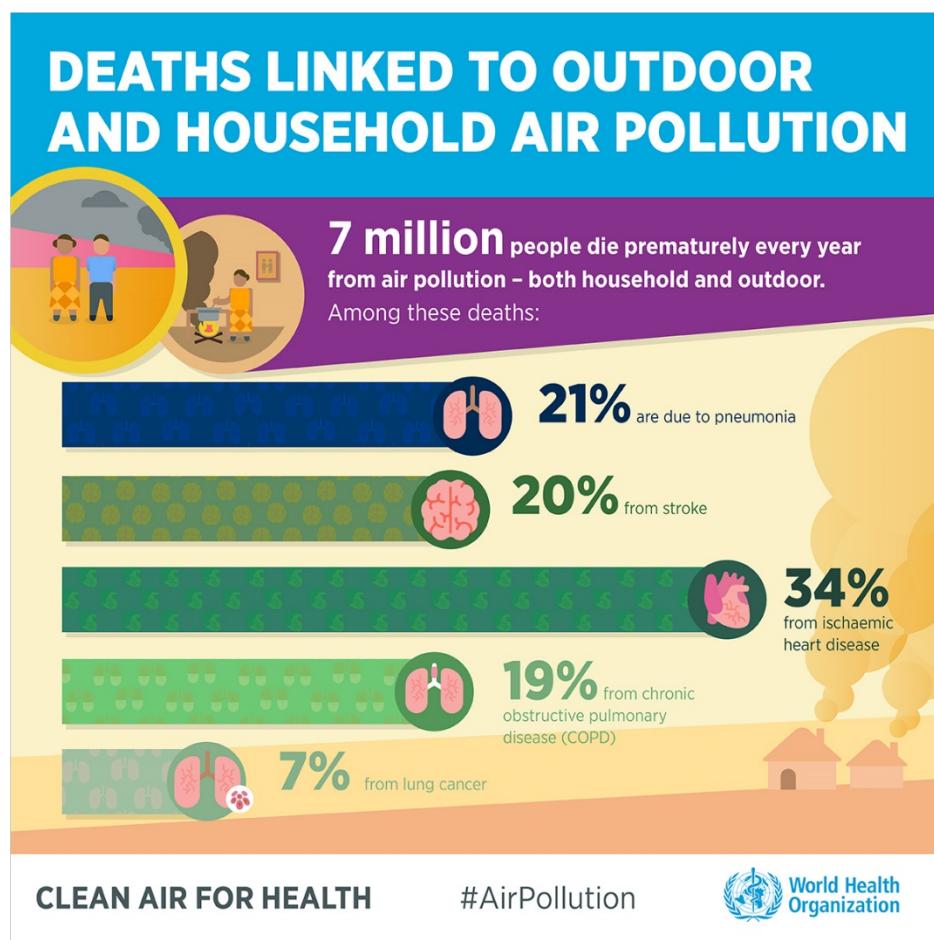


**Figure 2.4.** Cause of death from air pollution (WHO, 2020).

Surface ozone is associated with numerous harmful effects on respiratory health, at levels commonly found in urban areas throughout the world, contributing to morbidity and hospital admissions related to respiratory disease, even at low ambient levels (Entwistle et al., 2019). The high concentration of O<sub>3</sub> may lead to chest pain, coughing, throat irritation, and airway inflammation, and also reduce the function of the lung (US EPA, 2009).

Regarding particulate matter, for human health, small particles (PM<sub>2.5</sub>) are particularly dangerous as they can penetrate deeply into the lungs and be transported directly into the bloodstream (Wiśniewska et al., 2019). Furthermore, mixtures of NO<sub>2</sub>-PM<sub>2.5</sub>-O<sub>3</sub> exist in ambient environments, being the combinations of these pollutants more harmful to human health (a mixture with relatively low levels of some pollutants combined with relatively high levels of other pollutants, was found to be equally or more harmful than a mixture with high levels of all pollutants) (Liu & Peng, 2018). In Macao, traffic-related pollution is high, primarily due to high vehicle emissions and urban canyon topology (He et al., 2000).

Figure 2.5 shows the health effects of inhaling particulate matter (PM), which may cause different diseases to the brain, lungs and heart of a human body.



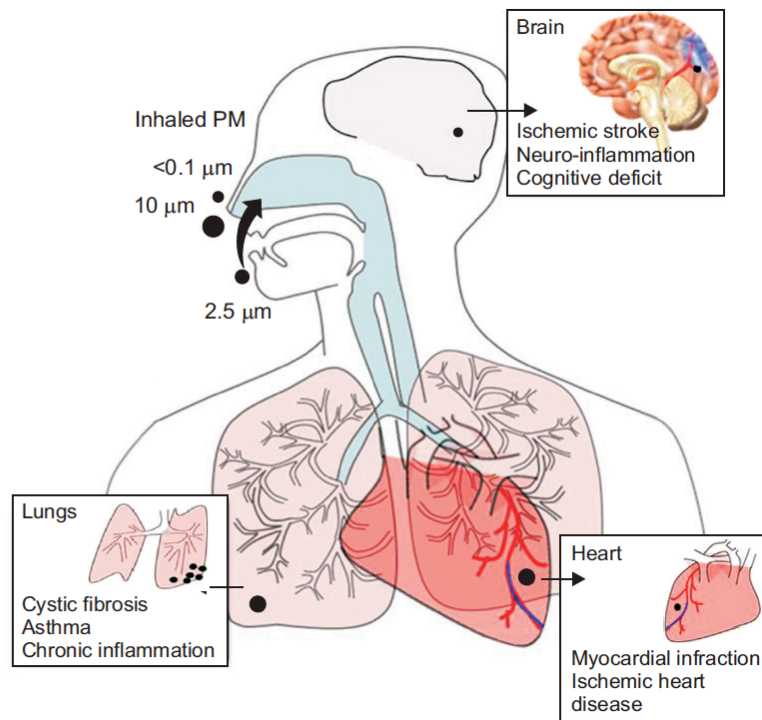


**Figure 2.5.** Diagrammatic representation of inhaled particulate matter of variable sizes and PM-linked respiratory, cardiovascular, and neurological diseases (Zaheer et al., 2018).

Figure 2.6 shows the health impacts of air pollution on humans, in particular of children and elderly being the most vulnerable groups. For instance, particulate matter (PM) can cause impact on the central nervous system, respiratory system and the reproductive system, while both PM and  $\text{O}_3$  can cause cardiovascular diseases and irritation of eyes, noses and throat. In addition,  $\text{NO}_2$  can cause impacts on liver, spleen, and blood (EEA, 2020). Table 2-1 showed the description of air pollutants including particulate matter (PM), nitrogen dioxide ( $\text{NO}_2$ ), ozone ( $\text{O}_3$ ) and sulphur dioxide ( $\text{SO}_2$ ).

### Health impacts of air pollution

Air pollutants can have a serious impact on human health. Children and the elderly are especially vulnerable.

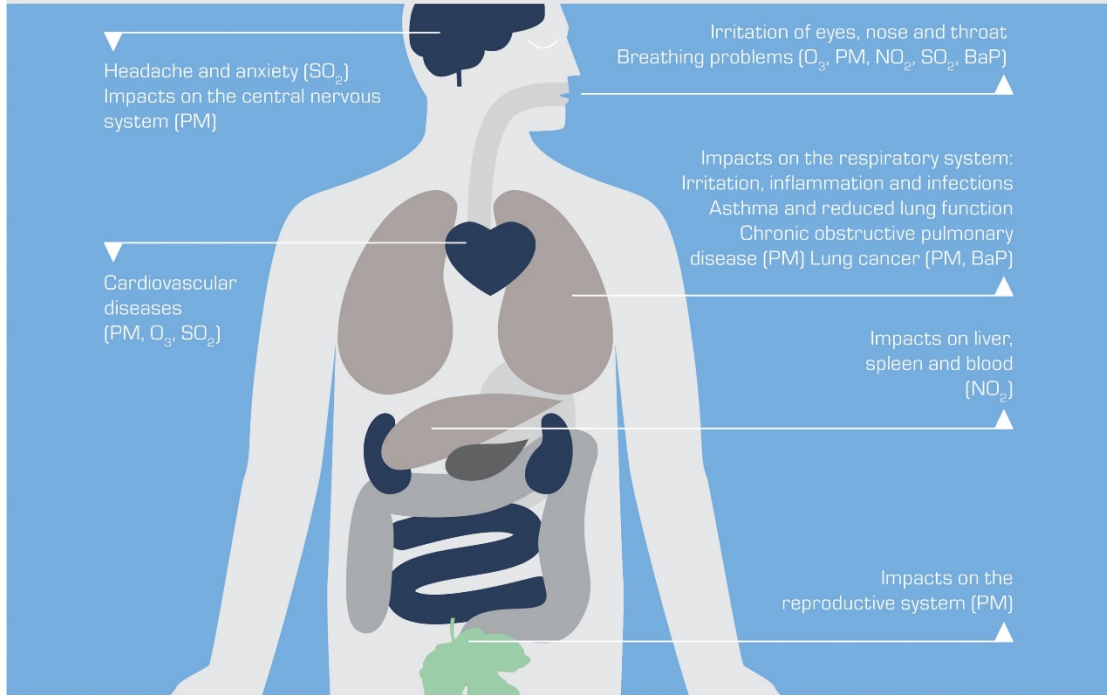


**Figure 2.6.** Health impacts of air pollution (EEA, 2020).

**Table 2-1.** Description of air pollutants. Adapted from (EEA, 2020).

Pollutants	Description
Particulate Matter (PM)	PM are particles that are suspended in the air. Sea salt, black carbon, dust and condensed particles from certain chemicals can be classed as a PM pollutant.
Nitrogen Dioxide (NO <sub>2</sub> )	NO <sub>2</sub> is formed mainly by combustion process such as those occurring in car engines and power plants.
Ozone (O <sub>3</sub> )	Ground level O <sub>3</sub> is formed by chemical reactions (triggered by sunlight) involving pollutants emitted into the air, including those by transport, natural gas extraction, landfills, and household chemicals.
Sulphur Dioxide (SO <sub>2</sub> )	SO <sub>2</sub> is emitted when sulphur containing fuels are burned for heating, power generation, and transport. Volcanoes also emit SO <sub>2</sub> into the atmosphere.

### 2.3 Source of Air Pollutants

Air pollution is normally associated with emission sources at alternating spatial scales from local, to regional and transboundary (Tong et al., 2018a), under certain

synoptic conditions. Estimates show that, for nitrogen oxides (NO<sub>x</sub>), mobile sources account for the majority of emissions (50%). For PM the industrial sector is the main emitter, followed by mobile sources (Zheng et al., 2009).

Figure 2.7 shows the source of air pollution, which includes industry and energy supply, transport, waste management, dust, agricultural practices, and household energy (WHO, 2020).

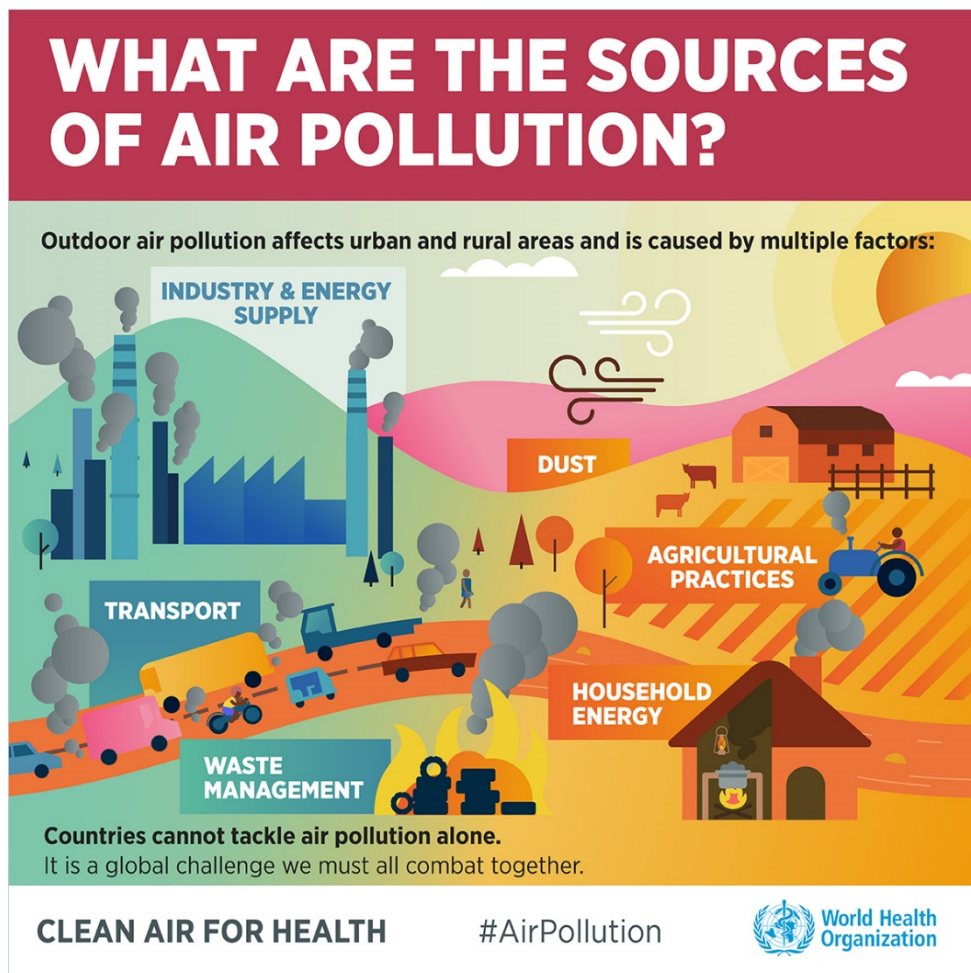


**Figure 2.7.** Source of air pollution (WHO, 2020).

The sources of  $PM_{10}$  and  $PM_{2.5}$  emissions include construction sites, unpaved roads, fires, power plants, industries and vehicles. Small particles less than 10 micrometers in diameter ( $PM_{10}$ ) poses the greatest problems, specifically due to the fine particles below 2.5 micrometers ( $PM_{2.5}$ ) that can get deep into the respiratory system, and some may even get into the bloodstream.

Coarse particles, also known as  $PM_{10}$ , are derived from suspension of dust, soil, sea salts, pollen, mold, and other crustal materials. Fine particles, also known as  $PM_{2.5}$ , are derived from emissions from combustion process, including vehicles powered by petrol and diesel, wood burning, coal burning, and other industrial processes. Ultrafine particles are derived from combustion related sources such as vehicle exhausts and atmospheric photochemical reactions (Pope & Dockery, 2006).

Figure 2.8 shows the size comparison of  $PM_{10}$ ,  $PM_{2.5}$ , human hair, and fine beach sand.

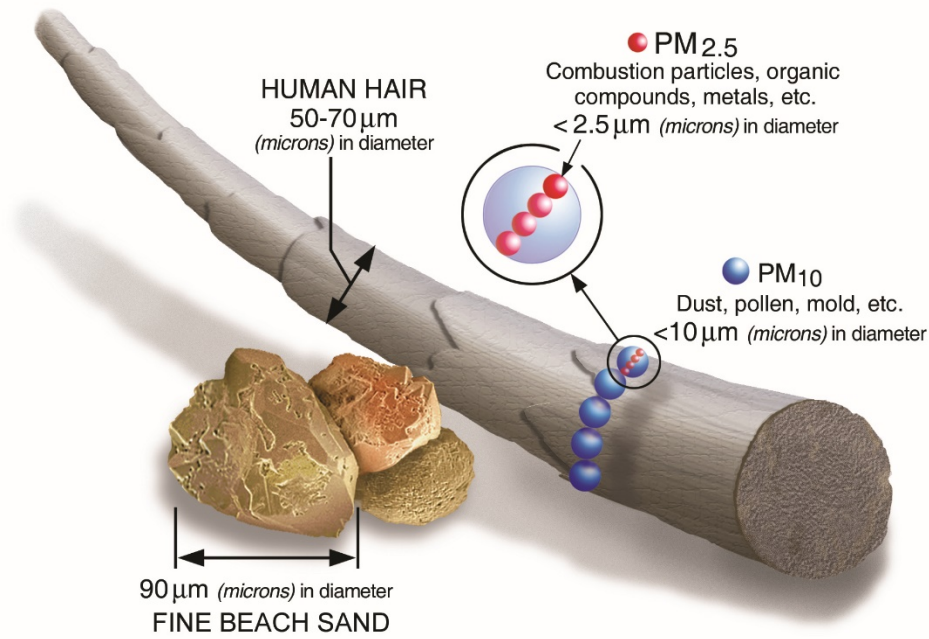


**Figure 2.8.** Size comparison of PM particles (EPA, 2020).

The sources of nitrogen dioxide ( $\text{NO}_2$ ) include the burning of fuel, emission from cars, trucks, and buses, and also power plants. The high concentration of  $\text{NO}_2$  may lead to different health impacts, which include the worsening of respiratory diseases such as asthma and also respiratory symptoms such as coughing, wheezing, and difficulty in breathing (US EPA, 2011).

Nitrogen oxides ( $\text{NO}_x$ ) are primarily emitted from transportation and combustion processes, while the emission of volatile organic compounds (VOCs) is primarily from road traffic and the use of products containing organic solvents (Li et al., 2020; Y. Wang et al., 2020).

Ozone ( $O_3$ ) is formed from a chemical reaction between nitrogen oxides ( $NO_x$ ) and VOCs. When  $NO_x$  and VOCs are emitted by cars, power plants, refineries, or chemical plants, and these pollutants react with sunlight, it may cause the formation of  $O_3$ . The levels of  $O_3$  concentration usually reach its highest levels under hot and sunny conditions, favorable for  $O_3$  formation.

Figure 2.9 shows the schematic representation of the photochemical formation of  $O_3$  in the presence of VOCs and  $NO_x$ .

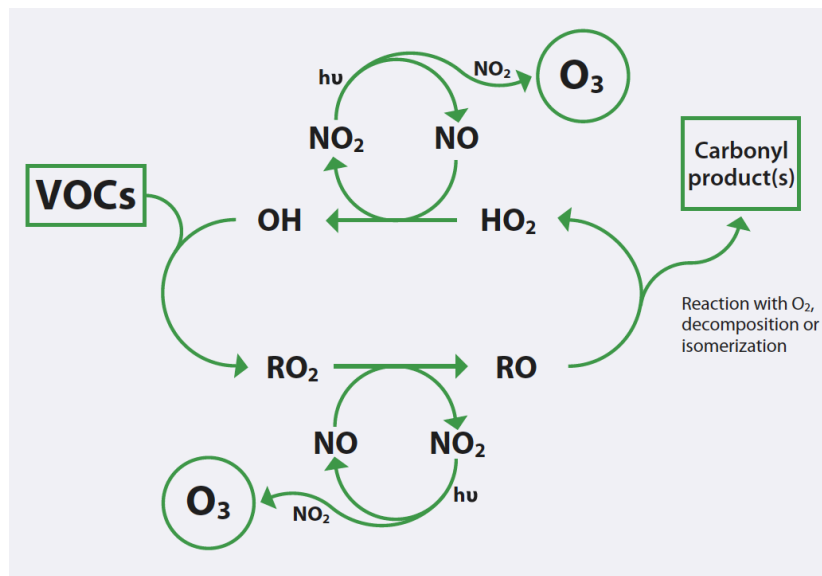


**Figure 2.9.** Schematic representation of the photochemical formation of ozone in the presence of VOCs and  $NO_x$ . (WHO Europe, 2008).

$O_3$  is the most important index substance for photochemical smog, one of the major air pollutants (Ghazali et al., 2010). The formation of ground-level  $O_3$  heavily depends on the concentration levels of VOCs and  $NO_x$  and meteorological factors

such as wind speed, insolation, and temperature. Nevertheless, the greater NO<sub>x</sub> emission reductions have contributed to a widespread shift in the O<sub>3</sub> production regime from NO<sub>x</sub>-saturated (high-NO<sub>x</sub>) to NO<sub>x</sub>-sensitive (low-NO<sub>x</sub>) in some urban areas, while O<sub>3</sub> production in rural areas is even more sensitive to NO<sub>x</sub>.

A study for Terengganu State, Malaysia, showed that high levels of O<sub>3</sub> occurring under dry and warm conditions during the southwest monsoon, were higher in industrial areas, and were positively correlated with the maximum daily temperature (Abdullah et al., 2017).

## **2.4 Air Quality Guidelines**

The World Health Organisation (WHO) has last updated their Air Quality Guidelines (AQG) in 2005. As shown in Table 2-2, WHO sets the threshold value of 24-hour mean concentration for PM<sub>10</sub> and PM<sub>2.5</sub> at 50 µg/m<sup>3</sup> and 25 µg/m<sup>3</sup>, respectively, 1-hour mean concentration of NO<sub>2</sub> at 200 µg/m<sup>3</sup>, and 8-hour mean concentration of O<sub>3</sub> at 100 µg/m<sup>3</sup> (WHO Europe, 2006). The Chinese National Ambient Air Quality Standards (NAAQS), GB 3095-2012, was first published in February 2012 as a replacement for GB 3095-1996, which became effective in January 2016. As shown in Table 2-2, there are two classes in the NAAQS, which set the standard value of 24-hour



mean concentration for PM<sub>10</sub> Classes 1 at 50 µg/m<sup>3</sup> and Classes 2 at 150 µg/m<sup>3</sup>, PM<sub>2.5</sub> Classes 1 at 35 µg/m<sup>3</sup> and Classes 2 at 75 µg/m<sup>3</sup>, 1-hour mean concentration for NO<sub>2</sub> Classes 1 and Classes 2 at 200 µg/m<sup>3</sup>, and 8-hour mean concentration for O<sub>3</sub> Classes 1 at 100 µg/m<sup>3</sup> and Classes 2 at 160 µg/m<sup>3</sup> (MEE, 2012).

Compliance with the thresholds set by the WHO for PM<sub>2.5</sub> could improve life expectancy in China by 0.14 years (Qi et al., 2020) and ambient air pollution has caused at least 3.7 million deaths in 2012, with more than 25% of deaths in Southeast Asia (Ai et al., 2016; Chen et al., 2018).

Table 2-2 shows the air quality standards for the levels of PM<sub>10</sub>, PM<sub>2.5</sub>, NO<sub>2</sub>, O<sub>3</sub> concentration set at different countries and institutions. Figures 2.10 to 2.13 show the comparison of different air quality standards amongst WHO, European Union (EU), US, China, Macao, and Hong Kong for PM<sub>10</sub>, PM<sub>2.5</sub>, NO<sub>2</sub>, and O<sub>3</sub>.

**Table 2-2.** Air quality standards set at different countries and/or by different institutions. Adapted from (MEE, 2012; SMG, 2019; WHO Europe, 2006).

Source	PM <sub>10</sub> (µg/m <sup>3</sup> )		PM <sub>2.5</sub> (µg/m <sup>3</sup> )		NO <sub>2</sub> (µg/m <sup>3</sup> )		O <sub>3</sub> (µg/m <sup>3</sup> )
	1 year	24 hours	1 year	24 hours	1 year	1 hour	8 hours
WHO	20	50	10	25	40	200	100
European Union	40	50	25		40	200	120
United States	50	150	15	65	100		157
China (Classes 1)	40	50	15	35	40	200	100
China (Classes 2)	70	150	35	75	40	200	160
Macao	70	150	35	75	40	200	160
Hong Kong	50	100	35	75	40	200	160
WHO Interim Target-1	70	150	35	75			160
WHO Interim Target-2	50	100	25	50			
WHO Interim Target-3	30	75	15	37.5			

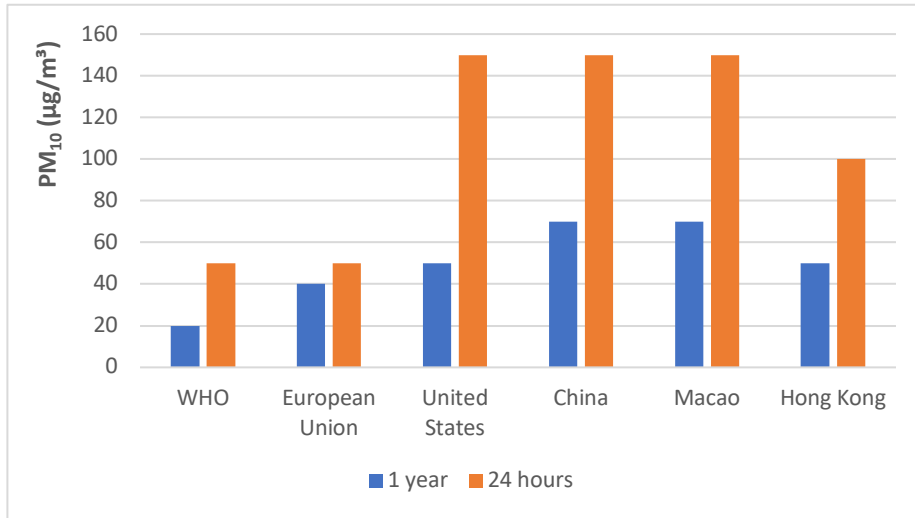


**Figure 2.10.** Comparison of air quality standards for PM<sub>10</sub>.

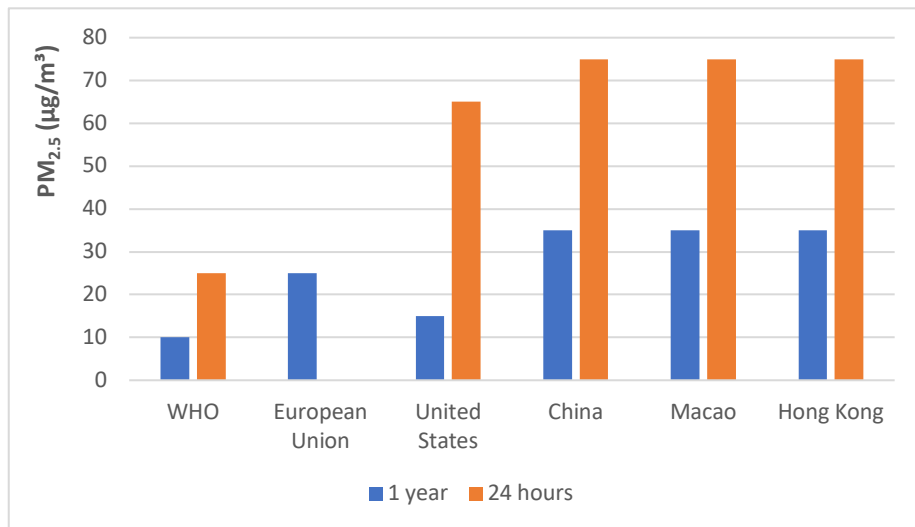


**Figure 2.11.** Comparison of air quality standards for PM<sub>2.5</sub>.

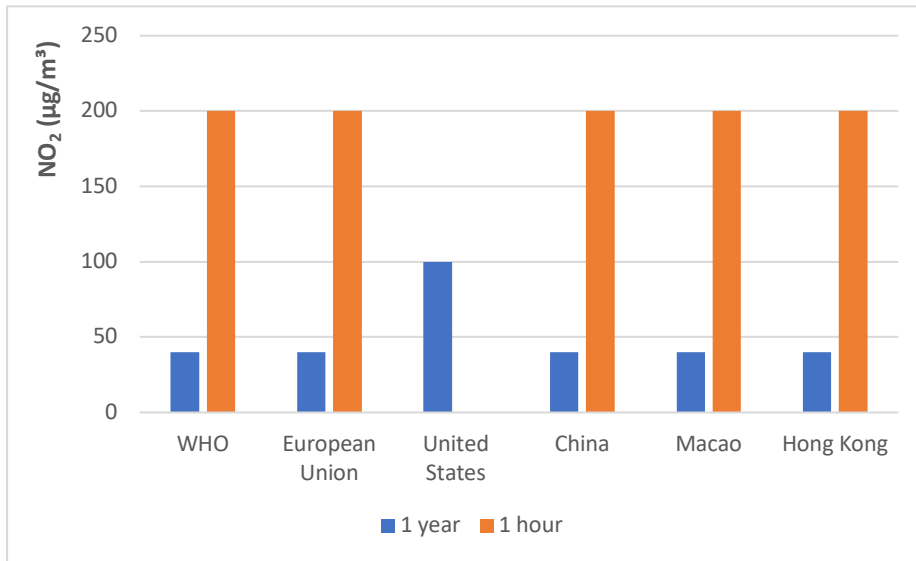


**Figure 2.12.** Comparison of air quality standards for nitrogen dioxide (NO<sub>2</sub>).

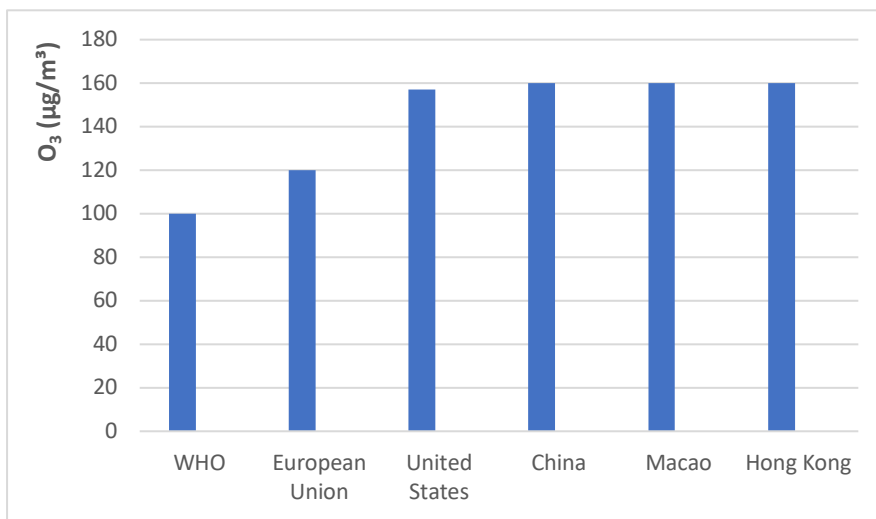


**Figure 2.13.** Comparison of air quality standards for 8-hour average ozone (O<sub>3</sub>).

Possible solutions to improve air pollution includes the investment in renewable and energy-efficient power generation, improve domestic industry and municipal waste management, reduce agricultural waste incineration, forest fires and certain

agro-forestry activities, make greener and more compact cities with energy-efficient buildings, provide universal access to clean, affordable fuels and technologies for cooking, heating and lighting, and build safe and affordable public transport systems and pedestrian and cycle-friendly networks (WHO, 2020).

## **2.5 Forecasting Models**

Several methodologies have been developed and applied to forecast air quality across the world, including deterministic, statistical, and machine learning methods (Lin et al., 2019; Ma et al., 2019; Masih, 2019; Pagowski et al., 2006). Deterministic methods, also known as numeric, can be applied to regions where a complete and fully detailed emission inventory is available. In contrast, those regions without a complete and reliable emission inventory can only use statistical methods, also known as stochastic, for forecasting air quality. Statistical methods primarily rely on historical data of air quality and meteorological data as the basis to develop the air quality forecast. The statistical approach learns from historical data and predicts the future behavior of the air pollutants.

Meteorological conditions significantly affect the levels of air pollution in the urban atmosphere, due to their important role in the transport and dilution of

pollutants, and as such there is a close relationship between the concentration of air pollutants and meteorological variables (Zhang & Ding, 2017). One approach to statistical forecasting is to train multiple linear regression models (MLR) based on existing measurements to predict concentrations of air pollutants in the future, according to the corresponding meteorological variables.

The development of air quality forecast models is essential for cities with high population density, including Macao, one of the most densely populated cities in the world, because by predicting pollution episodes authorities can provide warning to the local community in advance to avoid the exposure to poor air quality, which may lead to severe health consequences.

To be useful, these models should be robust to deal with extreme variations in pollution levels, in particular during high-pollution peak days. Factors leading to extreme variation in pollution levels are diverse and include both human activities and meteorological factors.

Some studies showed that statistical models are more accurate and efficient compared to deterministic models, particularly in regions with complex terrain (Kocijan et al., 2018; Lopes et al., 2016; Zhang et al., 2012). Moreover, prediction of

NO<sub>2</sub>, PM<sub>10</sub>, PM<sub>2.5</sub>, and O<sub>3</sub> MAX concentrations based on multiple linear regression (MLR) and classification and regression tree (CART) models have been successfully implemented in Bangkok, Changsha City, Beijing, Bilbao, and Pakistan (Ahmad et al., 2019; Chen & Wang, 2019; Sahanavin et al., 2018; Samadianfard et al., 2013; Zhao et al., 2018).

### **2.5.1 Deterministic Methods**

Deterministic models utilize all of the major meteorological, physical, and chemical processes that lead to the formation and accumulation of air pollutants. The equations must be determined for the mass of various species and transformation relationship among chemical species and physical states (Zhang et al., 2012).

Deterministic models perform the air quality forecast by constructing a simulation model of the dispersion and transport process of atmospheric chemistry. In addition, deterministic methods are computationally expensive and the forecasting results may be inaccurate due to the use of default parameters and the lack of real-time observations for air quality and meteorological variables. Some of the limitations for deterministic methods include the high computing costs needed to develop the model and the detailed knowledge required to input the different parameters into the model

(Catalano & Galatioto, 2017; Kukkonen et al., 2003; Ma et al., 2019; Suleiman et al., 2019).

Studies showed that deterministic models struggle to capture the relationship between the concentration of atmospheric pollutants and their source of emission. In addition, the deterministic methods may not capture the nonlinearity between air pollutants and the sources of their emission and dispersion, in particular of regions with complex terrain, which could lead to inaccurate results (Chen et al., 2017; Liu et al., 2017; Masih, 2019; Ritter et al., 2013; Shimadera et al., 2016). Some of the deterministic models that are most commonly used to predict air quality include Chemical Transport Models (CTMs), Weather Research and Forecast (WRF) Models, Operational Street Pollution Models (OSPM), and Nested Air Quality Prediction Modeling System (NAQPMS) (Ma et al., 2019; Saide et al., 2011; Stern et al., 2008; Wang et al., 2001).

Figure 2.14 shows the air quality forecast using different deterministic models, such as Weather Research Forecast (WRF), Chemical Transport Models (CTM), and CHIMERE (Guttikunda et al., 2011).



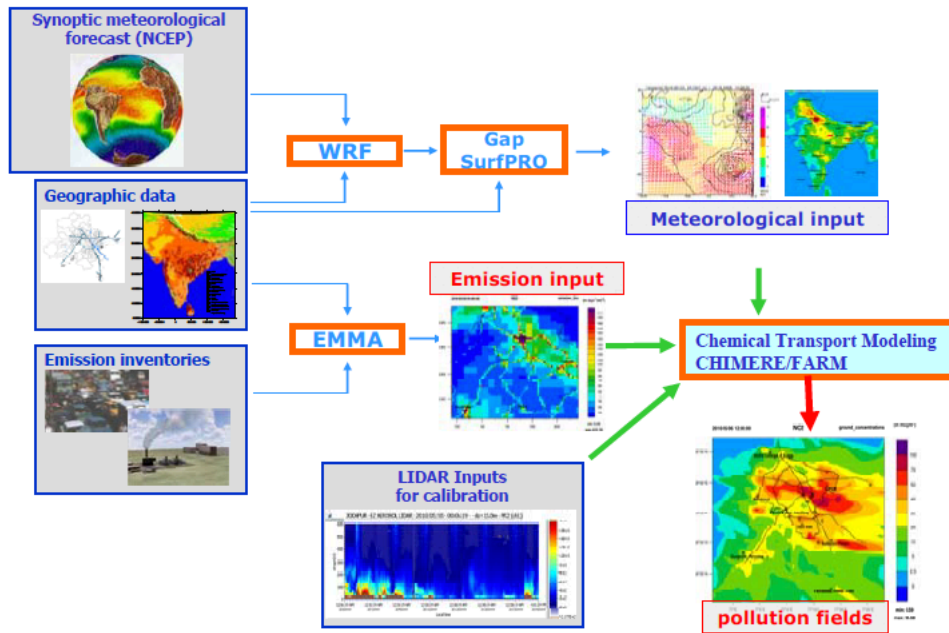


**Figure 2.14.** Air quality forecasting model using deterministic methods (Guttikunda et al., 2011).

As an example, air quality forecast using deterministic methods such as the Advanced Research Weather Research and Forecasting (WRF-ARW) model and the HYSPLIT model were used to predict air quality in the Pearl River Delta (PRD) region, which included Macao, Hong Kong, and Guangdong Province (Lopes et al., 2016, 2018).

Figure 2.15 shows the configuration of the four modeling domains in a deterministic model.

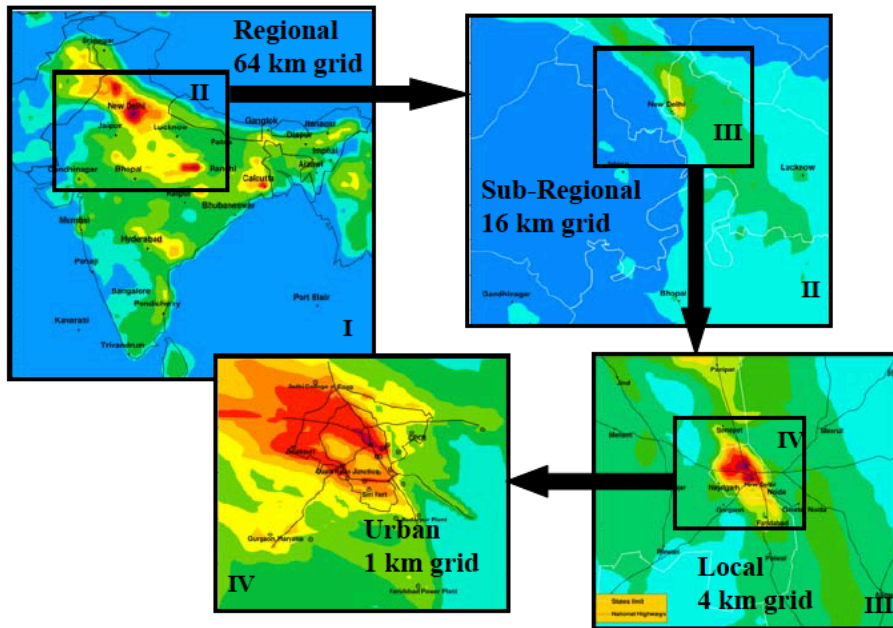


**Figure 2.15.** Different grids in deterministic models (Guttikunda et al., 2011).

### 2.5.2 Statistical Methods

Statistical models such as multiple linear regression (MLR) and classification and regression tree (CART) are developed based on historical measurements of meteorological and air quality variables. Statistical models are more accurate and efficient compared to deterministic models (Kocijan et al., 2018; Zhang et al., 2012).

Figure 2.16 shows the steps of model development for an air quality forecast using statistical methods in an operational forecast.

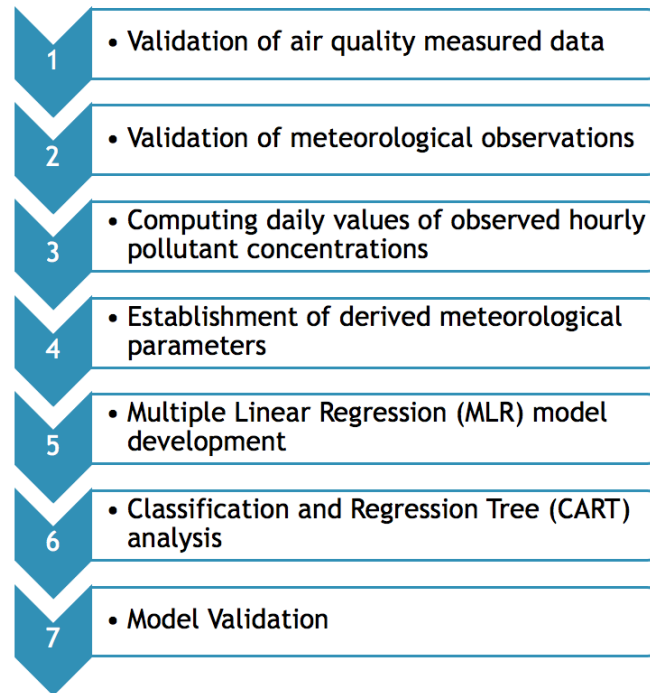


**Figure 2.16.** Steps of model development for an air quality forecast using statistical methods.

### 2.5.3 Machine Learning Techniques

According to recent studies, machine learning (ML) has been adopted by researchers to forecast air quality as a complement to the deterministic methods and particularly to statistical methods. ML is a branch of computer science which makes computers capable of performing a task without being explicitly programmed, while artificial neural network (ANN) attempts to simulate the structures and networks within the human brain to make decisions (Kang et al., 2018) and has been one of the most popular methods for air quality forecasting (Ma et al., 2019). In order to tackle the

limitations of traditional models, ML based on statistical algorithms seemed to be promising, because it does not consider physical and chemical processes in deterministic model, or strictly rely on historical data to make pollution predictions in statistical model (Lee et al., 2017; Masih, 2019; Nhung et al., 2017; Zafra et al., 2017).

Researchers believe that using ML to generate local emissions based on real-time observations is a promising approach and has been applied and improved the relevant air quality forecast when integrated with a data assimilation system (Lin et al., 2019).

Nevertheless, the shortcomings of ML include its incapacity to capture the time series patterns or learn from the long-term dependencies of air pollutant concentrations.

A combination of machine learning (ML) and statistical methods were used to successfully forecast air quality in Bogotá, Columbia. The integrated model reduced the variance of the forecast and diminished the probability of over fitting (Martínez et al., 2018). The integration of ML and ANN was used to successfully forecast the levels of PM<sub>2.5</sub> concentration in Beijing (Tao et al., 2019), the levels of SO<sub>2</sub> concentration in Mumbai (Bhalgat et al., 2019), the levels of PM<sub>10</sub> concentration in Northern Spain (García Nieto et al., 2018), the concentration of PM<sub>10</sub> and PM<sub>2.5</sub> in Tehran (Delavar et al., 2019; Zhang & Ding, 2017), the levels of O<sub>3</sub> concentrations in Hong Kong (Wang

et al., 2003; Zhang & Ding, 2017), and the levels of PM<sub>2.5</sub> concentrations in Pakistan (Ahmad et al., 2019).

In addition, recent studies using this methodology have been conducted to assess meteorological influence on air quality (Tong, et al., 2018; Xie et al., 2019), and related to air quality forecast (Lee et al., 2017; Deng et al., 2018).

## **Chapter 3: Background and Methodology**

---

### **3.1 Case Study of Macao**

Macao is located in Southern China and is one of the cities within the Greater Bay Area. The historical center of Macao has been awarded “World Cultural Heritage” status by the United Nations Educational, Scientific and Cultural Organizations (UNESCO) in 2005. Nevertheless, the land area of Macao is extremely limited due to rapid development and population growth in combination with lack of land resources and thus the United Nations World Prospects Report had listed Macao as the number 1 most densely populated region in the world (Sheng & Tang, 2013). Macao has a land area of 30.8 square kilometers with a population of 653,100, which is equivalent to a population density of 21,100 habitants per square kilometer (DSEC, 2018).

Macao is a special administrative region of China. The lack of land and natural resources makes it impossible for Macao to develop any heavy industries or construct any large scale factories within the region. As a result, the Macao government focused on the light industry, in particular of hotel and gaming as the primary industry. Macao had a long history of gambling, which started about 140 years ago. The Macao government’s decision to open up the gambling industry in 2002 revolutionized the development of casinos and gaming industry, making Macao as the only region in China

that allows legal gambling (Feng et al., 2012).

The geographical setting of Macao consists of the main peninsula, which is connected to the mainland China and two outlying islands known as Taipa and Coloane. The main peninsula and outlying islands are interconnected with roads and bridges. Due to the limited land area, the government of Macao utilized reclamation as a primary solution to keep up with the supply and demand of land. Due to land reclamation, the area of Macao has doubled its size since its designation as a city back in 1586 (Chaplain, 2002). The total area of Macao has raised from 11.6 square kilometers in the early 1900s to over 30.8 square kilometers in 2018, which showed that Macao has tripled its size in the last century (DSEC, 2018). The casinos and hotels are primarily constructed on the reclaimed land near the island of Taipa (Feng et al., 2012). The Cotai Strip is a reclaimed area that stretches between Taipa and Coloane, measuring approximately 6 square kilometers, and being primarily used for the constructions of casino and hotel (Chaplain, 2002). The newly opened hotel and casino has created an enormous amount of job opportunities, which attracted many of the foreign workers to work in Macao. Thus, the population size of Macao has continued to increase in the past decade. The population size of Macao is over 653,100 people.



Due to the high population density, the health impact of air pollution in Macao is significant. The levels of PM<sub>10</sub>, PM<sub>2.5</sub>, NO<sub>2</sub>, and O<sub>3</sub> concentration in Macao and its neighboring cities in the Greater Bay Area are extremely high and often exceeding the established limit values recommended by World Health Organization (WHO) Air Quality Guidelines (AQG).

### **3.2 Air Quality in Macao**

The air quality of Macao is under the influence of the nearby regions, in particular of cities from the Guangdong Province, due to their geographical proximity. Despite Macao and Hong Kong being amongst the lowest emission cities in China, nearby cities such as Zhuhai and Zhongshan are experiencing an increase of emissions due to industrialization, coal power plant and energy production within or in their vicinities (Tsai et al., 2006; Zhou et al., 2018).

The Guangdong-Hong Kong-Macao Regional Air Quality Monitoring Information System provides a platform to access the pollutant concentrations of PM<sub>10</sub>, PM<sub>2.5</sub>, NO<sub>2</sub>, and O<sub>3</sub> in the cities of Greater Bay Area in Southern China. Figure 3.1 shows the past 1-hour average ( $\mu\text{g}/\text{m}^3$ ) of pollutant concentrations of the monitoring stations in the Guangdong-Hong Kong-Macao Greater Bay Area (GBA).

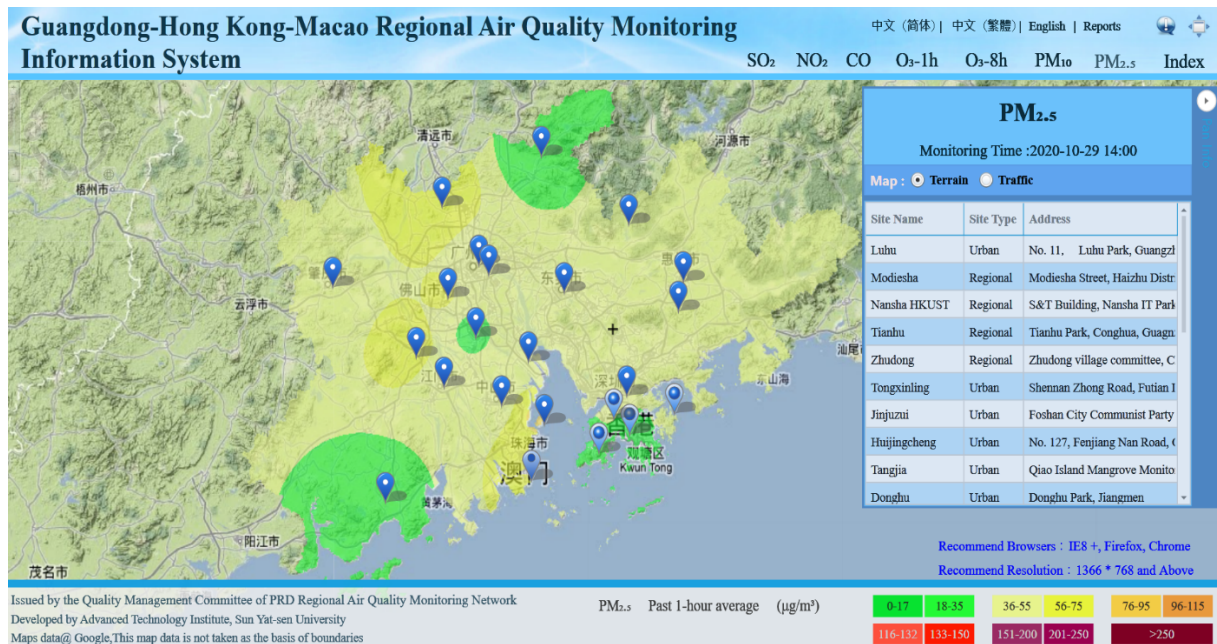


**Figure 3.1.** Guangdong-Hong Kong-Macao regional air quality monitoring information system (SMG, 2020).

There are two types of air quality monitoring stations, ambient and roadside stations, in which the ambient stations monitor the background and set the baseline levels of pollutant concentrations for a region, while the roadside stations monitor the roadside emission at a location close to the traffic. Figure 3.2 shows the settings of a typical ambient air quality monitoring station. Figure 3.3 shows the settings of a typical roadside air quality monitoring station. The air quality monitoring can be achieved by air quality monitoring stations (AQMS) setup by the local environmental authorities for their respective jurisdiction.



**Figure 3.2.** Settings of a Macao ambient station (SMG, 2020).



**Figure 3.3.** Settings of a Macao roadside station (SMG, 2020).

The air quality monitoring network of Macao measures particulate matters ( $PM_{10}$  and  $PM_{2.5}$ ), nitrogen dioxide ( $NO_2$ ), ozone ( $O_3$ ) and sulfur dioxide ( $SO_2$ ), in both ambient background and roadside locations. There are a total of six air quality

monitoring stations evenly spread throughout Macao, which include one high-intensity residential area and one roadside station in Macao, one high-intensity residential area and one ambient station in Taipa, one ambient station in Coloane, and one roadside station is Ka-Ho (SMG, 2017). Due to the small physical size of the region, the density of monitoring stations in Macao is considered to be high.

The SMG adopted the WHO interim target-1 (IT-1) for the threshold of pollutants, which has a less strict standard on the pollutants compared to the WHO Air Quality Guideline. Taipa Ambient is an ambient station in Macao which is also the background representative station. It is located at Taipa Grande, the headquarter of SMG. Figure 3.4 represents the spatial locations of air quality monitoring stations, within the 32.8 km<sup>2</sup> of Macao region.

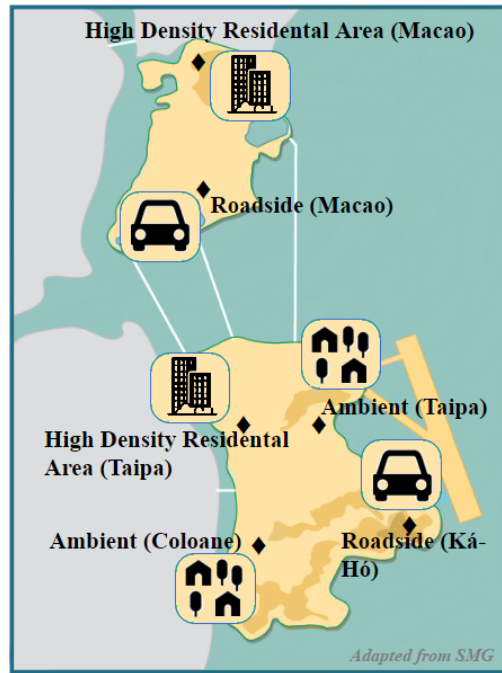








**Figure 3.4.** Map of Macao air quality monitoring stations network. Adapted from SMG (2019).

Currently, the Macao Meteorological and Geophysical Bureau (SMG) uses the past air quality data (the calculation period of the index is from 12:00 p.m. from the previous day to 12:00 p.m. of the current day) to provide an air quality index (AQI).

Figure 3.5 shows an example of the daily air quality index in Macao, from the Macao Meteorological and Geophysical Bureau (SMG).







Daily Air quality index on 2020–11–29 Daily Air quality index on

Station	Daily Air Quality Index	Air Quality	
Roadside (Macao)	62	Moderate	
High Density Residential Area (Macao)	57	Moderate	
High Density Residential Area (Taipa)	44	Good	
Ambient (Taipa)	76	Moderate	
Ambient (Coloane)	76	Moderate	
Roadside (Ka-Ho)	80	Moderate	

**Figure 3.5.** Daily air quality index in Macao (SMG, 2020).

Table 3-1 translates the AQI in terms of the influence on health and advises the public based on the air quality accordingly.

**Table 3-1.** Air quality index (AQI) of Macao (SMG, 2019).

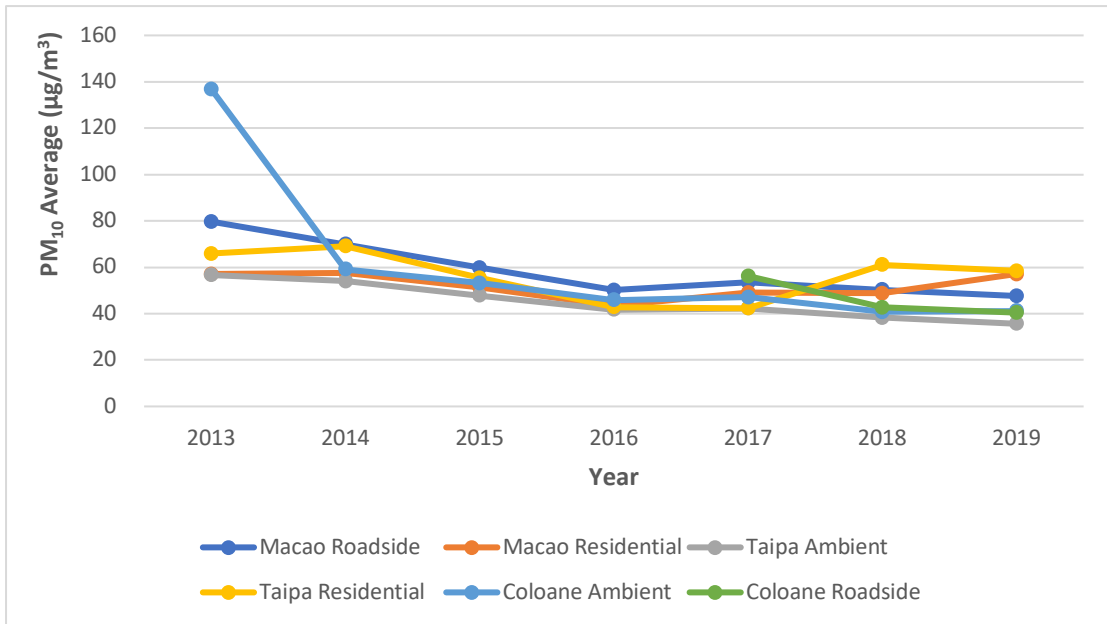
Air quality			Influence to health	Advise to public
Index	Quality			
0 - 50	Good 	No influence is expected.	No response action is required.	
51 - 100	Moderate 	The general public may not experience immediate effect. However, it may cause adverse health effects if people are exposed under this level for a long time.	No immediate response action is required. It may cause adverse health effects if people are exposed under this level for a long time.	
101 - 200	Bad 	For people who have cardiac or respiratory disease, symptom might become slightly worse. The general public might experience discomfort.	People who have cardiac and respiratory disease are advised to reduce physical exercise and outdoor activities.	
201 - 300	Very Bad 	For people who have cardiac or respiratory disease, symptom might be obviously affected. The general public would experience discomfort.	People are advised to reduce physical exercise and avoid outdoor activities.	
301 - 400	Severe 			
401 - 500	Harmful 			

[http://www.smg.gov.mo/smg/airQuality/e\\_daily\\_iqa\\_definition.htm](http://www.smg.gov.mo/smg/airQuality/e_daily_iqa_definition.htm)

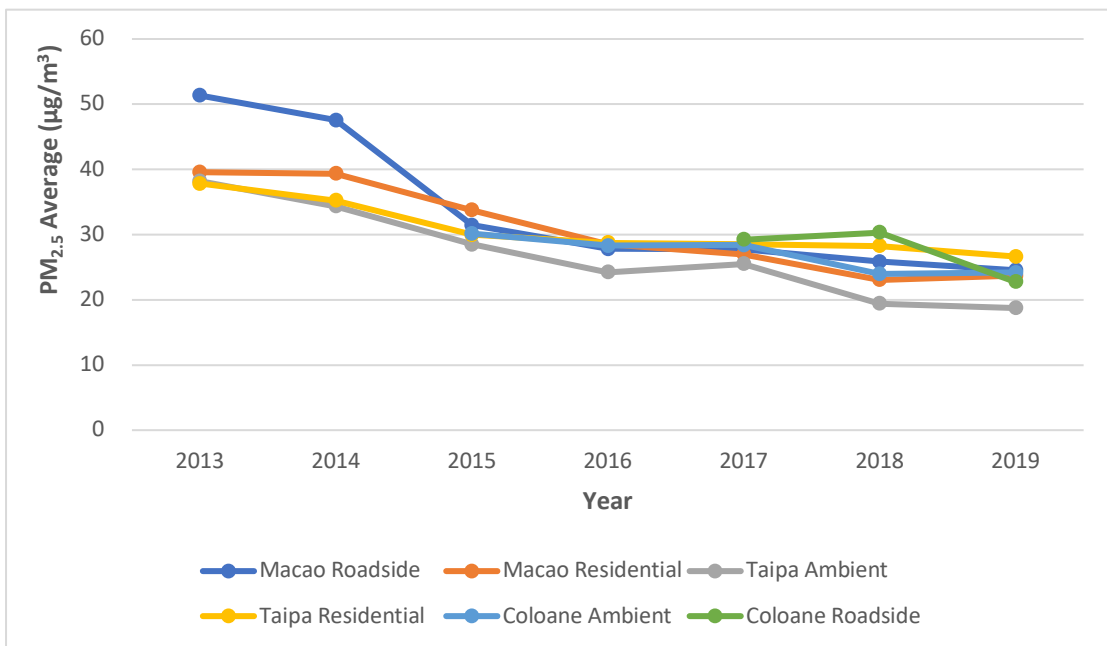
The higher levels of PM<sub>10</sub> and PM<sub>2.5</sub> concentration usually occur during the winter season, from December to February, due to the northern wind bringing the air pollutants to the region, lowering mixing height, fewer amount of rainfall, and lower frequency

of rainfall. In contrast, the levels of  $PM_{10}$  and  $PM_{2.5}$  concentration is usually measured lower during the summer season, from June to August, due to the southern winds from the China sea, higher mixing height, greater amount of rainfall, and higher frequency of rainfall, which allows for a better air pollution dispersion and deposition conditions (Lopes et al., 2016, 2018). In addition, Macao has a typical tropical oceanic climate which is hot and humid, with an annual average temperature of 22.3 °C and an annual average wind speed of 3.5 m/s, with northwestern wind dominant in winter and southeastern wind dominant in summer (He et al., 2000).

Figure 3.6 and 3.7 present for the Macao air quality monitoring stations the annual average levels of  $PM_{10}$  and  $PM_{2.5}$  concentrations, respectively, from 2013 to 2019. The figures show a decreasing trend in the yearly average concentration of  $PM_{10}$  and  $PM_{2.5}$  in all stations.



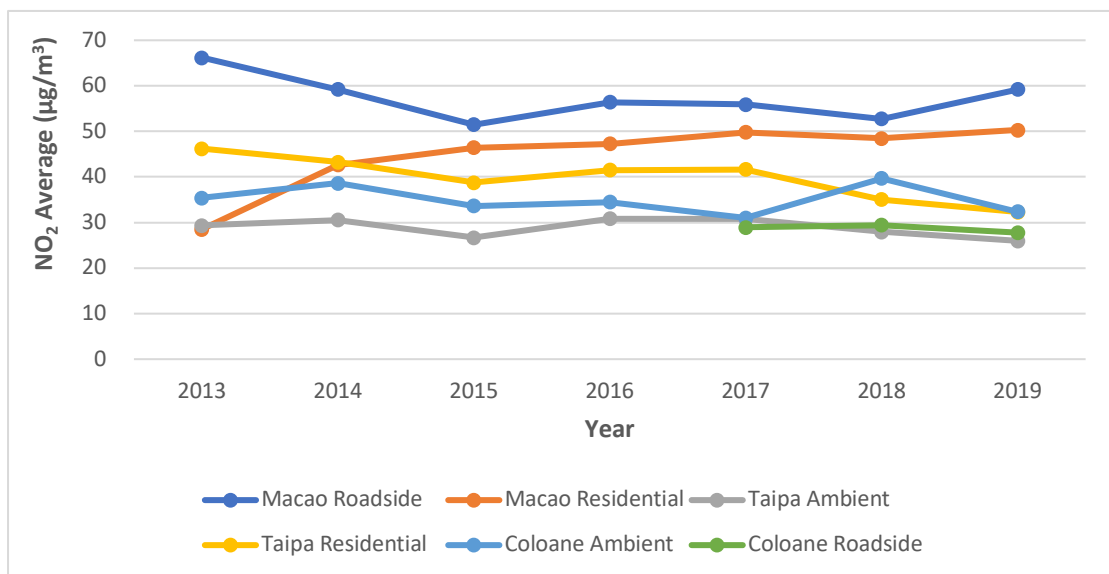
**Figure 3.6.** Yearly average levels of PM<sub>10</sub> in the Macao air quality monitoring stations (2013 to 2019).



**Figure 3.7.** Yearly average levels of PM<sub>2.5</sub> in the Macao air quality monitoring stations (2013 to 2019).



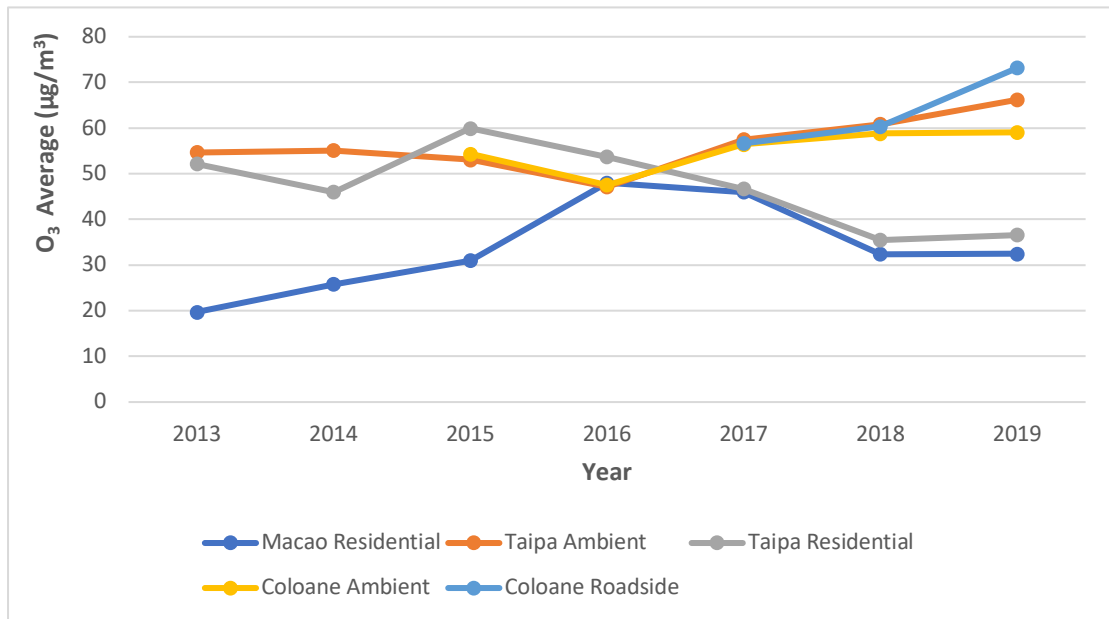
Figure 3.8 presents the average annual levels of NO<sub>2</sub> concentrations in the Macao air quality monitoring stations from 2013 to 2019. The figure shows that there is a decrease in the average yearly concentration of NO<sub>2</sub> in all stations from 2013 to 2019 with the exception of Macao Residential. This may be due to the increase traffic in the surrounding area of the Border Gate between Macao and China and the recently inaugurated Hong Kong-Zhuhai-Macao Bridge (HZMB), connecting Macao, Hong Kong and China.



**Figure 3.8.** Yearly average levels of NO<sub>2</sub> in the Macao air quality monitoring stations (2013 to 2019).

Figure 3.9 presents the average annual levels of O<sub>3</sub> concentrations in the Macao air quality monitoring stations from 2013 to 2019. An increase of the levels of O<sub>3</sub> concentration in all stations from 2013 to 2019 can be verified, with the exception of

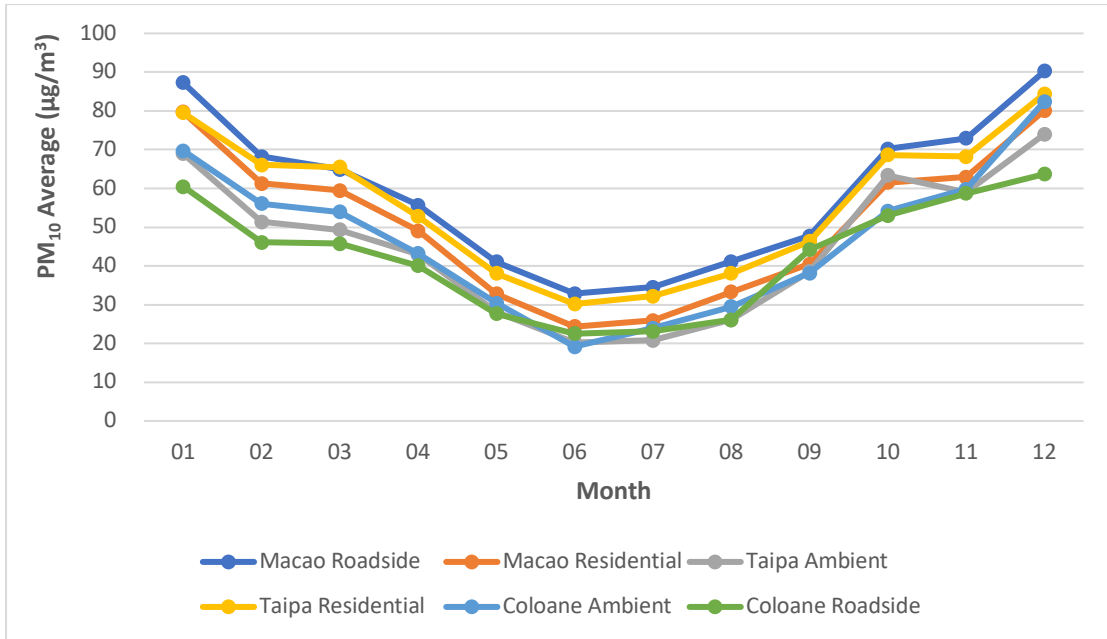
Taipa Residential.



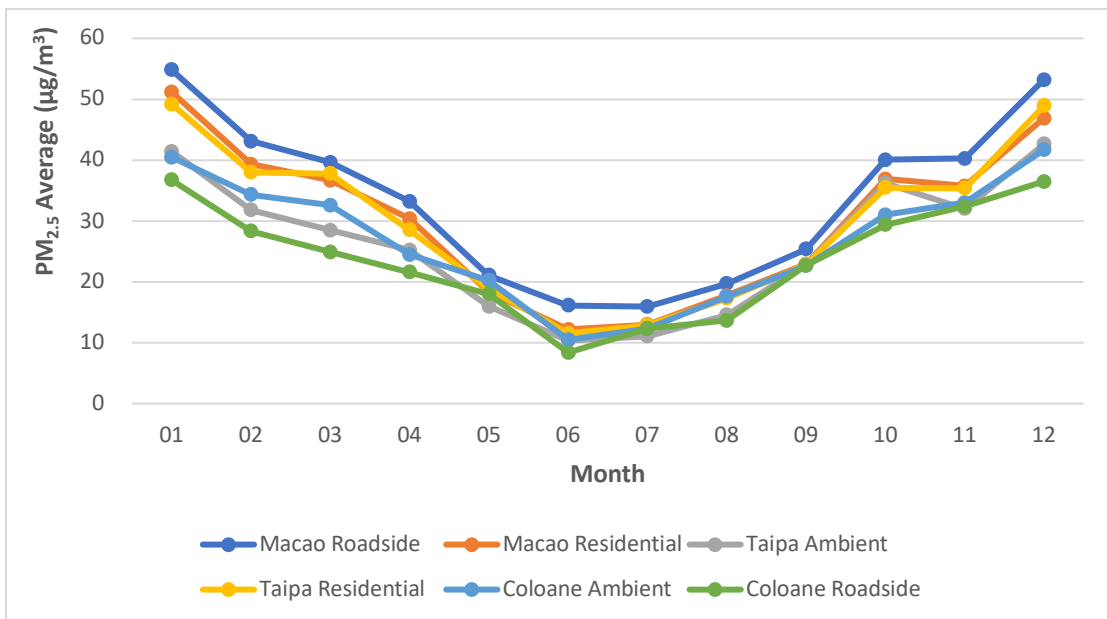
**Figure 3.9.** Yearly average levels of O<sub>3</sub> in the Macao air quality monitoring stations

(2013 to 2019).

Figure 3.10 and 3.11 present for the Macao air quality monitoring stations the average monthly levels of PM<sub>10</sub> and PM<sub>2.5</sub> concentrations, respectively, from 2013 to 2019. The figures show that the months from June to August recorded the lowest concentration of PM<sub>10</sub> and PM<sub>2.5</sub> in all stations. In contrast, the months from December to February recorded the highest concentration of these particles in all stations.



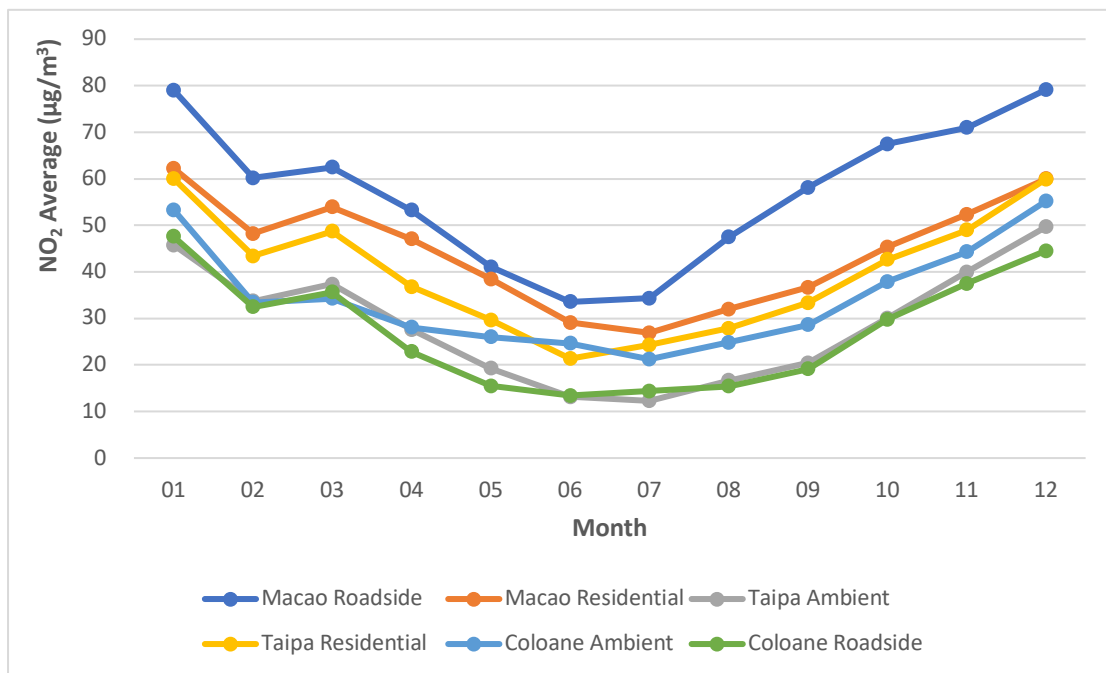
**Figure 3.10.** Monthly average levels of PM<sub>10</sub> in the Macao air quality monitoring stations (2013 to 2019).



**Figure 3.11.** Monthly average levels of PM<sub>2.5</sub> in the Macao air quality monitoring stations (2013 to 2019).

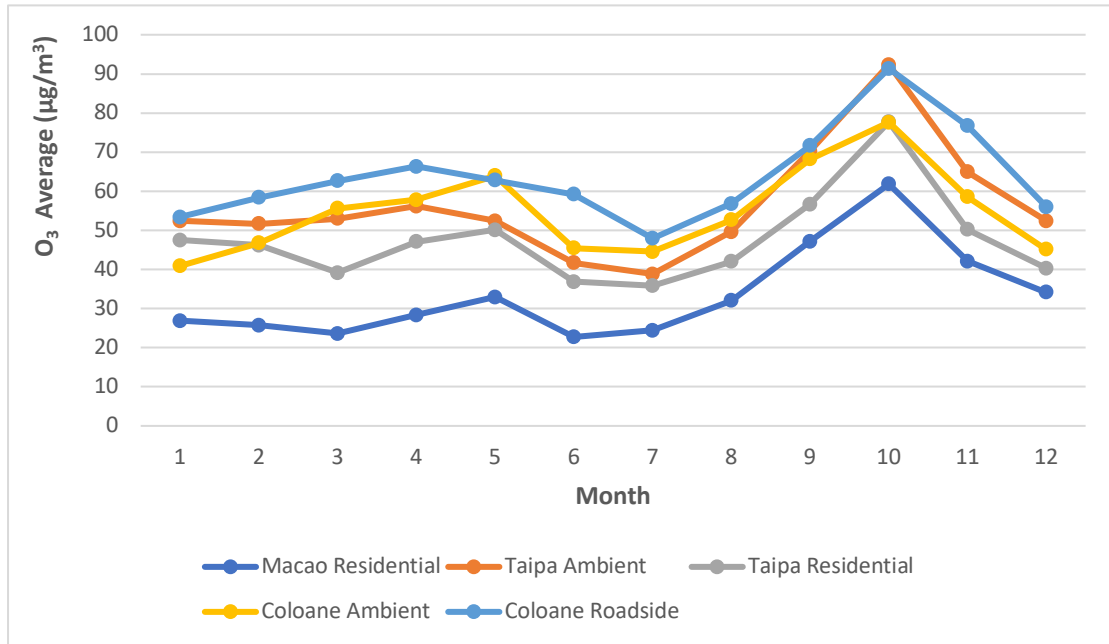
Figure 3.12 presents the monthly average levels of NO<sub>2</sub> concentration in the

Macao air quality monitoring stations from 2013 to 2019. The monthly average levels of NO<sub>2</sub> concentration were lowest during June and July and highest during December and January for all stations.



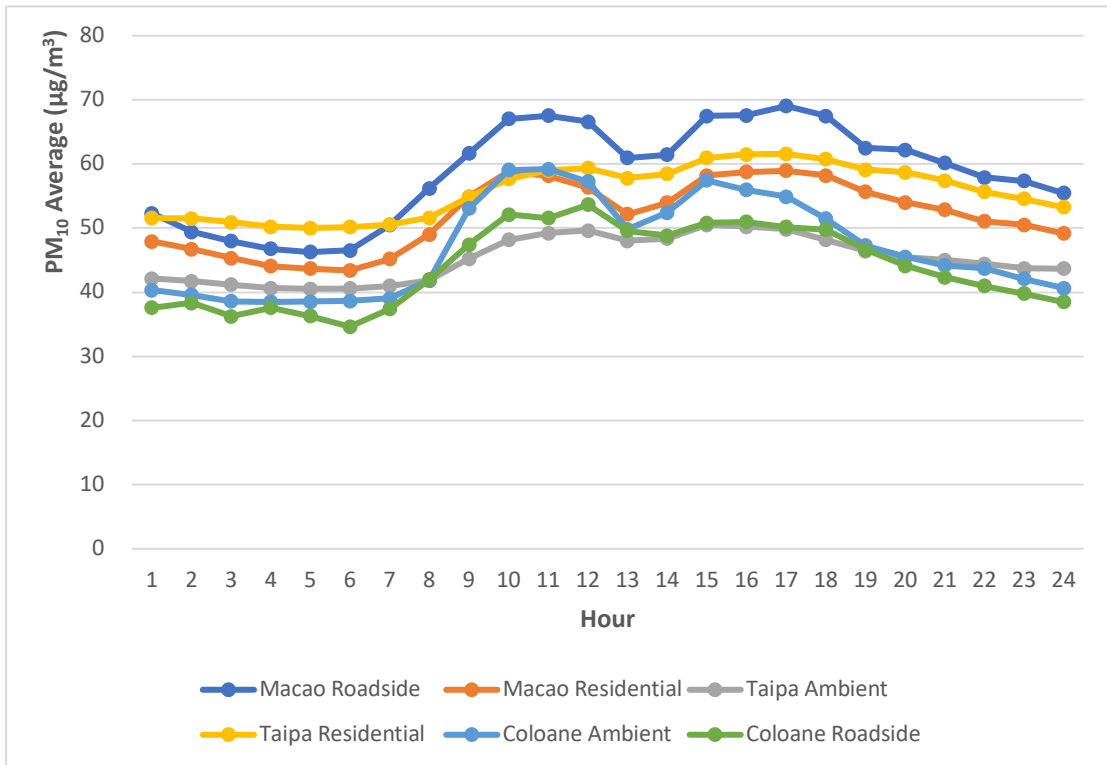
**Figure 3.12.** Monthly average levels of NO<sub>2</sub> in the Macao air quality monitoring stations (2013 to 2019).

Figure 3.13 presents the monthly average levels of O<sub>3</sub> concentration in the Macao air quality monitoring stations from 2013 to 2019. The levels of O<sub>3</sub> concentration were lowest between June and July, and highest in October in all stations.



**Figure 3.13.** Monthly average levels of O<sub>3</sub> in the Macao air quality monitoring stations (2013 to 2019).

Figure 3.14 and 3.15 presents for the Macao air quality monitoring stations the hourly average levels of PM<sub>10</sub> and PM<sub>2.5</sub> concentrations, respectively, from 2013 to 2019. Figure 3.14 shows that the hourly levels of PM<sub>10</sub> reached its highest concentration from 10:00h to 12:00h and 15:00h to 18:00h in all stations. Figure 3.15 shows that the hourly average levels of PM<sub>2.5</sub> concentration reached its highest concentration from 8:00h to 11:00h and 18:00h to 20:00h in all stations.



**Figure 3.14.** Hourly average levels of PM<sub>10</sub> in the Macao air quality monitoring stations (2013 to 2019).

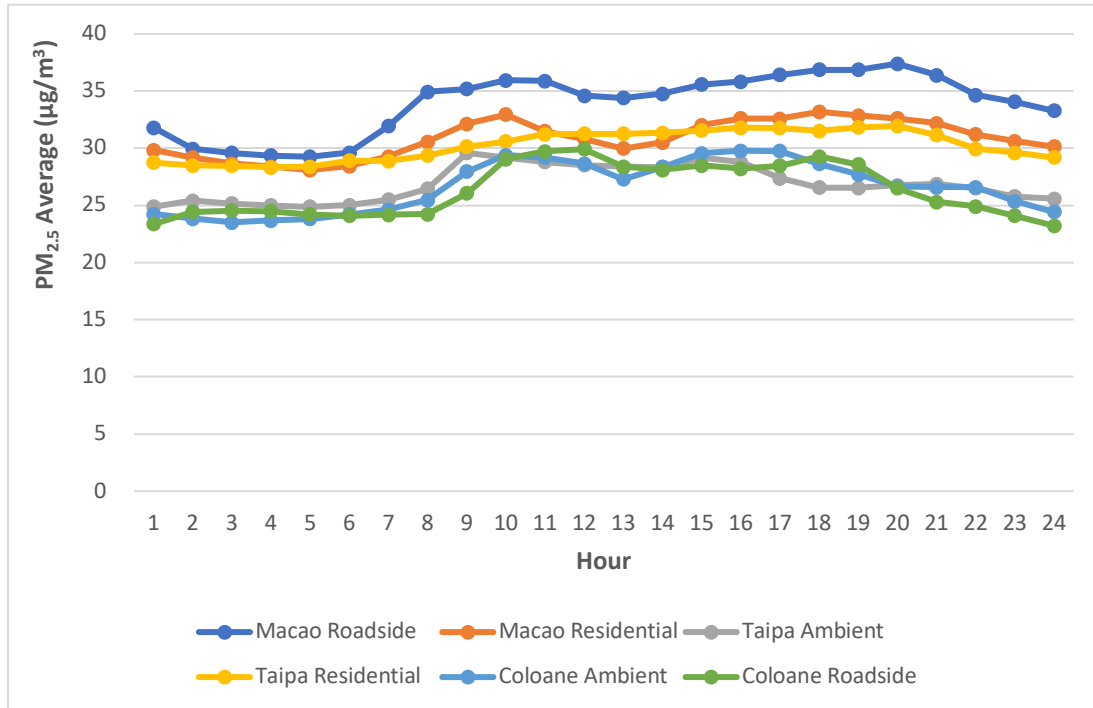


**Figure 3.15.** Hourly average levels of PM<sub>2.5</sub> in the Macao air quality monitoring stations (2013 to 2019).

Figure 3.16 presents the hourly average levels of NO<sub>2</sub> concentrations in the Macao air quality monitoring stations from 2013 to 2019. The figure shows that the hourly average levels of NO<sub>2</sub> concentration reached its highest concentration from 8:00h to 11:00h and 16:00h to 19:00h in all stations.

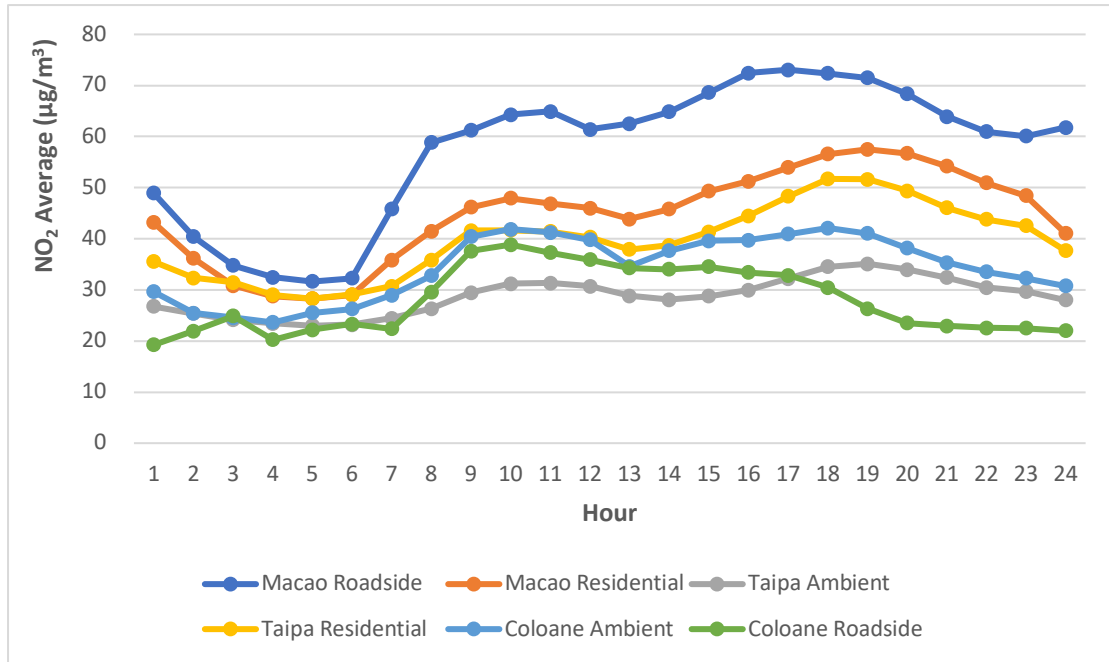


**Figure 3.16.** Hourly average levels of NO<sub>2</sub> in the Macao air quality monitoring stations (2013 to 2019).

Figure 3.17 presents the hourly average levels of O<sub>3</sub> concentrations in the Macao air quality monitoring station from 2013 to 2019. It shows that the hourly average levels of O<sub>3</sub> concentration increased rapidly after 12:00h and continued to reach its peak concentration at 16:00h. The temperature increase throughout the day creates more favorable condition for O<sub>3</sub> formation as ground-level O<sub>3</sub> is formed when nitrogen oxides (NO<sub>x</sub>) and volatile organic compounds (VOC), collectively called 'ozone precursors', react under photochemical processes.



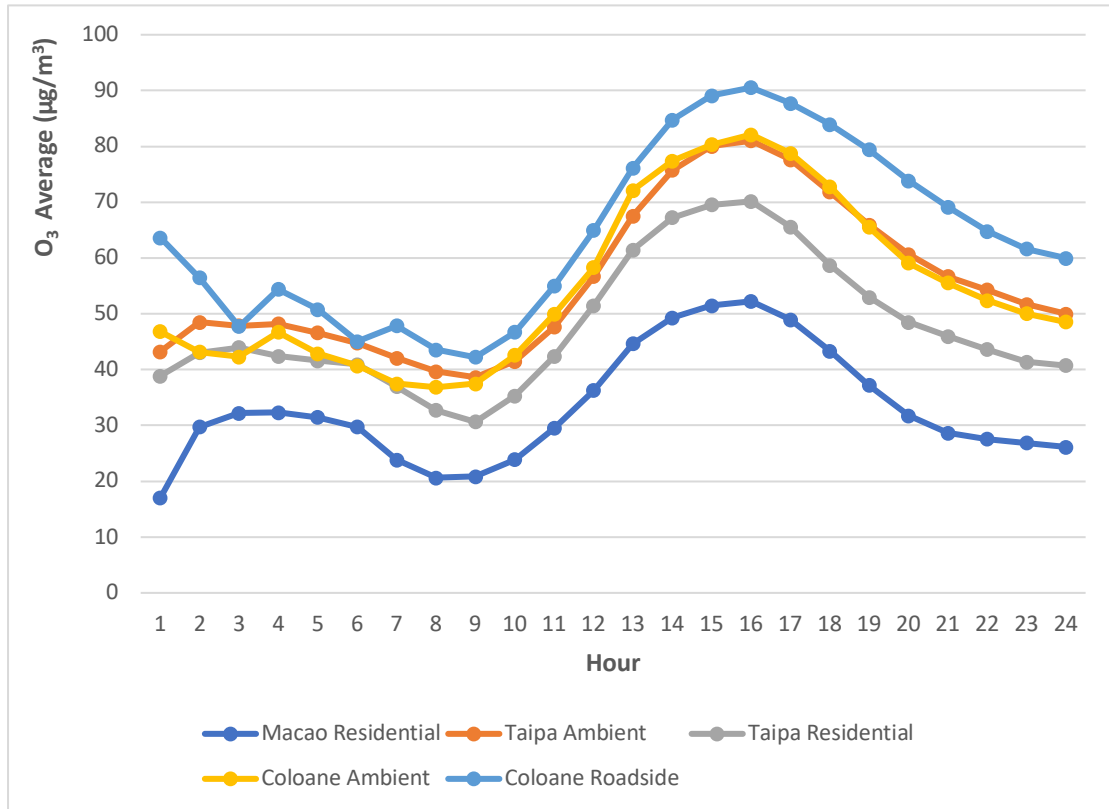


**Figure 3.17.** Hourly average levels of O<sub>3</sub> in the Macao air quality monitoring stations (2013 to 2019).

### 3.3 Meteorological Characteristics of Macao

The Greater Bay Area (GBA) of China consists of nine cities of Guangdong province, and the Special Administrative Region of Hong Kong and Macao. The synoptic situation of Macao and other cities of the GBA is closely related due to its geographic proximity. The GBA experiences a complex temporal and spatial climatic condition due to topographic variations, urban morphology, and land-water contrasts. Located along the southeast coast of Mainland China, Macao is surrounded by the sea

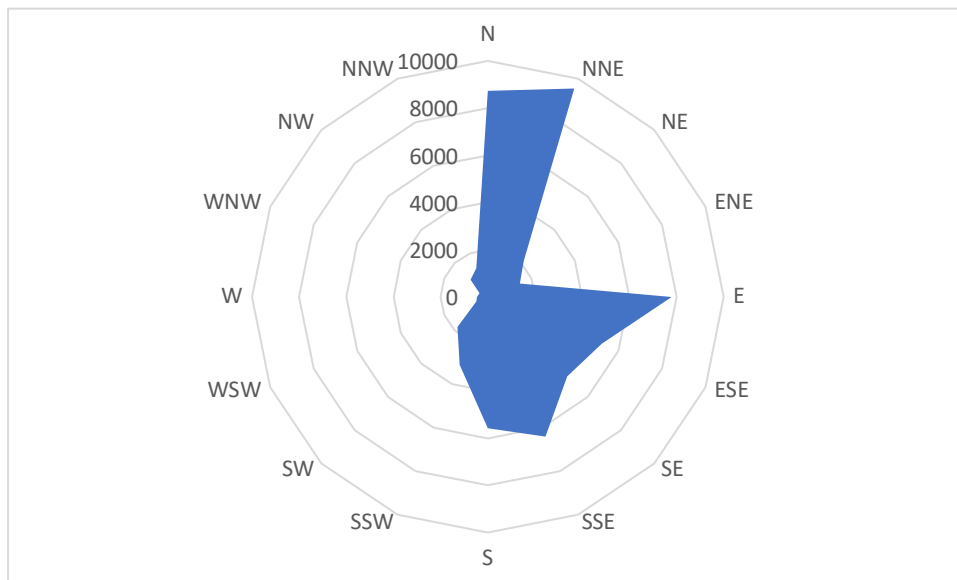
on three sides, with a subtropical oceanic monsoon climate that is characterized by high temperatures, high rates of evaporation, high levels of atmospheric moisture and abundant rainfall (SMG, 2014). In winter, Macao is influenced by the north monsoon, the climate is cold and dry with the predominant wind from the north quadrant. In summer, the northeast monsoon is replaced by the strong southwest monsoon with heavy rains. Spring and autumn are transition periods.

Recent studies (Tong et al., 2018) showed a rise of surface temperature and a drop of surface absolute humidity and wind speed at GBA due to the decline of vegetation and irrigated cropland. The landscape of GBA is characterized by a large flatland surrounded by the Nanling Mountains which can prevent air pollution from the central part of China reaching the GBA. Nevertheless, the northeast monsoon present during the winter may transport pollutants from northern and eastern China, along the coastline to the region of GBA (Tong, et al., 2018). PM levels are usually measured higher during the winter season, from December to February, due to the northern wind, bringing the air pollutants to the region, lowering mixing height, and fewer amount and lower frequency of rainfall. During summer season, from June to August, PM levels are usually measured lower due to the southern winds from the China sea, higher mixing

height, higher frequency and amount of rainfall, which allow for more favorable air pollution dispersion and deposition conditions (Lopes et al., 2016).

### 3.3.1 Key Meteorological Variables

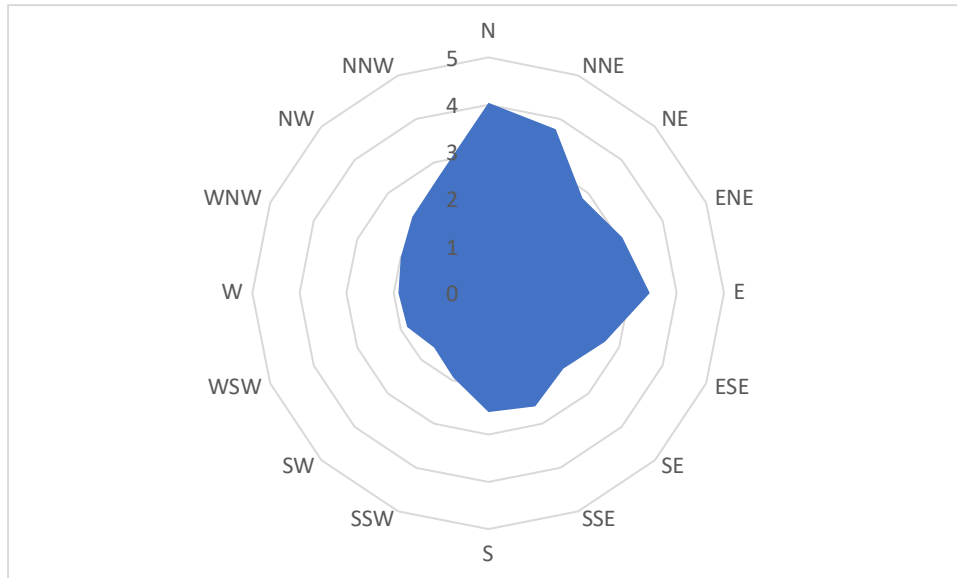
Figure 3.18 presents the wind rose of Macao from 2013 to 2019. It shows that the primary wind direction of Macao is from north (N) and north-northeast (NNE). This shows that the air pollutants such as  $PM_{10}$  and  $PM_{2.5}$  maybe transported by the wind from nearby regions, in particular of Guangdong Province, into the region of Macao.



**Figure 3.18.** Wind rose of Macao from 2013 to 2019 (hourly counts).

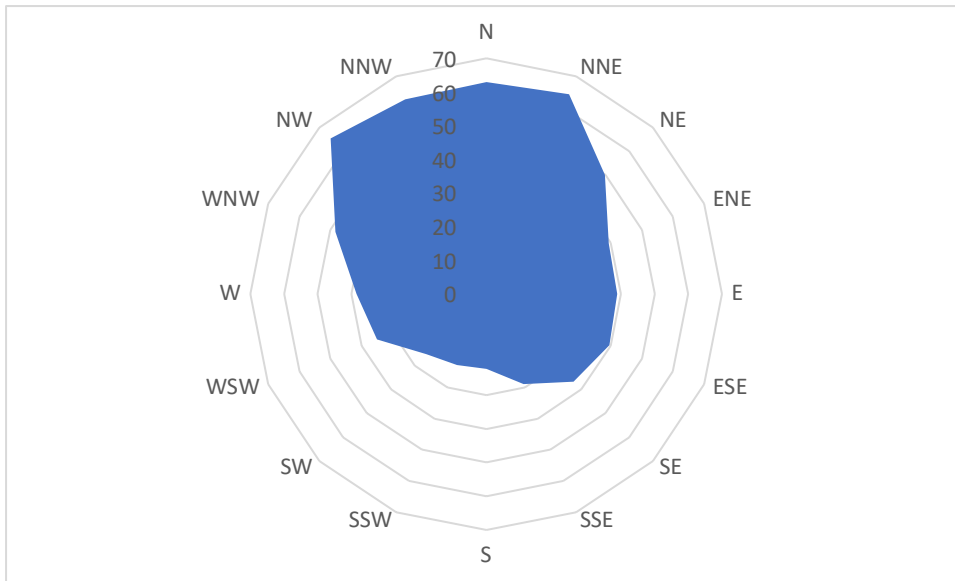
Figure 3.19 presents the wind speed of Macao from 2013 to 2019. The highest level of wind speed come from the north (N) and north-northeast (NNE), with an

average wind speed of 4 m/s. Being predominant from the northern quadrant, the high levels of wind speed may transport air pollutants such as  $PM_{10}$  and  $PM_{2.5}$  from nearby Guangdong Province into the Macao region.



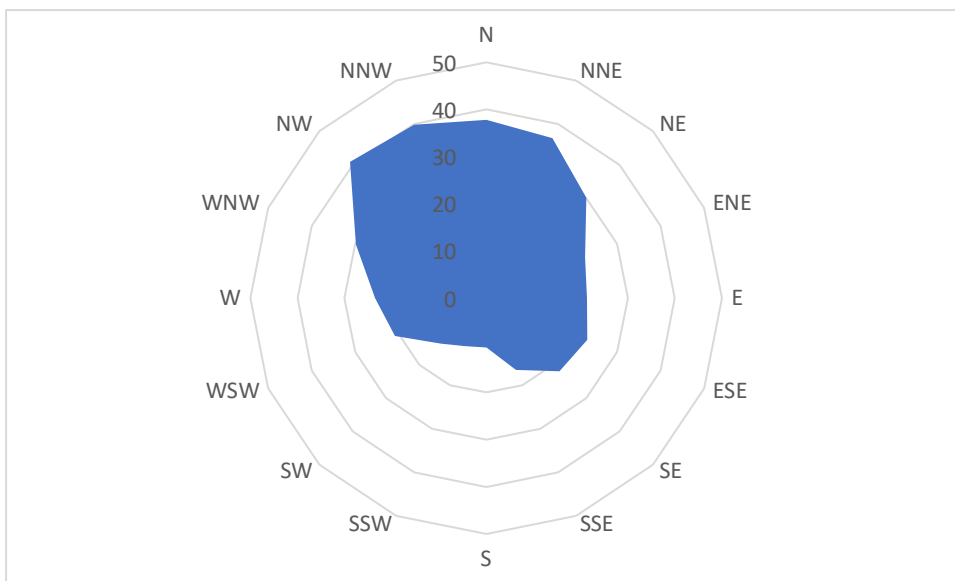
**Figure 3.19.** Wind speed (m/s) of Macao from 2013 to 2019.

Figure 3.20 presents the pollution rose of  $PM_{10}$  from 2013 to 2019. The figure shows the highest level of  $PM_{10}$  concentration to be coming from north-northeast (NNE) and northwest (NW), with an average concentration of  $64 \mu\text{g}/\text{m}^3$  and  $65 \mu\text{g}/\text{m}^3$ , respectively.



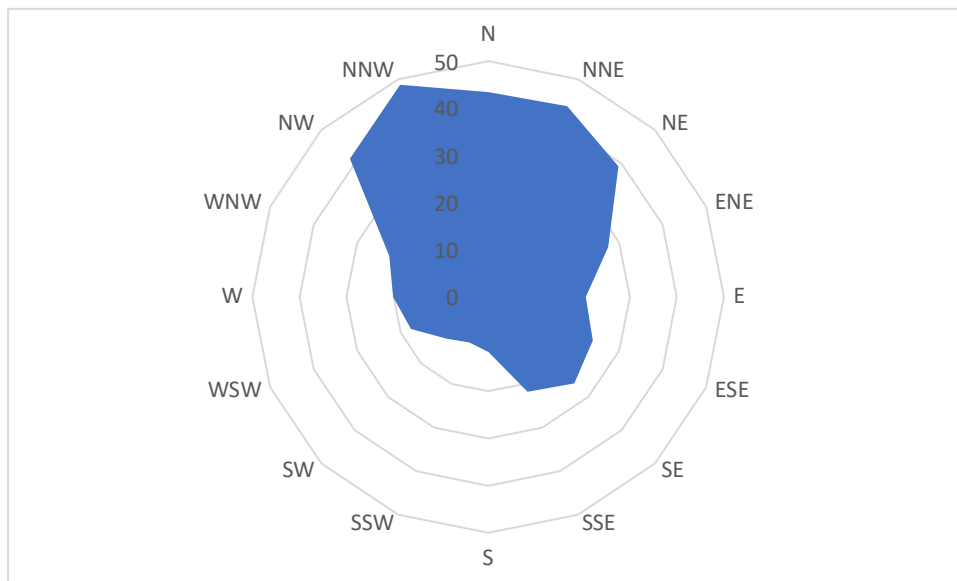
**Figure 3.20.** Pollution rose of PM<sub>10</sub> (µg/m<sup>3</sup>) from 2013 to 2019.

Figure 3.21 presents the pollution rose of PM<sub>2.5</sub> from 2013 to 2019. It shows the highest level of PM<sub>2.5</sub> concentration to be coming from northwest (NW) and north-northwest (NNW), with an average concentration of 41 µg/m<sup>3</sup> and 40 µg/m<sup>3</sup>, respectively.



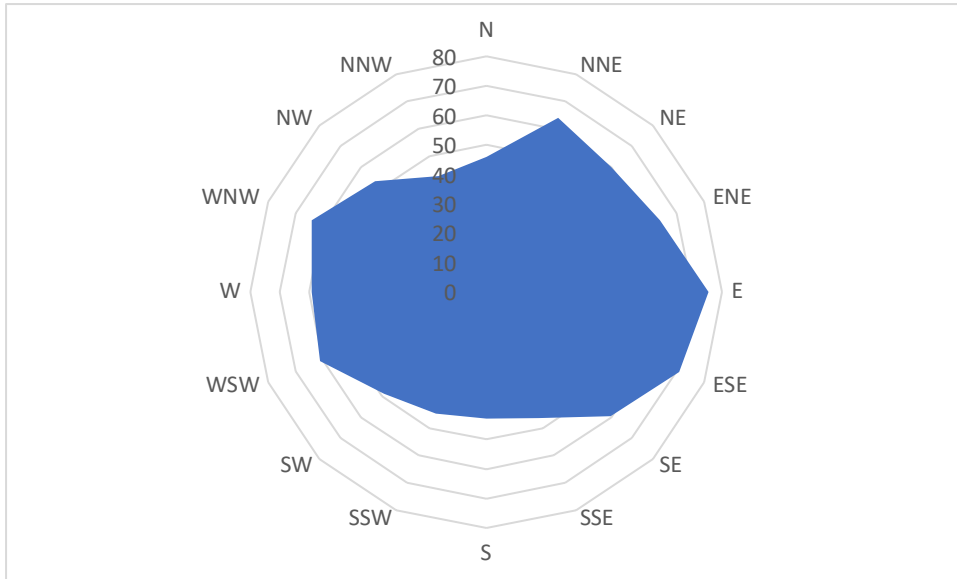
**Figure 3.21.** Pollution rose of PM<sub>2.5</sub> (µg/m<sup>3</sup>) from 2013 to 2019.

Figure 3.22 presents the pollution rose of NO<sub>2</sub> from 2013 to 2019. It shows the highest level of NO<sub>2</sub> concentration to be coming from north-northeast (NNE) and north-northwest (NNW), with an average concentration of 44 µg/m<sup>3</sup> and 49 µg/m<sup>3</sup>, respectively.



**Figure 3.22.** Pollution rose of NO<sub>2</sub> (µg/m<sup>3</sup>) from 2013 to 2019.

Figure 3.23 presents the pollution rose of O<sub>3</sub> from 2013 to 2019. It shows the highest level of O<sub>3</sub> concentration to be coming from east (E) and east-southeast (ESE), with an average concentration of 75 µg/m<sup>3</sup> and 71 µg/m<sup>3</sup>, respectively.



**Figure 3.23.** Pollution rose of O<sub>3</sub> (µg/m<sup>3</sup>) from 2013 to 2019.

Figure 3.24 presents the yearly average temperature of Macao from 2013 to 2019.

The yearly average temperature of Macao has increased by over 1 °C in 2019, in comparison to the yearly average temperature of 2013.

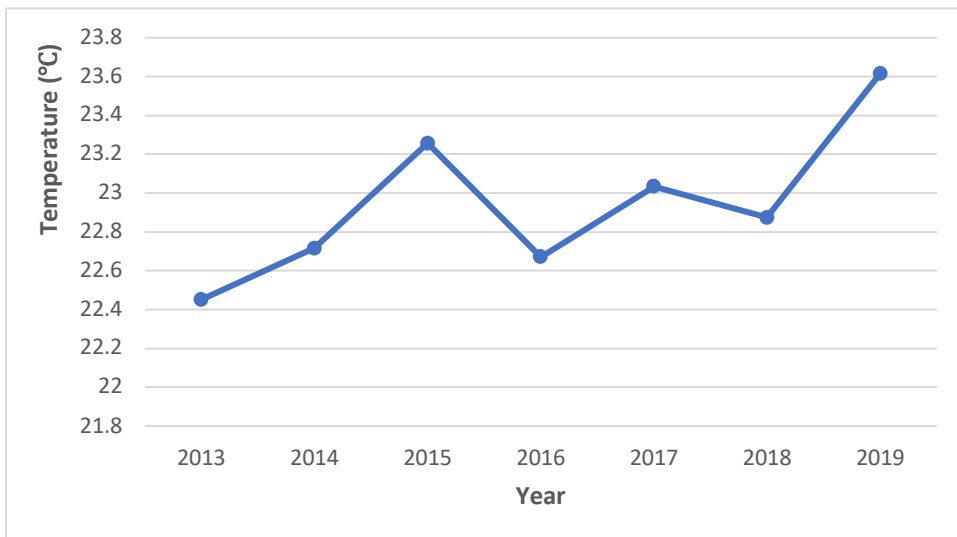


**Figure 3.24.** Yearly average temperature in Macao from 2013 to 2019.

Figure 3.25 presents the yearly total precipitation of Macao from 2013 to 2019.

The yearly total precipitation of Macao has decreased by over 300 mm in 2019, in comparison to the yearly total precipitation of 2013.

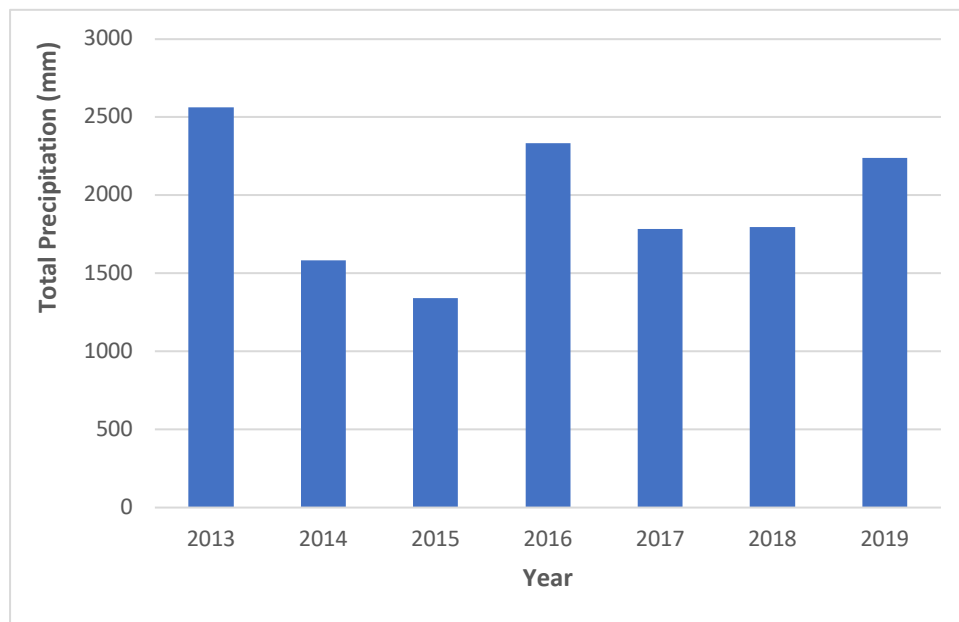


**Figure 3.25.** Yearly total precipitation in Macao from 2013 to 2019.

Figure 3.26 presents the monthly average temperature of Macao from 2013 to 2019. The hottest months in Macao were from June to September and the coldest from December to February. The high temperature between June and August creates a favorable condition for the formation of O<sub>3</sub> in Macao.



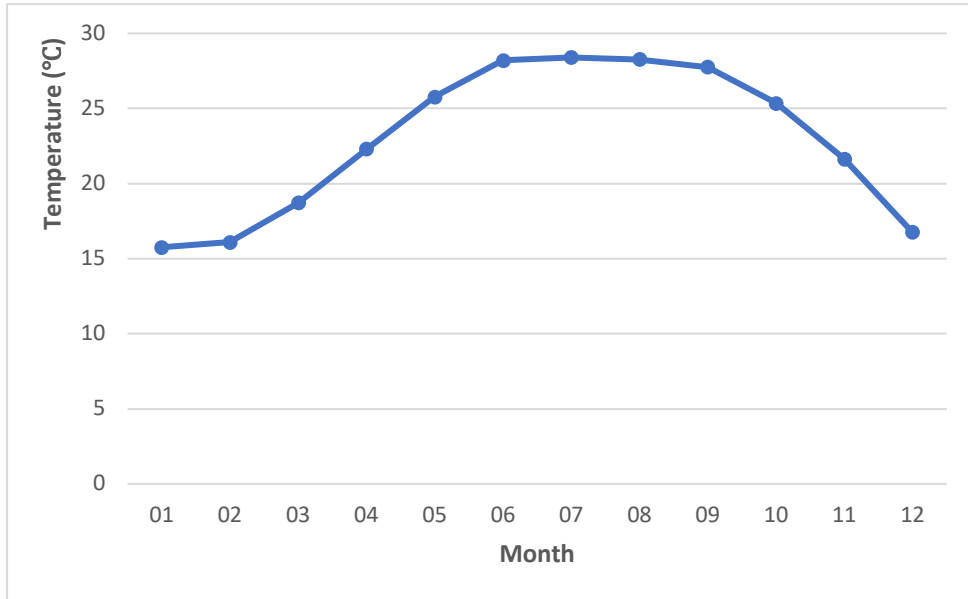


**Figure 3.26.** Monthly average temperature in Macao from 2013 to 2019.

Figure 3.27 presents the monthly average wind speed in Macao from 2013 to 2019. The wind speed was lowest during June to August and highest during October to December.

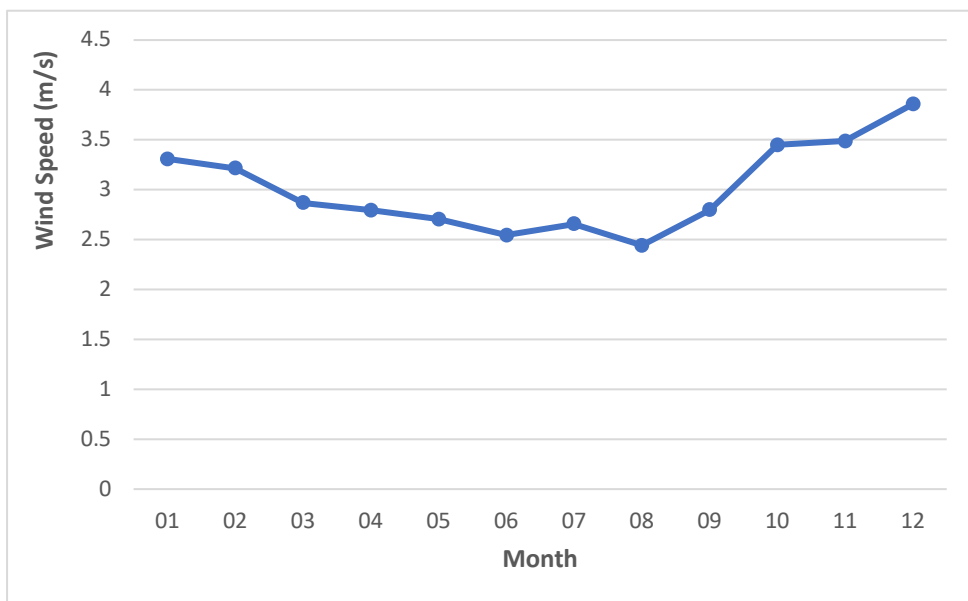


**Figure 3.27.** Monthly average wind speed in Macao from 2013 to 2019.

Figure 3.28 presents the monthly total precipitation in Macao from 2013 to 2019.

The monthly total precipitation in Macao was highest from May to August and lowest from November to February. The low precipitation levels between November and February may favor high concentrations of particulate matter (PM<sub>10</sub> and PM<sub>2.5</sub>) and NO<sub>2</sub> in Macao.

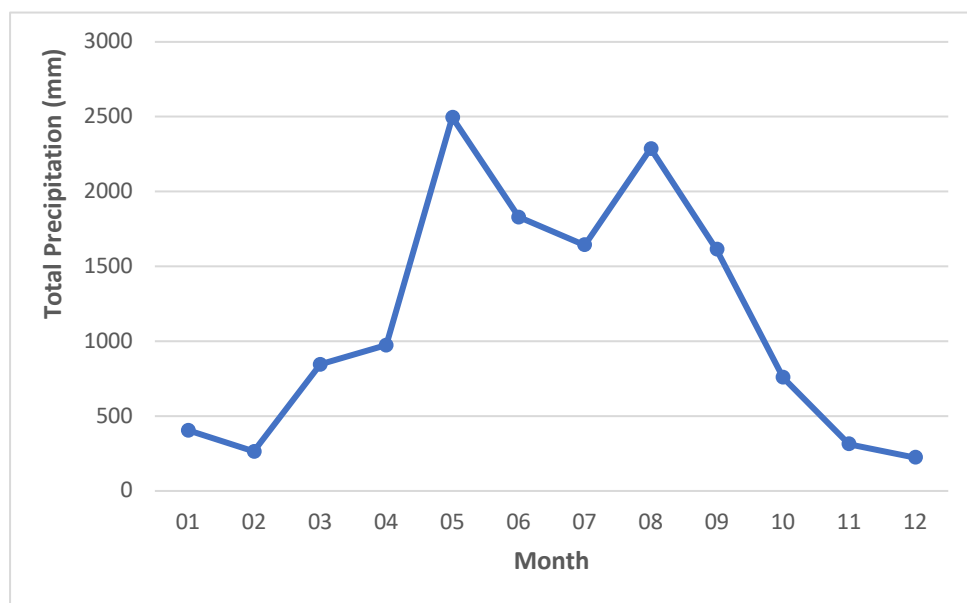


**Figure 3.28.** Monthly total precipitation in Macao from 2013 to 2019.

Figure 3.29 presents the hourly average temperature in Macao from 2013 to 2019. The highest temperature occurred from 12:00h to 15:00h and the lowest from 4:00h to 7:00h. The highest temperature is usually reached after noon, while the lowest temperature is usually reached before sunrise in Macao.

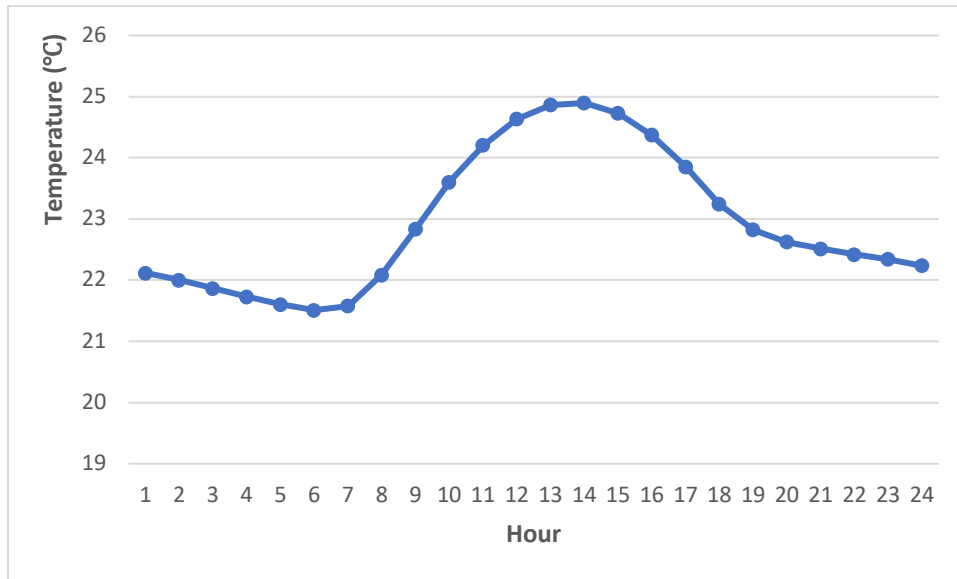


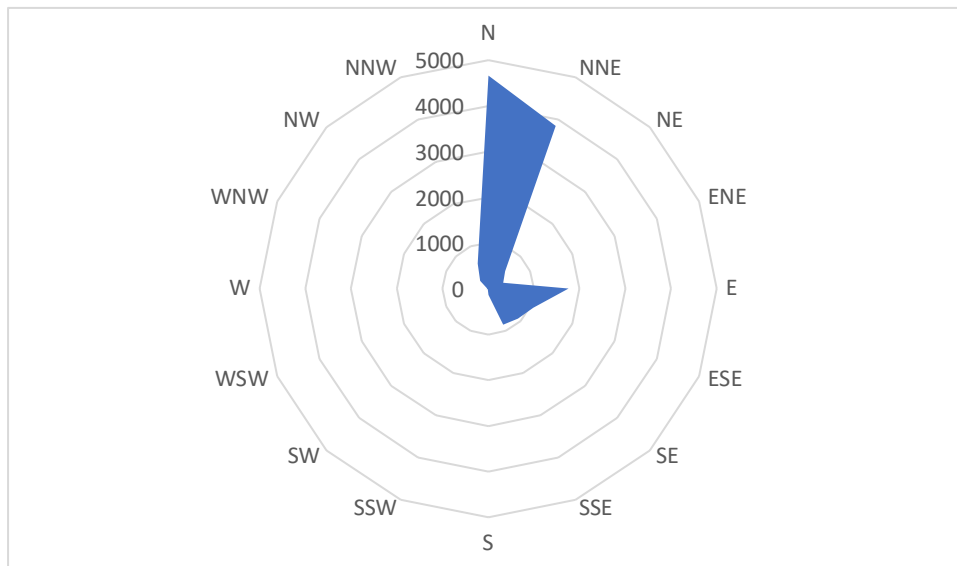
**Figure 3.29.** Hourly average temperature in Macao from 2013 to 2019.

### 3.3.2 Meteorological Seasonal Variation in Macao

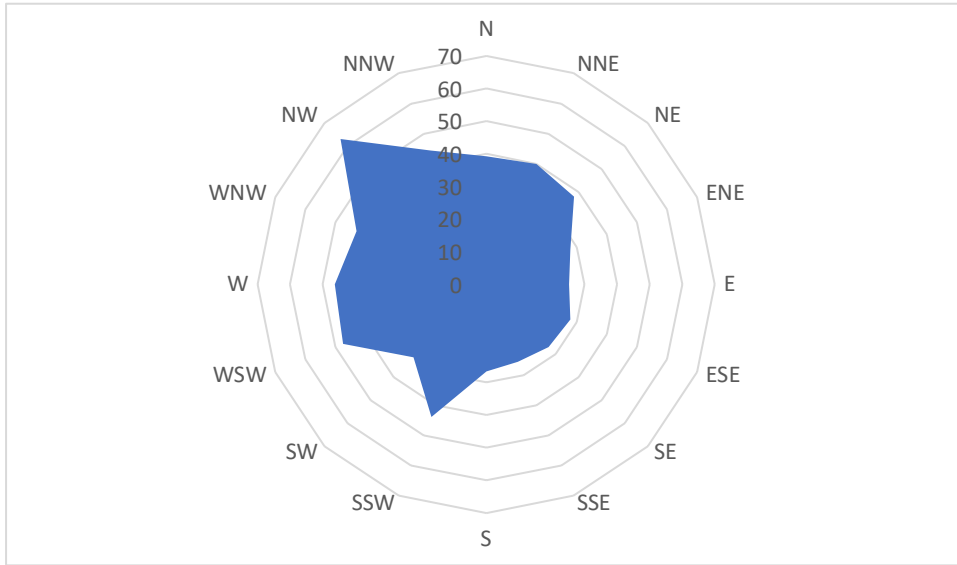
The Intertropical Convergence Zone (ITCZ) is the region that circles the Earth, near the equator, where the trade winds of the Northern and Southern Hemispheres come together. It is a low-pressure belt and migrates with the changing position of the thermal equator. The movement of the thermal equator shifts the belts of planetary winds and pressure systems to the north and to the south annually, which also affects the climate of Macao.

Figure 3.30 shows the wind rose of Macao during the winter season from 2013 to 2019. The wind direction during the winter season (from December to February) is predominantly from the north (N) and north-northeast (NNE). Figure 3.31 shows the pollution rose of PM<sub>2.5</sub> during the winter season from 2013 to 2019. Levels of PM<sub>2.5</sub>

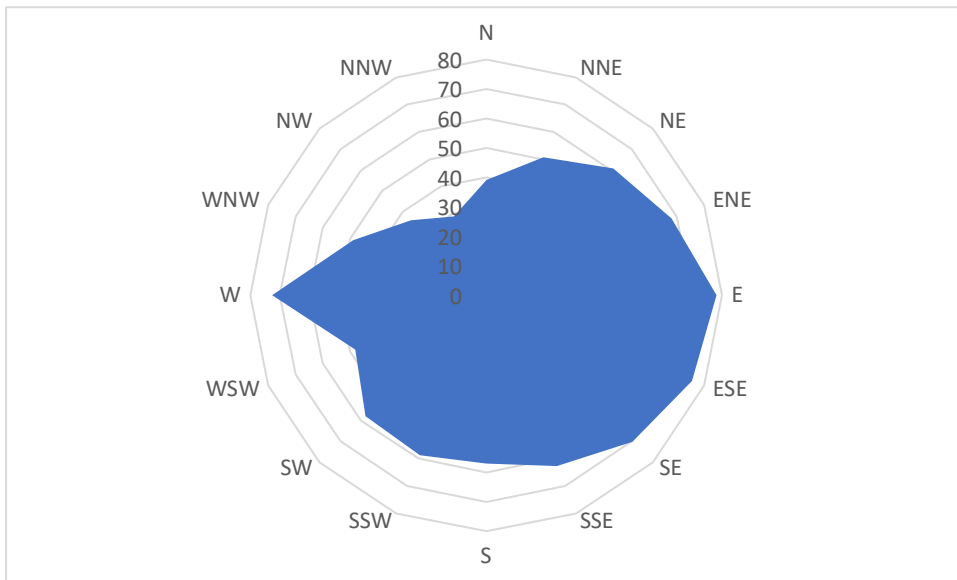
concentrations reached its peak when the wind direction is coming from northwest (NW) and north-northwest (NNW). Figure 3.32 shows the pollution rose of O<sub>3</sub> during the winter season from 2013 to 2019. The levels of O<sub>3</sub> concentration reached its peak when the wind direction is coming from the east (E) and east-southeast (ESE). Figure 3.33 shows the winter meteorological charts in Macao, which shows the winds are coming primarily from the north (N) during the winter season.



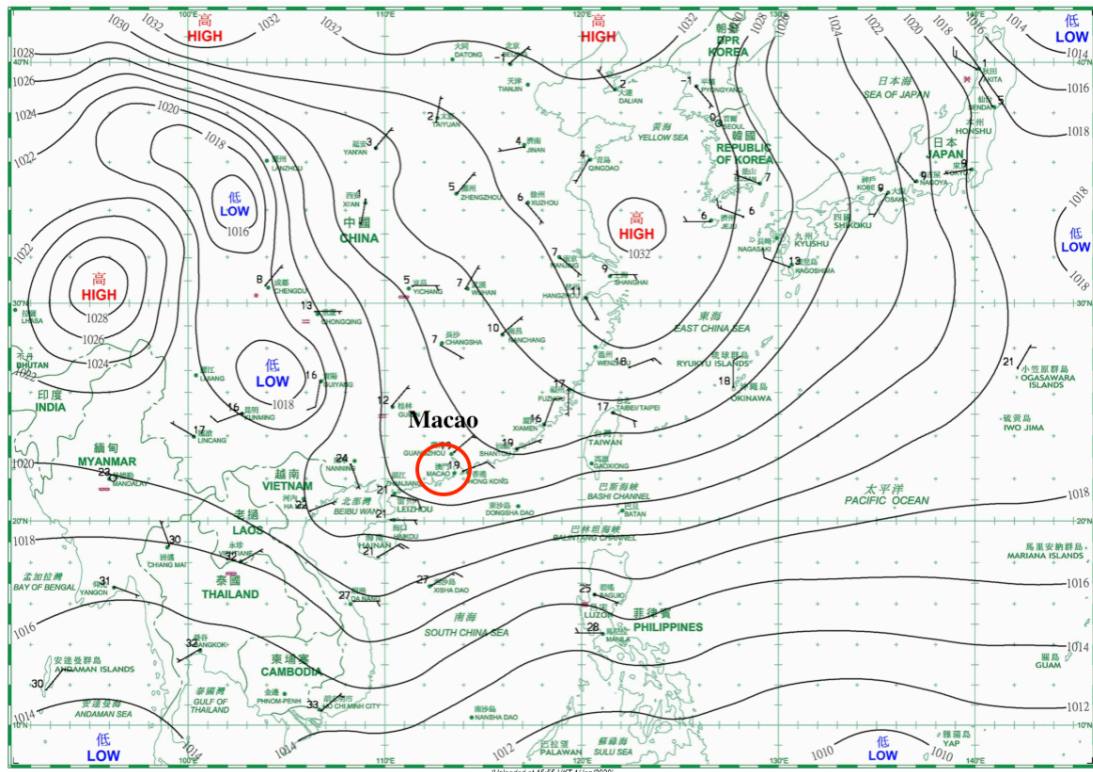
**Figure 3.30.** Wind rose of Macao in winter season from 2013 to 2019 (hourly counts).



**Figure 3.31.** Pollution rose of PM<sub>2.5</sub> (µg/m<sup>3</sup>) in winter season from 2013 to 2019.



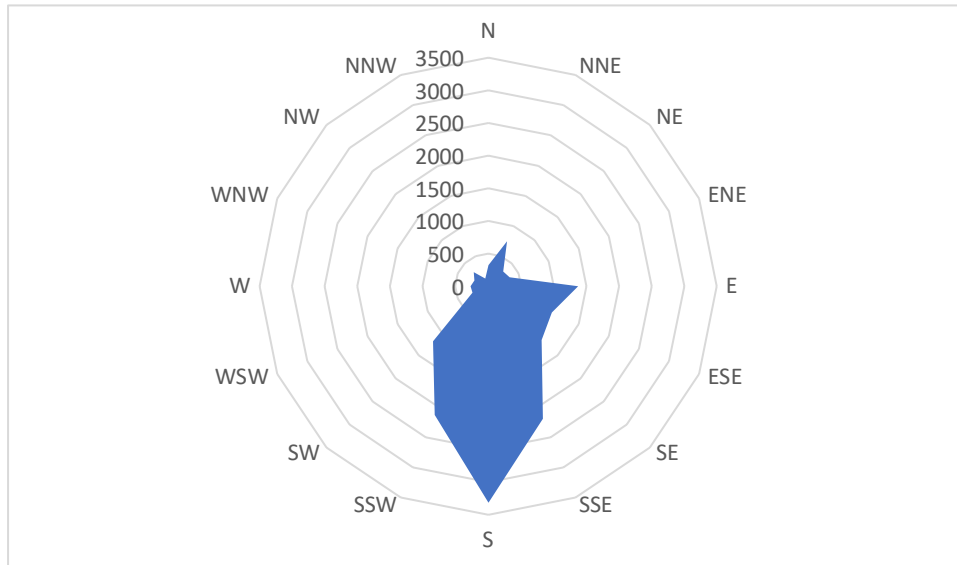
**Figure 3.32.** Pollution rose of O<sub>3</sub> (µg/m<sup>3</sup>) in winter season from 2013 to 2019.



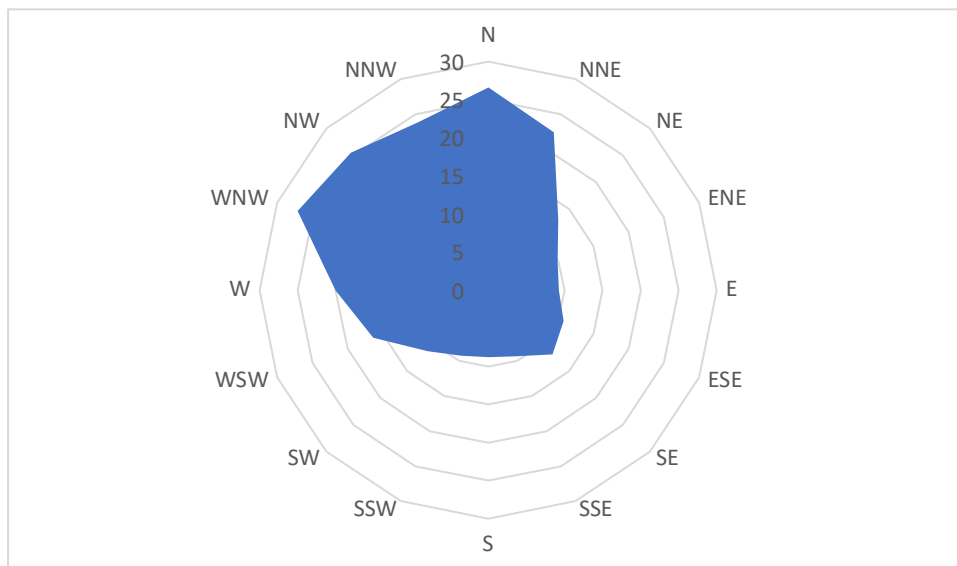
**Figure 3.33.** Typical winter meteorological surface chart of Macao (HKO, 2020).

Figure 3.34 shows the wind rose of Macao during the summer season (from June to August) from 2013 to 2019. The wind direction during the summer season is predominantly from the south (S) and south-southeast (SSE). Figure 3.35 shows the pollution rose of PM<sub>2.5</sub> during the summer season from 2013 to 2019. The levels of PM<sub>2.5</sub> concentrations reached its peak when the wind direction was coming from north (N) and west-northwest (WNW). Figure 3.36 shows the pollution rose of O<sub>3</sub> during the summer season from 2013 to 2019. The levels of O<sub>3</sub> concentration reached its peak when the wind direction was coming from the northwest (NW) and north-northeast (NNE). Figure 3.37 shows the summer meteorological charts in Macao,

with winds coming primarily from the south (S).



**Figure 3.34.** Wind rose of Macao in summer season from 2013 to 2019 (hourly counts).



**Figure 3.35.** Pollution rose of PM<sub>2.5</sub> (µg/m<sup>3</sup>) in summer season from 2013 to 2019.

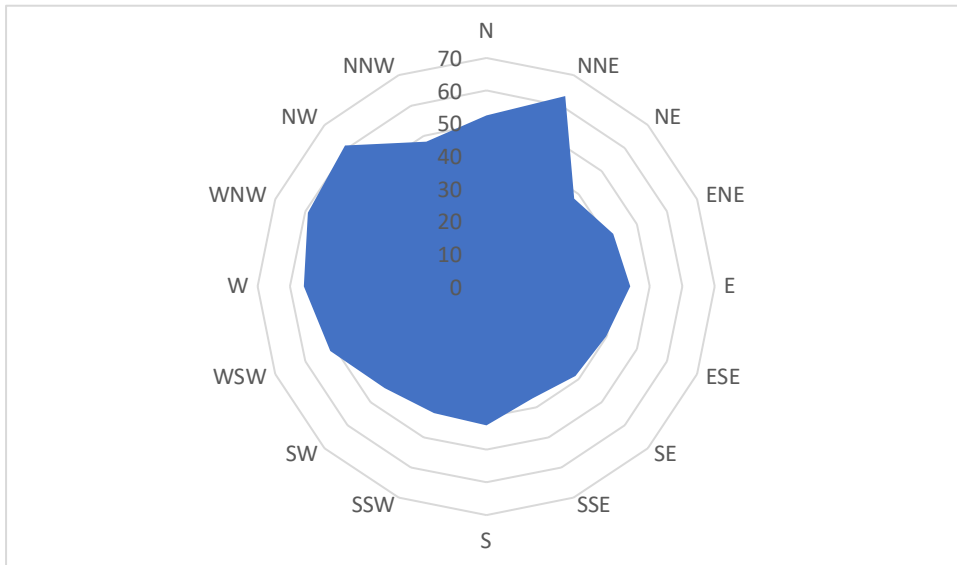


Figure 3.36. Pollution rose of O<sub>3</sub> (µg/m<sup>3</sup>) in summer season from 2013 to 2019.

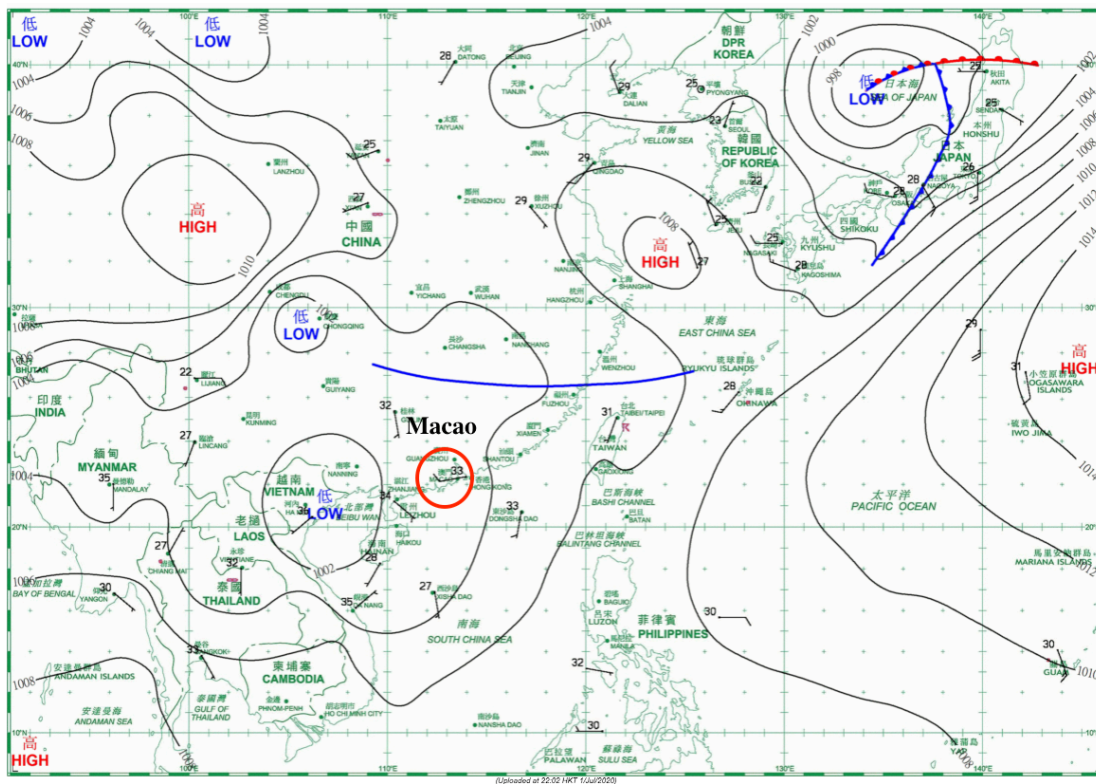


Figure 3.37. Typical summer meteorological surface chart in Macao (HKO, 2020).



### **3.4 Development of Air Quality Forecast Using Statistical Methods**

It is important to develop a reliable prediction methodology for the concentration of PM<sub>10</sub>, PM<sub>2.5</sub>, NO<sub>2</sub> and O<sub>3</sub>, which can provide alert for health hazards in advance.

Macao has been focusing on its economic development in the past decades and seriously overlooked the air pollution problem. There are no available forecast modeling tools to predict the air quality for Macao, which is necessary for the region to keep up with the international standards and the neighboring regions. An emission inventory for the roadside was developed with a high spatial-temporal resolution in Macao. However, due to the limited spatial and temporal scope of this inventory and its operational availability, it would be impossible to develop a deterministic model to predict air quality concentrations. Therefore, it is necessary to create a statistical air quality forecast model for the daily concentration of air pollutants in Macao, based on the historical air quality and meteorological data. For this, the sources of air pollution need to be identified to better understand the air quality trend in Macao. It is equally very important to explore the relationships between the air quality and meteorological parameters in Macao to develop a statistical forecast model for the next day levels of PM<sub>10</sub>, PM<sub>2.5</sub>, NO<sub>2</sub>, and O<sub>3</sub> concentration.

The statistical methods selected for this work were both multiple linear regression analysis (MLR) and classification and regression tree (CART). Those can be a useful and straightforward tool in air quality studies (Cassmassi, 1997; Clapp & Jenkin, 2001; Choi et al., 2013; Martinez et al., 2018). One of the advantages of the CART analysis is its effectiveness in explaining the variations in pollutant levels solely by a combination of meteorological conditions as regression trees can identify specific meteorological conditions that lead to low or elevated pollutant concentrations (Choi et al., 2013). The basic concept of the CART approach is to establish a hierarchy of binary decisions, each of which splits distribution/variation of a target variable into two mutually exclusive branches (groups) based on the explanatory variable/value showing the largest reduction in variations in target variable after the split (Choi et al., 2013).

Following precedent experiences (Cassmassi, 1997; US EPA, 2003; Durão et al., 2016; Oduro et al., 2016) the statistical models were initially created using MLR analysis. As an approach to obtain improved results, mainly regarding a better prediction of high pollutant levels, the CART analysis was chosen. Statistical models, based on MLR and CART, were applied to forecast the daily average concentration of NO<sub>2</sub>, PM<sub>10</sub>, PM<sub>2.5</sub>, and the maximum average hourly concentration of O<sub>3</sub> levels for the

next day, for each station of the air quality monitoring network in Macao.

The air quality and meteorological variables that were considered to build all of the air quality statistical models were obtained from Macao Meteorological and Geophysical Bureau (SMG). The air quality data was gathered from the air quality monitoring network, namely for: Macao Roadside, Macao Residential, Taipa Ambient, Taipa Residential, and Coloane Ambient stations, which have a suitable historic dataset of surface air quality measurements for the levels of NO<sub>2</sub>, PM<sub>10</sub>, PM<sub>2.5</sub>, and O<sub>3</sub> concentrations. These background stations (residential and ambient) can capture the regional contribution of PM<sub>10</sub> and PM<sub>2.5</sub>. There is a higher population and traffic density in the vicinity of the Macao Roadside and Macao Residential stations, which are located in the main peninsula, in comparison to Taipa Ambient, Taipa Residential, and Coloane Ambient stations, which are located on the outlying islands.

Meteorological data was obtained from surface observations at SMG's Taipa Grande Meteorological Station and consisted of hourly records from automatic weather stations, such as temperature, relative humidity, precipitation, average wind speed, and dew point temperature. Since the SMG does not release weather balloons to collect data, information for the upper air layers is not available in Macao.

Therefore, it is essential to identify the closest neighbor of Macao and obtain the upper air sounding data from this nearby station. Hong Kong Kings Park (station number 45004) was identified as the ideal station to provide data such as geopotential heights, thickness, stability, temperature, relative humidity, and dew point temperature at various altitudes.

The air quality variables considered included the levels of  $\text{NO}_2$ ,  $\text{PM}_{10}$ ,  $\text{PM}_{2.5}$ , and  $\text{O}_3_{\text{MAX}}$  concentration from 00:00 to 23:00 of the previous day, two days and three days ago, and from 16:00 of the previous day to 15:00 of today. The meteorological variables being considered included the upper-air observations from King's Park location, Hong Kong Observatory, surface observations and other variables from the monitoring network of Macao Meteorological and Geophysical Bureau (SMG), as previously mentioned.

Other variables were added to the analysis, as the flag for week/weekend day and the daily sunlight period duration. Table 3-2 presents all the variables considered as predictors in the MLR and CART forecast models.

**Table 3-2.** Variables considered as predictors in the multiple linear regression (MLR) and classification and regression tree (CART) models in all of the air quality forecast models.

<b>Variable Type</b>	<b>Variable Name</b>	<b>Variable Description (Units)/ Observations</b>
<b>Air quality variables</b>	NO <sub>2</sub> , PM <sub>10</sub> , PM <sub>2.5</sub>	Average hourly concentration values  (µg/m <sup>3</sup> )
	O <sub>3</sub> MAX	Maximum hourly concentration values  (µg/m <sup>3</sup> )
	16D#, 23D#	23D#: 24-h concentration averaging period  between 00h and 23h  16D#: 24-h concentration averaging period  between 16h of D1 and 15h of D0  e.g.: PM10_16D1, O3_MAX_23D1.
	D0, D1, D2, D3	D0: Forecast Day; D1: Previous Day  (Forecast Day-1); D2: Forecast Day-2; and  D3: Forecast Day-3.

<b>Meteorological variables</b>	Upper-air obs.*	H1000, H850, H700, H500	Geopotential Height at 1000 hPa, 850 hPa, 700 hPa, and 500 hPa (m)/Indicator of synoptic-scale weather pattern.
		TAR925, TAR850, TAR700	Air Temperature at 925 hPa, 850 hPa, and 700 hPa (°C)/Measure of strength and height of the subsidence inversion.
		HR925, HR850, HR700	Relative Humidity at 925 hPa, 850 hPa, and 700 hPa (%).

		TD925, TD850, TD700	Dew Point Temperature at 925 hPa, 850 hPa, and 700 hPa (°C).
		THI850, THI700, THI500	Thickness at 850 hPa, 700 hPa, and 500 hPa (m)/Related to the mean temperature in the layer.
		STB925, STB850, STB700	Stability at 925 hPa, 850 hPa, and 700 hPa (°C)/Indicator of atmospheric stability.

<b>Surface observations</b>	T_AIR_MX, T_AIR_MD, T_AIR_MN	Maximum, Average, and Minimum Air Temperature (°C)
	HRMX, HRMD, HRMN	Maximum, Average, and Minimum Relative Humidity (%)
	TD_MD	Average dew point temperature (ground level) (°C)
	RRTT	Precipitation (mm)/Associated with atmospheric washout
	VMED	Average wind speed (m/s)/Related to dispersion
<b>Other variables</b>	DD	Duration of the day: number of hours of sun per day (h)
	FF	Week-day indicator (flag): weekday = 0, weekend = 1

\* Meteorological variables: Daily sounding at 12H (GMT+8) at King's Park

Meteorological Station—Hong Kong Observatory.



The next step was to assess data efficiency levels, for each parameter, through the years, in order to reject lower annual efficiencies. The statistical models for Ká-Hó Roadside station were not feasible, due to the lack of sufficient air quality data. A complimentary analysis was conducted to observe air pollution trends, monthly, weekly and hourly patterns, and pollution roses. A preliminary exploratory data analysis, looking at basic statistics, like average, mode, histogram, distribution type, correlation between different variables, and principal component analysis, was performed to identify variables with similar behaviors. This strategy enabled to decide on the following steps to obtain the best model outcome.

A significance level of 0.05 was used in the linear MR analysis. Some variables initially selected were rejected from the forecast models due to collinearity. The final objective was to obtain prediction models with the lowest possible number of variables but with the maximum explained variance as translated by the  $R^2$ . The higher the number of variables used by the model, the higher the risk of compromising the operational forecast, due to lack of information/missing data in case one or more variables are not accessible.

The statistical model was built using IBM SPSS Statistics version 26 with MLR

(stepwise) and CART methods (Lei et al., 2019; Neto et al., 2009). SPSS is a statistical software that is applied to solve research problems through hypothesis testing and predictive analysis.

Model performance indicators were determined recurring to the following parameters: coefficient of determination ( $R^2$ ) (1), root mean square error (RMSE) (2), mean absolute error (MAE) (3), and systematic error (BIAS) (4).

$$R^2 = \frac{[\sum_{i=1}^n (f_i - \bar{f}) - (o_i - \bar{o})]^2}{[\sum_{i=1}^n (f_i - \bar{f})^2] [\sum_{i=1}^n (o_i - \bar{o})^2]} \quad (1)$$

$$RMSE = \sqrt{\frac{1}{n} \sum_{i=1}^n (f_i - o_i)^2} \quad (2)$$

$$MAE = \frac{1}{n} \sum_{i=1}^n |f_i - o_i| \quad (3)$$

$$Bias = \frac{1}{n} \sum_{i=1}^n (f_i - o_i) \quad (4)$$

Where  $f$  is forecast,  $\bar{f}$  is forecast average,  $o$  is observation, and  $\bar{o}$  is observation average, for each  $i$  case to the  $n$  number of cases.

Figure 3.38 shows the flowchart for model development of air quality forecast by statistical methods in Macao.

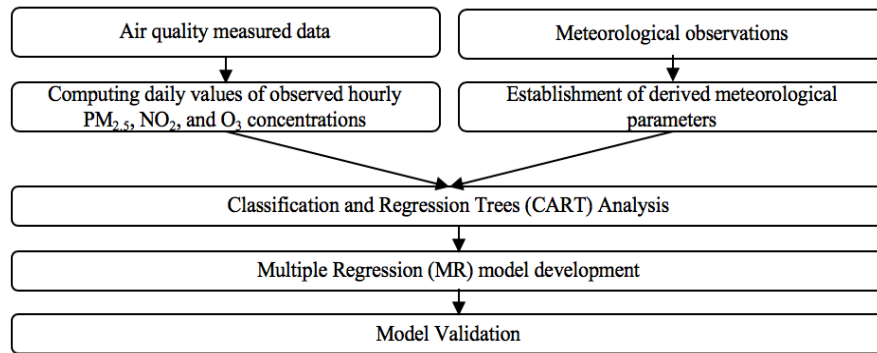


**Figure 3.38.** Flowchart for model development of air quality forecast by statistical methods.

In this study, meteorological and air quality variables for 2013 to 2016, 2015 to 2018, and 2013 to 2018 were used to build three separate forecasting models. The 2013 to 2016 model was constructed for the initial evaluation for the application of the statistical model to forecast air quality in Macao, while the 2015 to 2018 models and the 2013 to 2018 models are a follow-up, to determine if any improvement could be made with two additional years of data. The comparison of extended data ranging from 5 to 6 years are considered to be adequate lengths to test if there is any significant difference between the time series (Cassmassi, 1997). Simultaneously, it would not be ideal to trace back too far within the time series, because regional emissions are constantly changing, and therefore the level of pollutants concentration may also be changing. The dataset from 2017 was used to validate the 2013 to 2016 model, while the dataset from 2019 was used to validate the 2013 to 2016 model and

2013 to 2018 model. This study is a region-specific and empirical approach for Macao.

In order to test the performance of the selected and validated models, they were applied to forecast pollution levels during an extremely high pollution episode, and a low pollution period. The high and low pollution selected episodes were, respectively:

(i) the period of Chinese National Holiday, a week before the Chinese National Holiday from September 23rd to 30th, 2019, and the week during the Chinese National Holiday from October 1st to 7th, and (ii) the preventive measures period of COVID-19, from February 5th to 20th, 2020.

In a study for Beijing, China, the reduction of traffic flow and vehicle emissions in downtown areas during the Chinese National Holiday, reduced air pollution, while, in contrast, fireworks during the Chinese New Year Holiday had the opposite effect (Zheng et al., 2017). When highway tolls were being waived for passenger vehicles during the Chinese National Holiday across the entire nation of China, air pollution increased by 20% and visibility decreased by 1 km, causing economic losses due to negative health impacts estimated at RMB 0.95 billion (Fu & Gu, 2017).

Nevertheless, the Chinese National Holiday is known to be a golden week of

tourism, in which the Chinese tourist flock to different tourist destinations around the world to celebrate the national holiday. Due to the vibrant casinos and entertainment industry and close proximity to mainland China, Macao is also one of the favorite destinations for Chinese tourists, so the influx of tourist during the period of Chinese National Holiday may lead to an increase of emissions in Macao.

Likewise, the recent COVID-19 crisis has had an extreme impact in air pollution levels. The first case of COVID-19 was reported back in December 2019. Preventive measures were implemented soon after that, abruptly reducing industrial activities and transportation. Nevertheless, the levels of air pollutants, in particular of PM<sub>2.5</sub>, remained severe in northern China throughout the end of January 2020 due to adverse meteorological conditions that have overwhelmed the benefits of emission reduction in transportation and industrial sectors (Wang et al., 2020).

Previous work showed that there is an increase in the level of O<sub>3</sub> concentrations and a decrease in the level of NO<sub>2</sub>, PM<sub>10</sub>, and PM<sub>2.5</sub> concentration during the period of COVID-19 pandemic lockdown in several cities of China, due to the significant reduction of transportation and industrial activities (Bao & Zhang, 2020; Li et al., 2020; Shi & Brasseur, 2020; Wang et al., 2020).

## **Chapter 4: Result and Discussion**

---

#### **4.1 Air Quality Forecast Using 2013 to 2016 Data (Validated with 2017 Data)**

The statistical models based on MLR and CART analysis were developed to forecast NO<sub>2</sub>, PM<sub>10</sub>, PM<sub>2.5</sub>, and O<sub>3</sub> concentrations. The final objective is to be able to perform a daily forecast, for the next day, in an operational mode, by running the prediction models after 16H (due to the daily schedules of which the air quality data is made available). CART analysis was tested mainly in order to better predict the high concentration levels. For NO<sub>2</sub> and PM, CART analysis did not improve the quality of the overall predictions. Therefore, prediction models were based only on one MR model. In the case of O<sub>3</sub> forecast, for three stations (Taipa Ambient, Taipa Residential, and Coloane Ambient), CART analysis allowed to identify split nodes, for which O<sub>3</sub> prediction equations were determined afterwards by using MR for each node. Figure 4.1 represents an example of the CART trees obtained, in this case for O<sub>3</sub>MAX prediction at Taipa Ambient station.

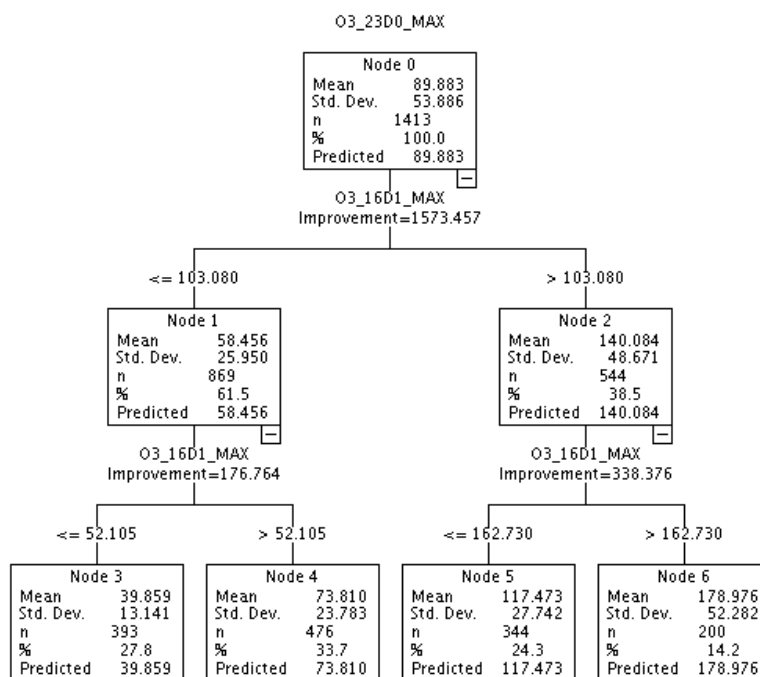


**Figure 4.1.** CART tree obtained for O<sub>3</sub> MAX prediction at Taipa Ambient station.

The output meteorological and air quality variables and equations obtained with MR (or CART and MR, in the O<sub>3</sub> MAX case), are listed in Table 4-1.

**Table 4-1.** Variables and model equations for each pollutant per air quality monitoring station for 2013-2016 model.

Station	Pollutant	Model equations
Macao Roadside	NO <sub>2</sub>	$NO_2 = 0.900 \times NO_{2\_16D1} + 0.012 \times H850 - 0.168 \times HRMN$
	PM <sub>10</sub>	$PM_{10} = 0.900 \times PM_{10\_16D1} + 0.019 \times H850 - 0.270 \times HRMD$
	PM <sub>2.5</sub>	$PM_{2.5} = 0.934 \times PM_{25\_16D1} + 0.009 \times H850 - 0.128 \times$



Station	Pollutant	Model equations
		HRMD
Macao Residential	NO <sub>2</sub>	$NO_2 = 0.919 \times NO_{2\_16D1} + 0.007 \times H850 - 0.098 \times HRMN$
	PM <sub>10</sub>	$PM_{10} = 0.884 \times PM_{10\_16D1} + 0.019 \times H850 - 0.274 \times$ HRMD
	PM <sub>2.5</sub>	$PM_{2.5} = 0.915 \times PM_{25\_16D1} + 0.005 \times H850 - 0.242 \times$ TD_MD
	O <sub>3</sub> MAX	$O_{3\ MAX} = 1.123 \times O_{3\_max\_16D1} - 0.314 \times O_{3\_max\_23D1} -$ $0.055 \times HR925 + 0.440 \times T\_AIR\_MX$
Taipa Ambient	NO <sub>2</sub>	$NO_2 = 0.915 \times NO_{2\_16D1} + 0.004 \times H850 + 0.758 \times STB925$
	PM <sub>10</sub>	$PM_{10} = 0.891 \times PM_{10\_16D1} + 0.018 \times H850 - 0.261 \times$ HRMD
	PM <sub>2.5</sub>	$PM_{2.5} = 0.918 \times PM_{25\_16D1} + 0.009 \times H850 - 0.128 \times$ HRMD
	O <sub>3</sub> MAX	If $[O_{3\ MAX\_16D1}] \leq 103.08$  $O_{3\ MAX} = 1.111 \times O_{3\_max\_16D1} - 0.207 \times O_{3\_max\_23D1} -$  $0.721 \times STB850$

Station	Pollutant	Model equations
		<p>If <math>[O_3_{MAX\_16D1}] = ]103.08; 162.73]</math></p> $O_3_{MAX} = 1.237 \times O_{3\_max\_16D1} - 0.433 \times O_{3\_max\_23D1} - 1.690 \times STB850$ <p>If <math>[O_3_{MAX\_16D1}] &gt; 162.73</math></p> $O_3_{MAX} = 0.930 \times O_{3\_max\_16D1} - 0.473 \times O_{3\_max\_23D1} - 8.608 \times STB850$
Taipa Residential	NO <sub>2</sub>	$NO_2 = 0.848 \times NO_{2\_16D1} + 0.008 \times H850 - 0.315 \times TDMD$
	PM <sub>10</sub>	$PM_{10} = 0.894 \times PM_{10\_16D1} + 0.017 \times H850 - 0.237 \times HRMD$
	PM <sub>2.5</sub>	$PM_{2.5} = 0.937 \times PM_{25\_16D1} - 0.651 \times TDMD + 0.746 \times TAR925$
	O <sub>3</sub> MAX	<p>If <math>[O_3_{MAX\_16D1}] \leq 129.05</math></p> $O_3_{MAX} = 1.043 \times O_{3\_max\_16D1} - 0.240 \times O_{3\_max\_23D1} + 0.016 \times H850 - 0.163 \times HRMN$ <p>If <math>[O_3_{MAX\_16D1}] = ]129.05; 205.47]</math></p> $O_3_{MAX} = 0.997 \times O_{3\_max\_16D1} - 0.387 \times O_{3\_max\_23D1} +$

Station	Pollutant	Model equations
		$0.055 \times H850 - 0.677 \times HRMN$  If $[O_3_{MAX\_16D1}] > 205.47$  $O_3_{MAX} = 1.170 \times O_3_{max\_16D1} - 0.482 \times O_3_{max\_23D1} +$  $0.124 \times H850 - 2.632 \times HRMN$
Coloane    Ambient	NO <sub>2</sub>	$NO_2 = 0.930 \times NO_2\_16D1 - 0.617 \times TDMD + 0.739 \times$  TAR925
	PM <sub>10</sub>	$PM_{10} = 0.875 \times PM_{10\_16D1} + 0.023 \times H850 - 0.331 \times$  HRMD
	PM <sub>2.5</sub>	$PM_{2.5} = 0.903 \times PM_{25\_16D1} + 0.008 \times H850 - 0.121 \times$  HRMN
	O <sub>3 MAX</sub>	If $[O_3_{MAX\_16D1}] \leq 113.96$  $O_3_{MAX} = 1.014 \times O_3_{max\_16D1} - 0.197 \times O_3_{max\_23D1} +$  $0.834 \times T\_AIR\_MX - 0.129 \times HRMN$  If $[O_3_{MAX\_16D1}] = ]113.96; 181.61]$  $O_3_{MAX} = 1.054 \times O_3_{max\_16D1} - 0.394 \times O_3_{max\_23D1} +$  $2.676 \times T\_AIR\_MX - 0.597 \times HRMN$

Station	Pollutant	Model equations
		<p data-bbox="544 338 895 376">If <math>[O_3_{MAX\_16D1}] &gt; 181.61</math></p> $O_3_{MAX} = 0.666 \times O_{3\_max\_16D1} - 0.448 \times O_{3\_max\_23D1} + 7.298 \times T\_AIR\_MX - 1.561 \times HRMN$

The models were validated with collected data from 2017. The results show a good agreement between modelled and observed concentrations, being statistically significant at the 95% confidence level. The selected models provide a good relationship between meteorological and air quality variables, when performing an air quality forecast under different situations. Table 4-2 contains the obtained model performance indicators, such as,  $R^2$ , RMSE, MAE, and Bias.

**Table 4-2.** Model performance indicators for the 2013 to 2016 model validation with 2017 data.

Station	Pollutant	Model performance indicator				Model built using only MR or CART and MR	
		R <sup>2</sup>	RMSE	MAE	BIAS	MR	CART
Macao Roadside	PM <sub>10</sub>	0.91	9.2	6.6	1.5	✓	
	PM <sub>2.5</sub>	0.90	5.9	4.0	1.5	✓	
	NO <sub>2</sub>	0.89	7.9	5.8	0.9	✓	
Macao Residential	PM <sub>10</sub>	0.91	8.3	5.8	1.2	✓	
	PM <sub>2.5</sub>	0.86	5.9	3.6	0.9	✓	
	NO <sub>2</sub>	0.87	7.8	5.6	-0.2	✓	
	O <sub>3</sub> MAX	0.81	23.2	14.0	0.0	✓	
Taipa Ambient	PM <sub>10</sub>	0.92	6.8	4.5	1.1	✓	
	PM <sub>2.5</sub>	0.89	5.0	3.2	1.1	✓	
	NO <sub>2</sub>	0.90	6.1	4.4	0.4	✓	
	O <sub>3</sub> MAX	0.82	25.7	15.0	1.3	✓	✓

Taipa Residential	PM <sub>10</sub>	0.92	6.4	4.1	1.5	✓	
	PM <sub>2.5</sub>	0.89	4.9	3.3	-0.3	✓	
	NO <sub>2</sub>	0.84	6.7	4.6	-0.5	✓	
	O <sub>3</sub> MAX	0.87	21.1	12.2	3.7	✓	✓
Coloane Ambient	PM <sub>10</sub>	0.93	7.7	5.7	1.9	✓	
	PM <sub>2.5</sub>	0.90	5.4	3.6	0.9	✓	
	NO <sub>2</sub>	0.85	6.4	4.1	0.0	✓	
	O <sub>3</sub> MAX	0.78	27.4	16.9	-1.5	✓	✓

The models, as assessed by R<sup>2</sup> values, performed better for PM (between 0.86 and 0.93 and, in all cases, greater for PM<sub>10</sub> than for PM<sub>2.5</sub>), followed by NO<sub>2</sub> (between 0.84 and 0.90), being the lowest explained variance achieved for O<sub>3</sub> (between 0.78 and 0.87).

Models did not show a defined trend on the forecasts by type of station, presenting undistinctive R<sup>2</sup> for roadside, residential and ambient stations. The monitored and forecasted concentrations, in 2017, for the models with the highest and lowest R<sup>2</sup> are depicted in Figure 4.2 and 4.3, being respectively, the one for PM<sub>10</sub> Coloane Ambient and O<sub>3</sub> MAX Coloane Ambient, in 2017. The poorest results obtained in Coloane Ambient is related with the fewest cases available to build the model (N=546).

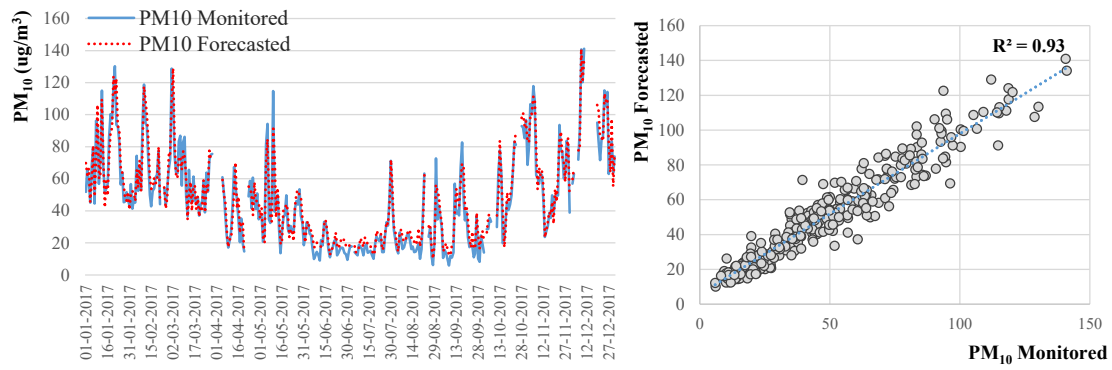


**Figure 4.2.** Observed and predicted PM<sub>10</sub> concentrations for Coloane Ambient in 2017.

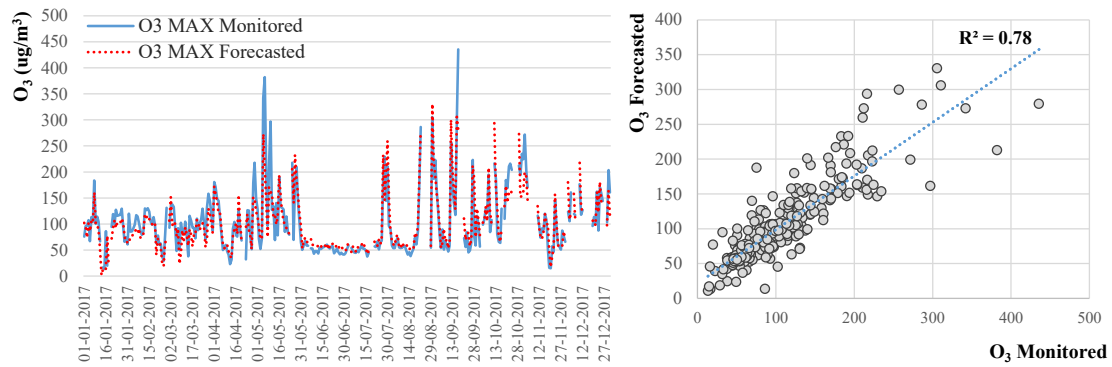


**Figure 4.3.** Observed and predicted O<sub>3</sub> MAX concentrations for Coloane Ambient in 2017.

Regarding the RMSE, all models presented the same trend observed for R<sup>2</sup>, being the RMSE lower for PM (between 4.9 µg/m<sup>3</sup> and 9.2 µg/m<sup>3</sup>), followed by NO<sub>2</sub> (between 6.1 µg/m<sup>3</sup> and 7.9 µg/m<sup>3</sup>), and the highest for O<sub>3</sub> (between 21.1 µg/m<sup>3</sup> and 27.4 µg/m<sup>3</sup>). In the case of O<sub>3</sub>, the high RMSE obtained values were due to abrupt variations, on consecutive days, influencing the predicted values, since statistical models are sensitive

to this kind of fluctuations.

Regarding CART analysis for O<sub>3</sub> prediction, three equation nodes were used. The number of cases considered in each node (N), the coefficient of determination (R<sup>2</sup>), the correlation coefficient (r), and the standard error of the estimate are presented in Table 4-3. The obtained standard error of the estimate, which is a measure of the prediction's accuracy, was higher for higher concentrations prediction categories. The highest obtained standard error of the estimate for Node 1 was of 17.2 µg/m<sup>3</sup> in Coloane Ambient station, for Node 2 was of 28.8 µg/m<sup>3</sup> and for Node 3 was of 43.6 µg/m<sup>3</sup>, both in Taipa Residential station. This reflects the difficulty of the model in predicting the highest O<sub>3</sub> concentration ranges. Traffic-related pollutants, such as PM and NO<sub>2</sub>, are dependent on meteorological conditions as well as emission rates. Because O<sub>3</sub> is produced in the atmosphere through photochemical processes, the major meteorological factors affecting ozone concentrations are different from those for traffic-related primary pollutants (Choi et al., 2013).



**Table 4-3.** CART model performance indicators for 2013 to 2016 model.

Station	Nodes split	N	Model performance indicator		
			R <sup>2</sup>	r	Standard error of the estimate
Taipa Ambient	$[O_3_{MAX\_16D1}] \leq 103.08$	873	0.93	0.97	16.57
	$[O_3_{MAX\_16D1}] = ]103.08; 162.73]$	347	0.97	0.98	22.70
	$[O_3_{MAX\_16D1}] > 162.73$	200	0.96	0.98	38.59
Taipa Residential	$[O_3_{MAX\_16D1}] \leq 129.05$	930	0.95	0.98	15.96
	$[O_3_{MAX\_16D1}] = ]129.05; 205.47]$	242	0.97	0.98	28.84
	$[O_3_{MAX\_16D1}] > 205.47$	99	0.96	0.98	43.62
Coloane Ambient	$[O_3_{MAX\_16D1}] \leq 113.96$	389	0.94	0.97	17.25
	$[O_3_{MAX\_16D1}] = ]113.96; 181.61]$	106	0.97	0.99	24.32
	$[O_3_{MAX\_16D1}] > 181.61$	52	0.96	0.98	40.73

In all the cases, the variable that represents the last 24-hour pollutant concentrations (16D1) is the most prevalent, being selected at all the forecast equations (Table 4-2).

The geopotential height at 850 hPa (H<sub>850</sub>), indicator of synoptic-scale weather pattern, is also frequently present in the forecast of NO<sub>2</sub> and PM. Specifically, in the case of

PM<sub>10</sub>, relevant variables are H\_850 and the medium relative humidity (HRMD), while for PM<sub>2.5</sub>, for both residential stations, average dew point temperature (TD\_MD) and air temperature at 925 hPa (TAR\_925, a measure of the strength and height of the subsidence inversion) figure in the final equations. Atmospheric stability at 925 hPa and at 850hPa (STB\_925 and STB\_850, respectively) figure in final equations in the case of NO<sub>2</sub> and O<sub>3</sub> MAX at Taipa Ambient. This temperature differences between layers provide information about atmospheric stability.

The used statistical methods depend on the past series of data. If the historical data is insufficient, forecasted data will be less reliable. In particular, if emission sources change considerably or if meteorological variables also change due to factors related to new weather patterns eventually motivated by climate change, the data series of the past will not represent the updated situation, and models need to be recalculated with more recent data.

#### **4.2 Air Quality Forecast Using 2013 to 2018 Data (Validated with 2019 Data)**

Table 4-4 shows there is no significant difference in the coefficient of determination ( $R^2$ ) and only minor improvements in the RMSE, MAE, and BIAS between the 2013 to 2016 model and the 2013 to 2018 model in predicting next-day

concentrations levels in 2019, with high  $R^2$  between predicted and observed daily average concentrations (between 0.78 and 0.89 for all pollutants).

Regarding model performance indicators obtained per pollutant and station, the majority of models show a good agreement and similar  $R^2$  range values (from 0.81 to 0.89), except for  $O_3_{MAX}$  (from 0.78 to 0.86), which is more difficult to predict. MLR was used for all pollutants, while CART analysis was used in almost all the  $O_3_{MAX}$  models (Table 4-2). This CART analysis complement was an approach to obtain improved results, mainly regarding a better prediction of high pollutant levels.

**Table 4-4.** Model performance indicators for the 2013 to 2016 model and the 2013 to 2018 model, validation with 2019 data.

Station	Pollutant	Model Performance Indicator (the 2013 to 2016 Model)				Model Performance Indicator (the 2013 to 2018 Model)			
		$R^2$	RMSE	MAE	BIAS	$R^2$	RMSE	MAE	BIAS
Macao	PM <sub>10</sub>	0.88	8.6	5.8	1.8	0.88	8.4	5.6	1.5
	PM <sub>2.5</sub>	0.86	5.4	3.7	1.5	0.87	5.2	3.3	0.2
Roadside	NO <sub>2</sub>	0.89	8.0	5.9	0.4	0.89	7.9	5.8	-0.1

	PM <sub>10</sub>	0.89	8.8	5.9	-0.3	0.89	8.8	5.9	-0.1
Macao	PM <sub>2.5</sub>	0.87	5.2	3.3	0.7	0.87	5.2	3.3	0.8
Residential	NO <sub>2</sub>	0.86	7.7	5.5	-0.4	0.86	7.7	5.5	0.0
	O <sub>3</sub> MAX	0.85	23.2	14.0	0.0	0.85	23.2	14.0	0.0
	PM <sub>10</sub>	0.88	7.9	5.4	1.7	0.88	7.8	5.1	0.8
Taipa	PM <sub>2.5</sub>	0.86	5.1	3.6	1.6	0.86	4.8	3.1	0.2
Ambient	NO <sub>2</sub>	0.87	6.1	4.2	0.9	0.87	6.1	4.2	1.0
	O <sub>3</sub> MAX	0.86	24.4	14.8	-2.1	0.86	23.7	14.7	-1.6
	PM <sub>10</sub>	0.87	8.0	5.2	0.1	0.88	7.9	5.1	0.2
Taipa	PM <sub>2.5</sub>	0.88	5.7	3.5	-0.1	0.88	5.6	3.5	-0.1
Residential	NO <sub>2</sub>	0.87	5.6	4.2	0.8	0.87	5.6	4.1	0.6
	O <sub>3</sub> MAX	0.78	20.9	12.7	1.3	0.78	20.9	12.7	1.3
	PM <sub>10</sub>	0.88	8.7	6.2	2.4	0.89	8.3	5.7	1.2
Coloane	PM <sub>2.5</sub>	0.86	5.4	3.7	1.3	0.86	5.3	3.6	1.0
Ambient	NO <sub>2</sub>	0.81	7.8	5.5	-0.2	0.81	7.8	5.5	-0.1
	O <sub>3</sub> MAX	0.79	24.7	15.9	-3.6	0.79	24.3	15.3	-3.0

Table 4-5 presents the final model equations obtained for each pollutant, per air quality monitoring station, in the 2013 to 2018 model. Additionally, the final equations used to predict the levels of NO<sub>2</sub>, PM<sub>10</sub>, PM<sub>2.5</sub>, and O<sub>3</sub> MAX concentrations are presented in Table 4-5.

**Table 4-5.** Variables and model equations for each pollutant per air quality monitoring station in the 2013 to 2018 model.

<b>Station</b>	<b>Pollutant</b>	<b>Model Equations</b>
<b>Macao Roadside</b>	NO <sub>2</sub>	$\text{NO}_2 = 0.897 \times \text{NO}_{2\_16\text{D1}} + 0.011 \times \text{H850}$ $- 0.151 \times \text{HRMN}$
	PM <sub>10</sub>	$\text{PM}_{10} = 0.913 \times \text{PM}_{10\_16\text{D1}} + 0.015 \times$ $\text{H850} - 0.208 \times \text{HRMD}$
	PM <sub>2.5</sub>	$\text{PM}_{2.5} = 0.943 \times \text{PM}_{25\_16\text{D1}} + 0.006 \times$ $\text{H850} - 0.091 \times \text{HRMD}$
<b>Macao Residential</b>	NO <sub>2</sub>	$\text{NO}_2 = 0.913 \times \text{NO}_{2\_16\text{D1}} + 0.007 \times \text{H850}$ $- 0.087 \times \text{HRMN}$
	PM <sub>10</sub>	$\text{PM}_{10} = 0.896 \times \text{PM}_{10\_16\text{D1}} + 0.016 \times$ $\text{H850} - 0.224 \times \text{HRMD}$

	PM <sub>2.5</sub>	$PM_{2.5} = 0.926 \times PM_{25\_16D1} + 0.004 \times H850 - 0.176 \times TD\_MD$
	O <sub>3 MAX</sub>	$O_{3\ MAX} = 1.089 \times O_{3\_MAX\_16D1} - 0.344 \times O_{3\_MAX\_23D1} - 1.303 \times TD\_MD + 1.437 \times T\_AIR\_MX$
<b>Taipa Ambient</b>	NO <sub>2</sub>	$NO_2 = 0.914 \times NO_{2\_16D1} + 0.004 \times H850 + 0.734 \times STB925$
	PM <sub>10</sub>	$PM_{10} = 0.905 \times PM_{10\_16D1} + 0.014 \times H850 - 0.205 \times HRMD$
	PM <sub>2.5</sub>	$PM_{2.5} = 0.928 \times PM_{25\_16D1} + 0.006 \times H850 - 0.093 \times HRMD$
	O <sub>3 MAX</sub>	<p>If <math>[O_{3\ MAX\_16D1}] \leq 105.50</math></p> $O_{3\ MAX} = 1.034 \times O_{3\_max\_16D1} - 0.214 \times O_{3\_max\_23D1} + 0.019 \times H850 - 0.236 \times HRMN$ <p>If <math>[O_{3\ MAX\_16D1}] = ]105.50; 181.87]</math></p> $O_{3\ MAX} = 0.994 \times O_{3\_max\_16D1} - 0.433 \times$

---

$$O_{3\_max\_23D1} + 0.051 \times H850 - 0.529 \times$$

HRMN

If  $[O_{3\_MAX\_16D1}] > 181.87$

$$O_{3\_MAX} = 1.006 \times O_{3\_max\_16D1} - 0.472 \times$$

$$O_{3\_max\_23D1} + 0.12 \times H850 - 2.025 \times$$

HRMN

---

**Taipa Residential**

NO<sub>2</sub>

$$NO_2 = 0.859 \times NO_{2\_16D1} + 0.007 \times H850$$

$$- 0.271 \times TD\_MD$$

---

PM<sub>10</sub>

$$PM_{10} = 0.902 \times PM_{10\_16D1} + 0.015 \times$$

$$H850 - 0.204 \times HRMD$$

---

PM<sub>2.5</sub>

$$PM_{2.5} = 0.938 \times PM_{25\_16D1} - 0.607 \times$$

$$TD\_MD + 0.703 \times TAR925$$

---

O<sub>3</sub> MAX

If  $[O_{3\_MAX\_16D1}] \leq 129.12$

$$O_{3\_MAX} = 1.028 \times O_{3\_max\_16D1} - 0.238 \times$$

$$O_{3\_max\_23D1} + 0.019 \times H850 - 0.216 \times$$

HRMN

If  $[O_{3\_MAX\_16D1}] = ]129.12; 207.10]$

---

---

$$O_{3\text{ MAX}} = 0.958 \times O_{3\text{ max\_16D1}} - 0.381 \times$$

$$O_{3\text{ max\_23D1}} + 0.061 \times H850 - 0.751 \times$$

HRMN

If  $[O_{3\text{ MAX\_16D1}}] > 207.10$

$$O_{3\text{ MAX}} = 1.12 \times O_{3\text{ max\_16D1}} - 0.5 \times$$

$$O_{3\text{ max\_23D1}} + 0.14 \times H850 - 2.818 \times$$

HRMN

---

**Coloane Ambient**

NO<sub>2</sub>

$$NO_2 = 0.931 \times NO_{2\_16D1} - 0.503 \times$$

$$TD\_MD + 0.628 \times TAR925$$

---

PM<sub>10</sub>

$$PM_{10} = 0.904 \times PM_{10\_16D1} + 0.015 \times$$

$$H850 - 0.214 \times HRMD$$

---

PM<sub>2.5</sub>

$$PM_{2.5} = 0.927 \times PM_{2.5\_16D1} + 0.005 \times$$

$$H850 - 0.069 \times HRMN$$

---

O<sub>3 MAX</sub>

If  $[O_{3\text{ MAX\_16D1}}] \leq 116.20$

$$O_{3\text{ MAX}} = 1.021 \times O_{3\text{ max\_16D1}} - 0.233 \times$$

$$O_{3\text{ max\_23D1}} + 1.650 \times T\_AIR\_MX -$$

$$1.392 \times TD\_MD$$

---



---

If  $[O_3_{MAX\_16D1}] = ]116.20; 186.92]$

$$O_3_{MAX} = 0.831 \times O_{3\_max\_16D1} - 0.397 \times$$

$$O_{3\_max\_23D1} + 4.929 \times T\_AIR\_MX -$$

$$3.384 \times TD\_MD$$

If  $[O_3_{MAX\_16D1}] > 186.92$

$$O_3_{MAX} = 0.921 \times O_{3\_max\_16D1} - 0.482 \times$$

$$O_{3\_max\_23D1} + 8.868 \times T\_AIR\_MX -$$

$$8.582 \times TD\_MD$$

---

### 4.3 Air Quality Forecast Using 2013 to 2018 Data, for Two days ahead (D2)

The air quality forecast for two days ahead (D2) is setup by using the forecasted data of one day ahead (D1) as the 16D1 and 23D1 for the air quality variables, and the forecasted meteorological variables for two days ahead (D2) obtained from ECMWF weather forecast model. The equations used in the two days ahead (D2) forecast model is identical to the one day ahead (D1) forecast model, as shown in Table 4-5 for Taipa Ambient.

The model performance indicators obtained for the 2013 to 2018 model, validated with 2019 data, for two days ahead (D2) and one day ahead (D1) are listed

in Table 4-6. The forecast for two days ahead (D2) is considerably less accurate compare to one day ahead (D1), with a decrease in the coefficient of determination ( $R^2$ ) and an increase in root mean square error (RMSE), mean absolute error (MAE), and biases (BIAS) for all pollutants. Nevertheless, the result shows that  $PM_{10}$  is more resilient, while the levels of  $PM_{2.5}$ ,  $NO_2$ , and  $O_3$  have a greater variation possibly related to weather change.

**Table 4-6.** Model performance indicators for the 2013 to 2018 model validation with 2019 data, for two days ahead (D2) and one day ahead (D1).

Station	Pollutant	Model Performance				Model Performance			
		Indicator (D2)				Indicator (D1)			
		$R^2$	RMSE	MAE	BIAS	$R^2$	RMSE	MAE	BIAS
	$PM_{10}$	0.51	16.2	11.6	1.6	0.88	7.8	5.1	0.8
Taipa	$PM_{2.5}$	0.37	10.8	7.7	0.3	0.86	4.8	3.1	0.2
Ambient	$NO_2$	0.39	13.9	10.0	1.6	0.87	6.1	4.2	1.0
	$O_{3MAX}$	0.43	49.6	34.2	-13.2	0.86	23.7	14.7	-1.6

#### 4.4 Air Quality Forecast During a High Pollution Episode

The air quality of Macao, a territory with only 32.8 km<sup>2</sup>, is heavily influenced by external factors, in particular by human activities that occur in the much larger and neighboring Guangdong province. Our study shows the extent to which an increase in mobility associated with Chinese National Holiday impacts air quality in Macao.

Taipa Ambient is the most representative background location for Macao, and was chosen to assess the background levels of PM<sub>2.5</sub> and O<sub>3</sub> during the extreme pollution episode. The influx of tourists coming to Macao, in light of the Chinese National Holiday, contributed to a high pollution episode that occurred during late September and early October 2019, with peak daily levels of PM<sub>2.5</sub> concentration exceeding 55 µg/m<sup>3</sup> and maximum hourly levels of O<sub>3</sub> MAX concentration exceeding 400 µg/m<sup>3</sup>, largely exceeding the threshold level recommended by the WHO. The levels of PM<sub>2.5</sub> and O<sub>3</sub> MAX concentrations for Taipa Ambient during the Chinese National Holiday in 2019 (from September to November) are presented in Figures 4.4 and 4.5. They show the comparison of daily average PM<sub>2.5</sub> and O<sub>3</sub> MAX concentration during 2018 and 2019, from a month before in September and a month after in November of the Chinese National Holiday. The pollution episode of 2019 occurred

just before and going well into the period of Chinese National Holiday (1 to 7 October).

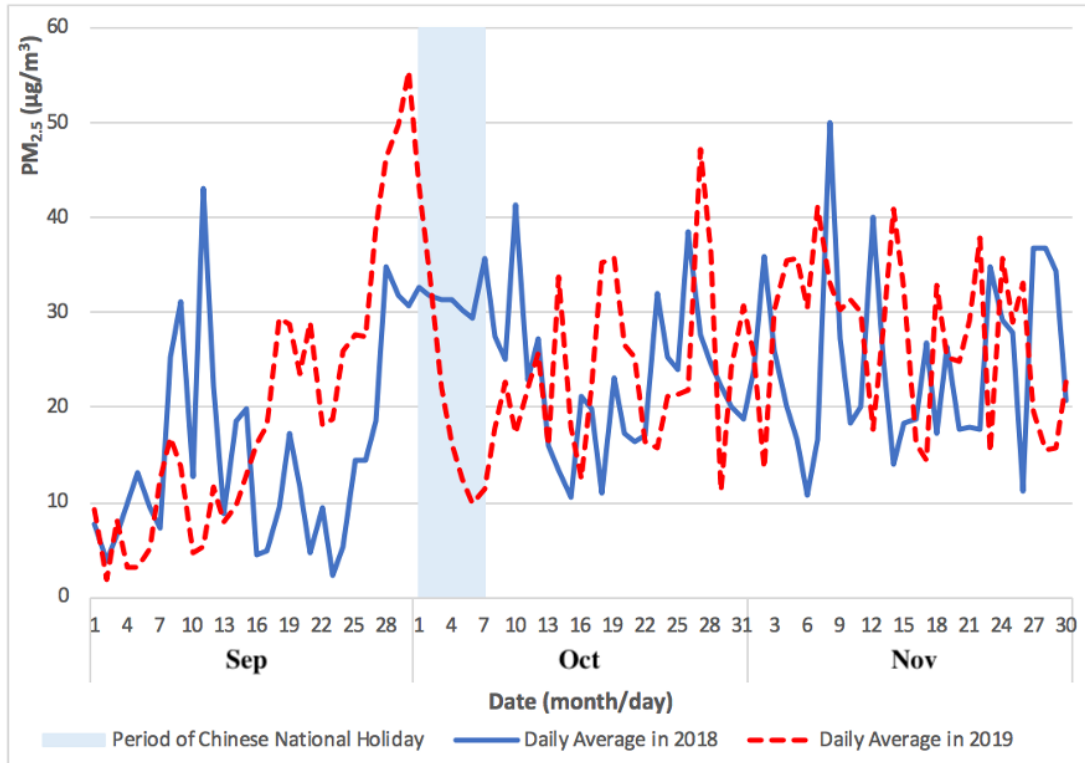


**Figure 4.4.** PM<sub>2.5</sub> concentrations for Taipa Ambient highlighting a pollution episode immediately before, and during, the Chinese National Holiday of 2018 and 2019 (September to November).

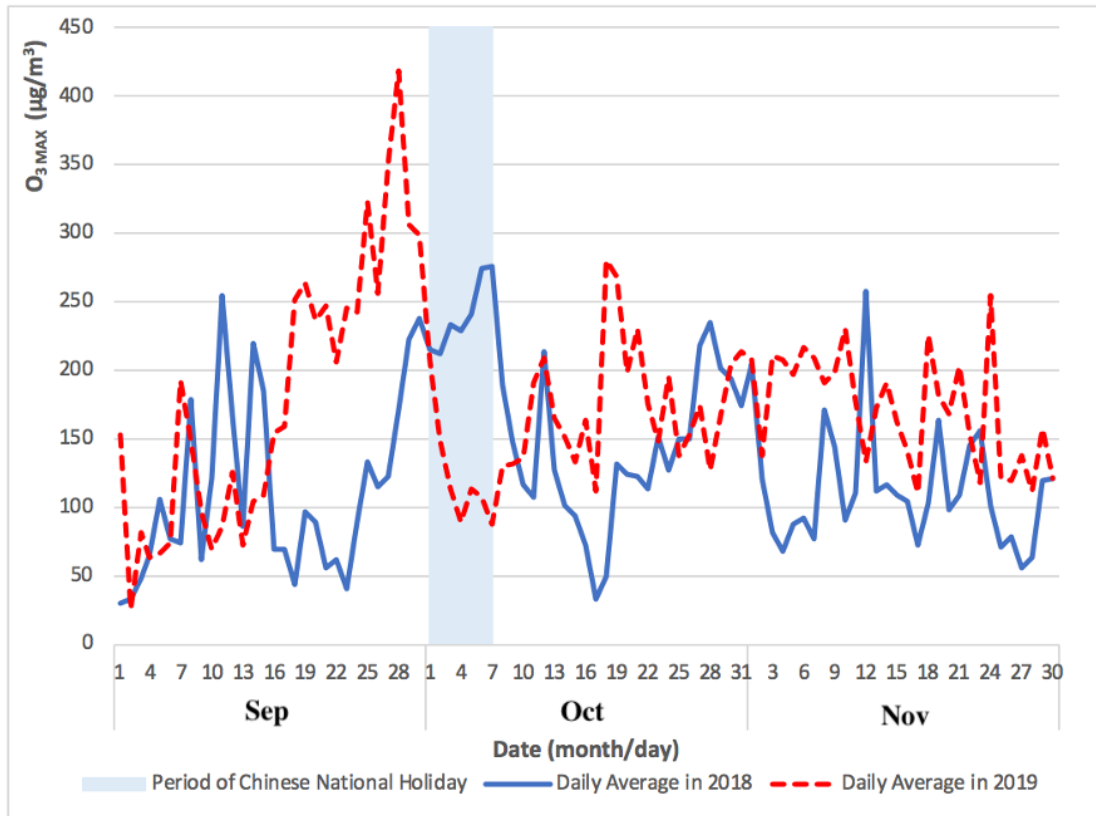


**Figure 4.5.**  $O_3$  MAX concentrations for Taipa Ambient highlighting a pollution episode immediately before, and during, the Chinese National Holiday of 2018 and 2019 (September to November).

As shown in Figures 4.4 and 4.5, the levels of  $PM_{2.5}$  and  $O_3$  MAX concentration peaked immediately before, and during, the Chinese National Holiday in late September and early October 2019. The monthly mean concentration of  $PM_{2.5}$  (from September to November) during the Chinese National Holiday in 2019 was  $19 \mu\text{g}/\text{m}^3$ ,  $24 \mu\text{g}/\text{m}^3$ , and  $28 \mu\text{g}/\text{m}^3$ , respectively. In addition, the monthly mean concentration of  $O_3$  MAX (from September to November) during the Chinese National Holiday in 2019

was 181  $\mu\text{g}/\text{m}^3$ , 163  $\mu\text{g}/\text{m}^3$ , and 172  $\mu\text{g}/\text{m}^3$ , respectively.

The levels of  $\text{O}_3$  MAX concentrations reached its peak during the late September and early October due to meteorological factors including predominant winds from the north and east, from the Guangdong Province and Hong Kong, respectively.

Temperatures were high in conjunction with low wind speed. The average daily temperature during the ozone peak episode that took place the two-weeks before the Chinese National Holiday (October 1st) was 28 °C, while the maximum daily average was 31 °C. Average wind speed was 2.5 m/s.

Due to the shutdown of nearby industrial sectors during the period of Chinese National Holiday, there were lower emissions of nitrogen oxides associated with the decreased load from the coal power plants in the northern region, usually supporting the operation of the factories. Therefore, this caused a decrease  $\text{NO}_x$ , the precursor of  $\text{O}_3$ . However, the increase in emissions of VOCs and  $\text{NO}_x$  by vehicles, with chemical reactions in the presence of sunlight, may have caused the peak levels of ozone concentrations under these high temperature favorable conditions.

Regarding the model behavior in predicting  $\text{PM}_{2.5}$  and  $\text{O}_3$  MAX during the high pollution episode (Chinese National Holiday), observed and predicted  $\text{PM}_{2.5}$  and

$O_3_{MAX}$  concentrations are presented in Figures 4.6 and 4.7. The levels of  $PM_{2.5}$  and  $O_3_{MAX}$  concentration peaked during late September and early October 2019. The  $PM_{2.5}$  predicted levels followed the primary trend of the measured concentration peak represented in Figure 4.6. The model for  $O_3_{MAX}$  also followed the primary trend, but it was more difficult to represent the concentration peak. The forecast model for  $PM_{2.5}$  has a higher  $R^2$  in comparison to the model of  $O_3_{MAX}$ , because the maximum hourly concentration of  $O_3_{MAX}$  is more challenging to predict in comparison to the 24 h average of  $PM_{2.5}$ , as there is influence from the regional precursor sources, and the complex chemistry with solar radiation for  $O_3$  formation also led to a higher degree of variability.

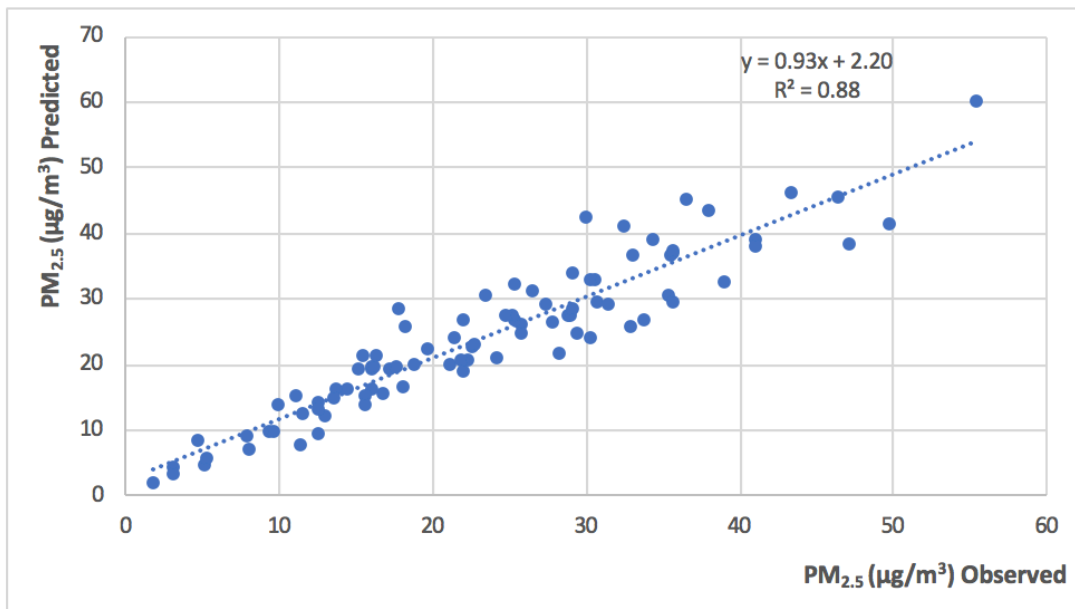
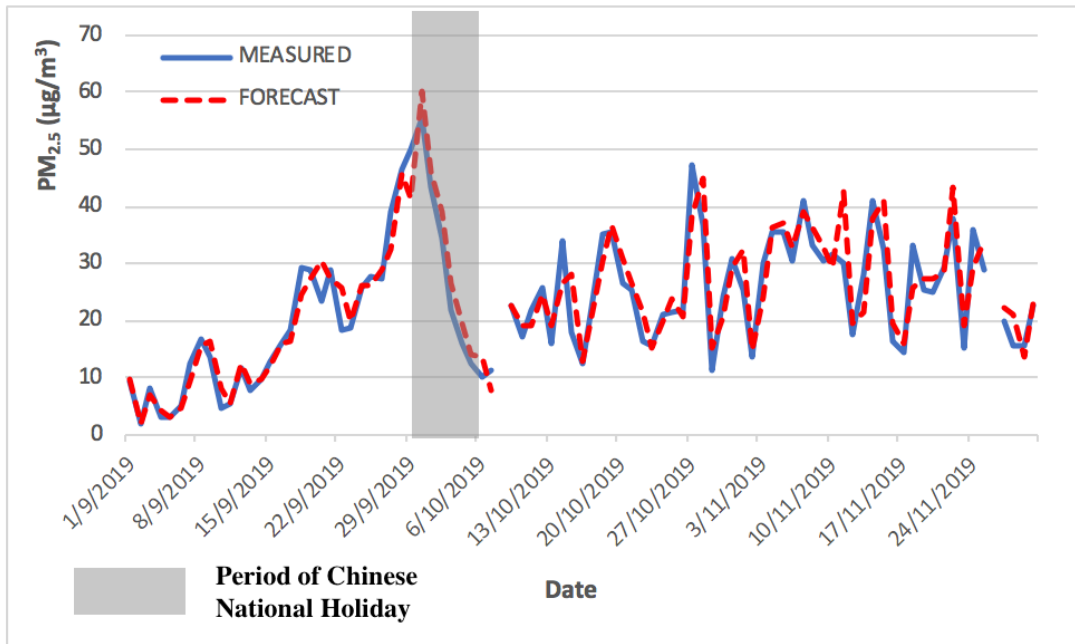


**Figure 4.6.** Observed and predicted PM<sub>2.5</sub> concentrations for Taipa Ambient during Chinese National Holiday (from September to November 2019).



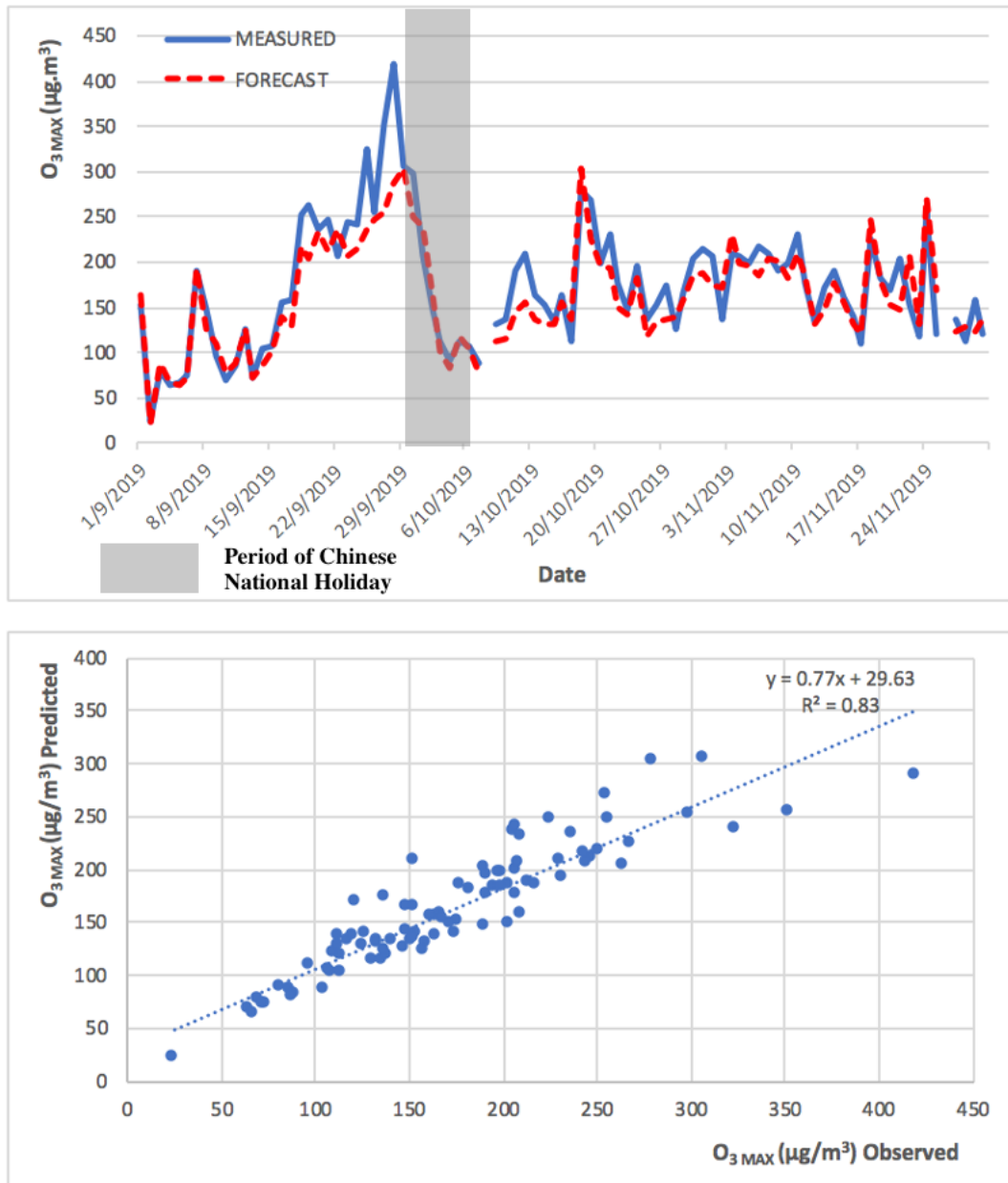


**Figure 4.7.** Observed and predicted  $O_3$  MAX concentrations for Taipa Ambient during Chinese National Holiday (from September to November 2019).

#### 4.5 Air Quality Forecast During a Low Pollution Episode

The levels of  $\text{PM}_{2.5}$  concentrations significantly reduced after the first confirmed case of COVID-19 pandemic in Macao on January 22<sup>nd</sup>, 2020, which caused panic

and anxiety in the local population, and continued by the announcement of casino closures by the Macao government as part of the preventive measures for COVID-19 from February 5th to 20th, 2020. Also, the COVID-19 pandemic has led to the Macao government's decision to temporarily suspend the operation of the casinos and entertainment industry and highly restrict cross border movements, as a preventive measure to reduce population mobility to and from Macao. As a result, it has caused a low pollution episode during late January and early February 2020, with daily levels of PM<sub>2.5</sub> concentration reaching a record low at 2 µg/m<sup>3</sup> and maximum hourly O<sub>3</sub> MAX concentration at 50 µg/m<sup>3</sup>. The reduction of population mobility, and consequently, of traffic emissions in Macao and its nearby Guangdong Province, lead to this lowest PM<sub>2.5</sub> concentration levels recorded.

As shown in Figure 4.8, the levels of PM<sub>2.5</sub> concentrations remained low during the initial outbreak of COVID-19 pandemic in Macao (from January to February 2020), slowly recovering to pre-COVID-19 values in March 2020. As shown in Figure 4.9, the levels of O<sub>3</sub> MAX concentration remained high during the initial outbreak of COVID-19 pandemic in Macao (from January to February 2020) and the high levels continued into March 2020. The higher levels of O<sub>3</sub> MAX concentration

were associated with lower NO<sub>x</sub> emissions, which led to a weakened O<sub>3</sub> titration by NO during the COVID-19 pandemic lockdown in the nearby Guangdong Province (Li et al., 2020).

Despite industrial emission being a major contributor to the PM<sub>2.5</sub> pollution in China prior to COVID-19 pandemic lockdown period, the residential emission contributed to 39% of total PM<sub>2.5</sub> emissions in China, so the emissions of PM<sub>2.5</sub> during the lockdown period may have originated from residential areas (Wang et al., 2020).

The comparison of PM<sub>2.5</sub> and O<sub>3</sub> MAX concentrations for Taipa Ambient during the previous year of 2019 and COVID-19 pandemic in 2020 (January to March) is presented in Figures 4.8 and 4.9.

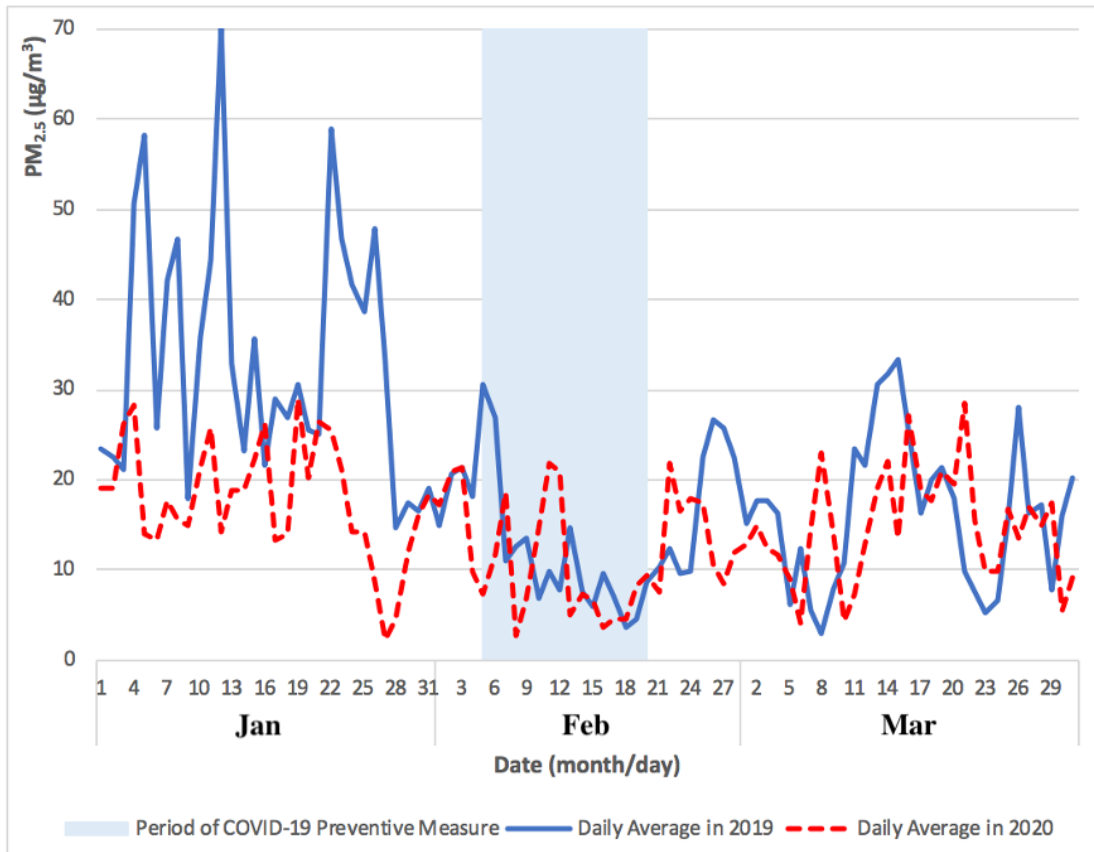


**Figure 4.8.** Comparison of PM<sub>2.5</sub> concentrations for Taipa Ambient during the previous year of 2019 and COVID-19 pandemic in 2020 (January to March).

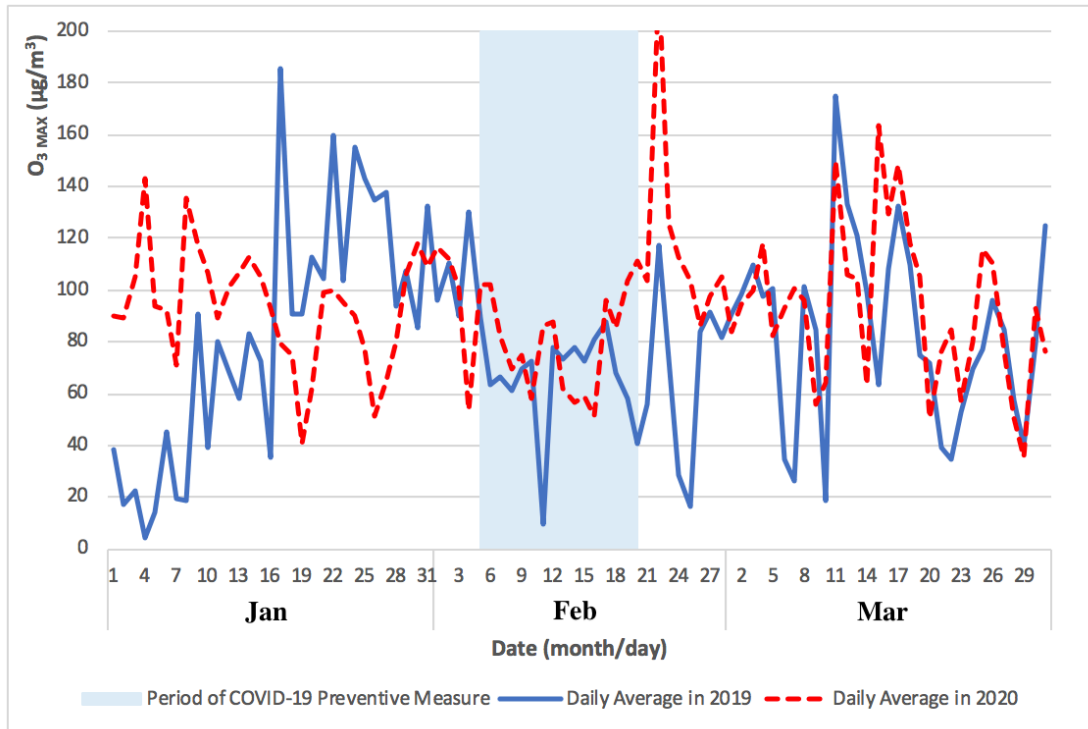


**Figure 4.9.** Comparison of O<sub>3</sub> MAX concentrations for Taipa Ambient during the previous year of 2019 and COVID-19 pandemic in 2020 (January to March).

As shown in Figure 4.10, the difference between monthly mean concentration (from January to March) of PM<sub>2.5</sub> concentration in 2019 and 2020 was 16 µg/m<sup>3</sup>, 2 µg/m<sup>3</sup>, and 1 µg/m<sup>3</sup>, respectively. As shown in Figure 4.9, the difference between monthly mean concentration (from January to March) of O<sub>3</sub> MAX concentration in 2019 and 2020 was 12 µg/m<sup>3</sup>, 21 µg/m<sup>3</sup>, and 9 µg/m<sup>3</sup>, respectively.

The monthly mean concentration of PM<sub>2.5</sub> and O<sub>3</sub> MAX concentration for Taipa Ambient during the previous year of 2019 and COVID-19 pandemic in 2020 (January to March) is presented in Figure 4.10 and 4.11. Overall, the preventive measures of

COVID-19 pandemic may not have caused a significant difference in the levels of PM<sub>2.5</sub> and O<sub>3</sub> concentration in Macao, as the levels from February to March 2020 were similar to that of the previous year, 2019.

In addition, as some of the preventive measures, in particular, the 15 days mandatory casino closure have been lifted, the fear and tension of the local residents has eased, which has promoted population mobility. Although the levels of PM<sub>2.5</sub> concentrations in Macao improved significantly during late January and early February 2020, the levels of PM<sub>2.5</sub> concentrations gradually returned to normal in March 2020 after some of the preventive measures began to be lifted in Macao and its nearby Guangdong Province.

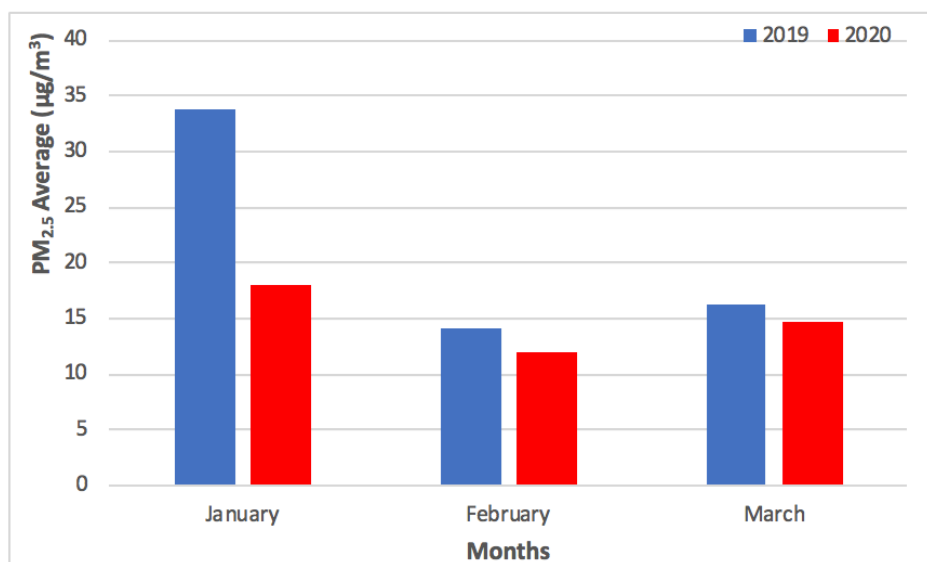


**Figure 4.10.** Monthly mean PM<sub>2.5</sub> concentrations for Taipa Ambient during the previous year of 2019 and COVID-19 pandemic in 2020 (January to March).

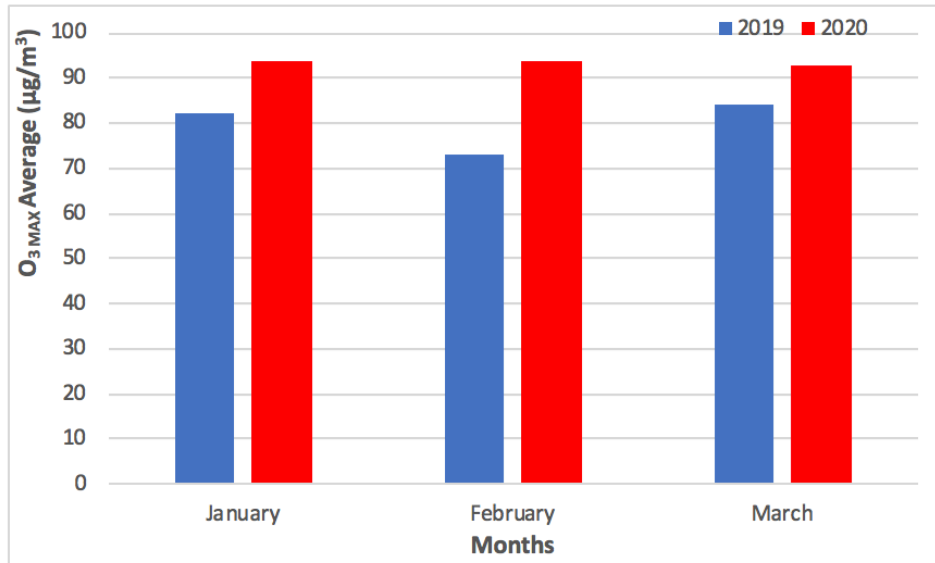


**Figure 4.11.** Monthly mean  $O_3_{MAX}$  concentrations for Taipa Ambient during the previous year of 2019 and COVID-19 pandemic in 2020 (January to March).

Due to the different nature of  $PM_{2.5}$  and  $O_3_{MAX}$ , the forecast model performed better in the prediction of  $PM_{2.5}$  in comparison to  $O_3_{MAX}$ . This can be demonstrated in the higher  $R^2$  values in the  $PM_{2.5}$  forecast model. The observed and predicted  $PM_{2.5}$  and  $O_3_{MAX}$  concentrations, during the low pollution episode (implementation of COVID-19 preventive measures), are presented in Figure 4.12 and 4.13.

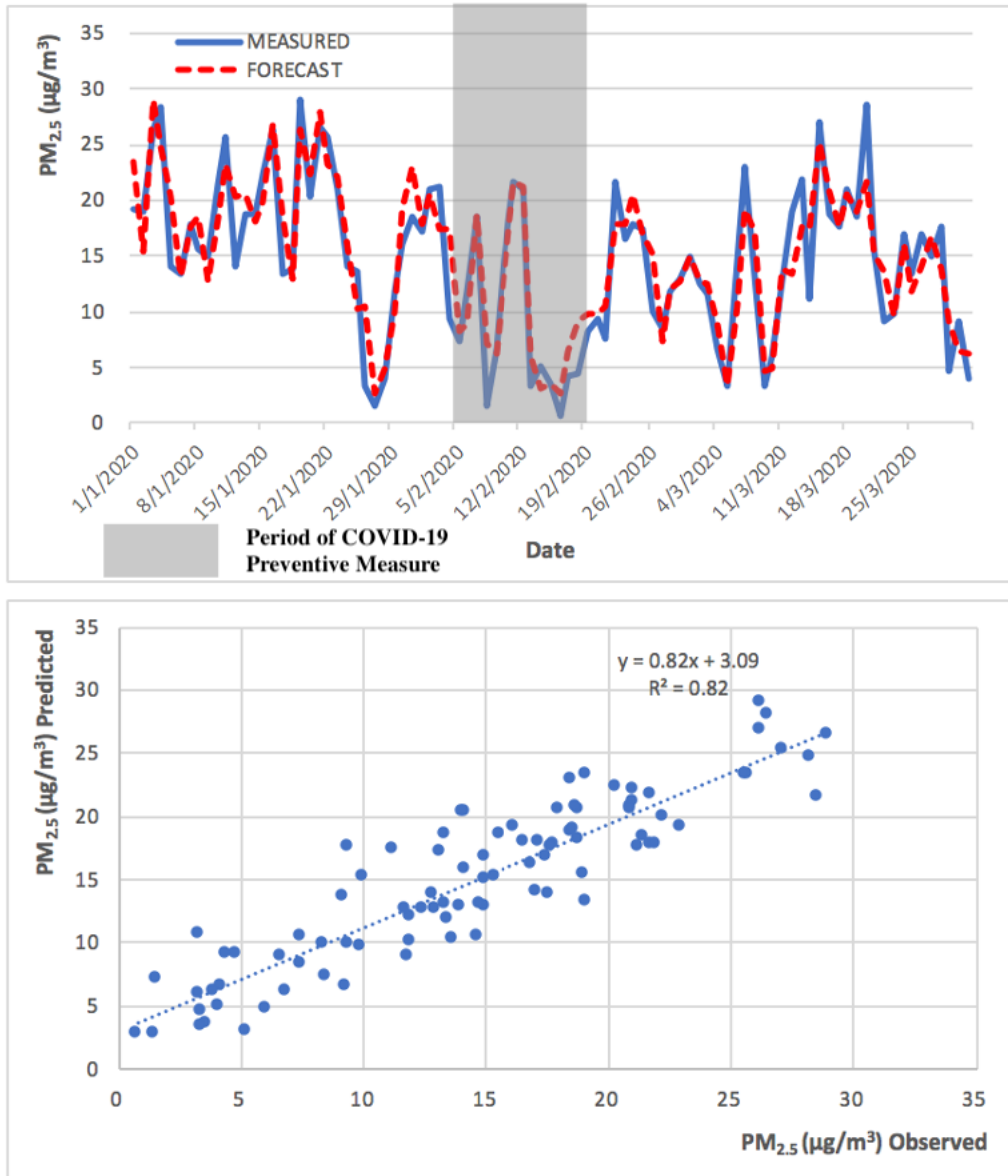


**Figure 4.12.** Observed and predicted PM<sub>2.5</sub> concentrations for Taipa Ambient during preventive measures of COVID-19 pandemic (from January to March 2020).



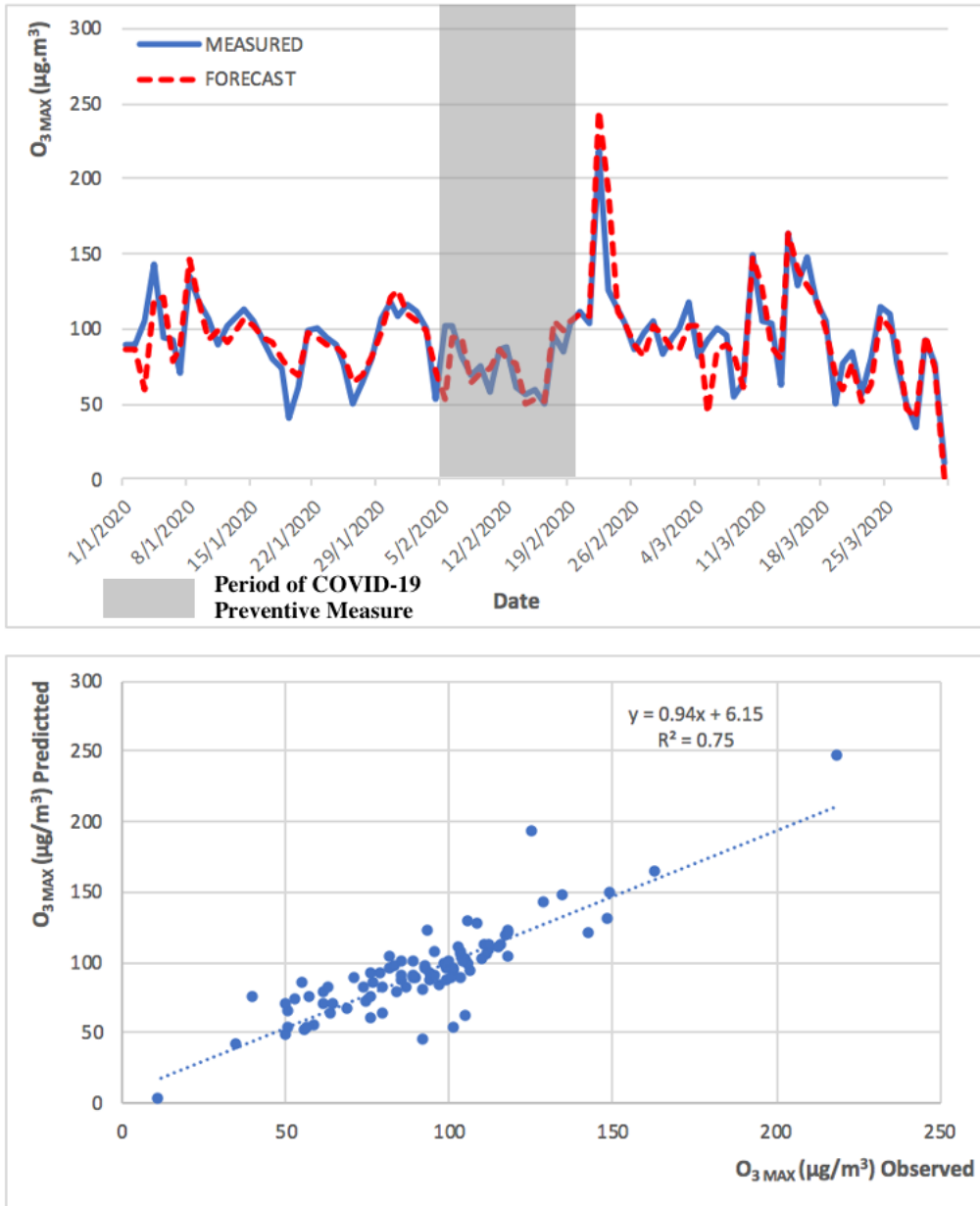


**Figure 4.13.** Observed and predicted  $O_3_{MAX}$  concentrations for Taipa Ambient during preventive measures of COVID-19 pandemic (from January to March 2020).

The 2013 to 2018 model successfully predicted both the high and low pollution episodes, for  $PM_{2.5}$  and  $O_3_{MAX}$ , obtaining a significant  $R^2$  of 0.88 and 0.83, respectively, for the high pollution period (from September to November 2019), and

an  $R^2$  of 0.82 and 0.75, respectively, for the low pollution period (from January to March 2020). The  $R^2$  obtained for the entire year of 2019 was 0.86 for both  $PM_{2.5}$  and  $O_3_{MAX}$ . The statistical forecast model has been shown to be capable to predict, with a high coefficient of determination, the next 24 h.



**Chapter 5: Future measures that could be implemented to improve air quality  
in Macao**

---

In order to improve the air quality in Macao, a group of measures implemented in European and Asian megacities were explored.

The Low Emission Zones (LEZ) have been widely implemented in European capitals such as Lisbon (Portugal), London (United Kingdom), and Berlin (Germany) for many years, while the license plate restriction policy and license plate lottery policy has been widely implemented in Asian capitals such as Beijing (China) and Delhi (India) in the recent years. Both of these measures have been successful to improve the air quality in their respective city center.

The Macao government has adopted several measures to improve air quality such as tax exemptions of EV and exclusive corridor for public transportation (bus only). Nevertheless, the Macao government may also consider adopting LEZ and license plate restriction and lottery policies as the next step to further improve the air quality in Macao.

Nevertheless, the comparison of the measures to improve air quality amongst European cities, Asian cities, and Macao is valuable, as these precedent cases may serve as an example for the Macao government to follow.

## 5.1 Low Emission Zone (LEZ)

In order to achieve the strict emission threshold set by the World Health Organization (WHO), local, regional, and national governments across the world have taken different measures in their city center to reduce the anthropogenic emission of particulate matter (PM<sub>10</sub> and PM<sub>2.5</sub>) and nitrogen oxides (NO<sub>x</sub>), one of the major pollutants from vehicle emissions. In order to discover the best measures to improve air quality in Macao, it would be important to learn from the difference measures across the world, in particular of megacities in Europe and Asia. In European cities, the majority has adopted a Low Emission Zone (LEZ) as a measure to improve air quality, which has been successful in reducing vehicle emissions in city centers. A Low Emission Zone (LEZ) is a defined area where access by the most polluting vehicles is restricted, which means that the older vehicles with higher emission cannot enter this area.

A study showed that the levels of PM<sub>10</sub> and NO<sub>2</sub> concentrations in Lisbon have been exceeding the thresholds set by European Union and national legislation in 2001 (Ferreira et al., 2015). The Lisbon Regional Agency developed a first Air Quality Action Plan in 2006, publishing the respective Enforcement Plan in 2009, and the

LEZ implementation took place by the municipality of Lisbon in 2011, as a measure to reduce air pollution related to road traffic. Figure 5.1 shows the LEZ of Lisbon and the locations of the monitoring sites. The current LEZ phase 3 consist of Euro 3 emission standards in the city center (Zone 1) and Euro 2 emission standards in the rest of the LEZ area (Zone 2). A comparison between before the LEZ measures (2011) and after the LEZ measures (2013) showed that there was a 23% decrease of annual mean PM<sub>10</sub> concentration and 12% decrease of annual mean NO<sub>2</sub> concentration after the implementation of the LEZ. Nevertheless, the reduction attained in the levels of NO<sub>2</sub> concentration was not as effective as in comparison to other European cities such as Berlin and London (Ferreira et al., 2015).

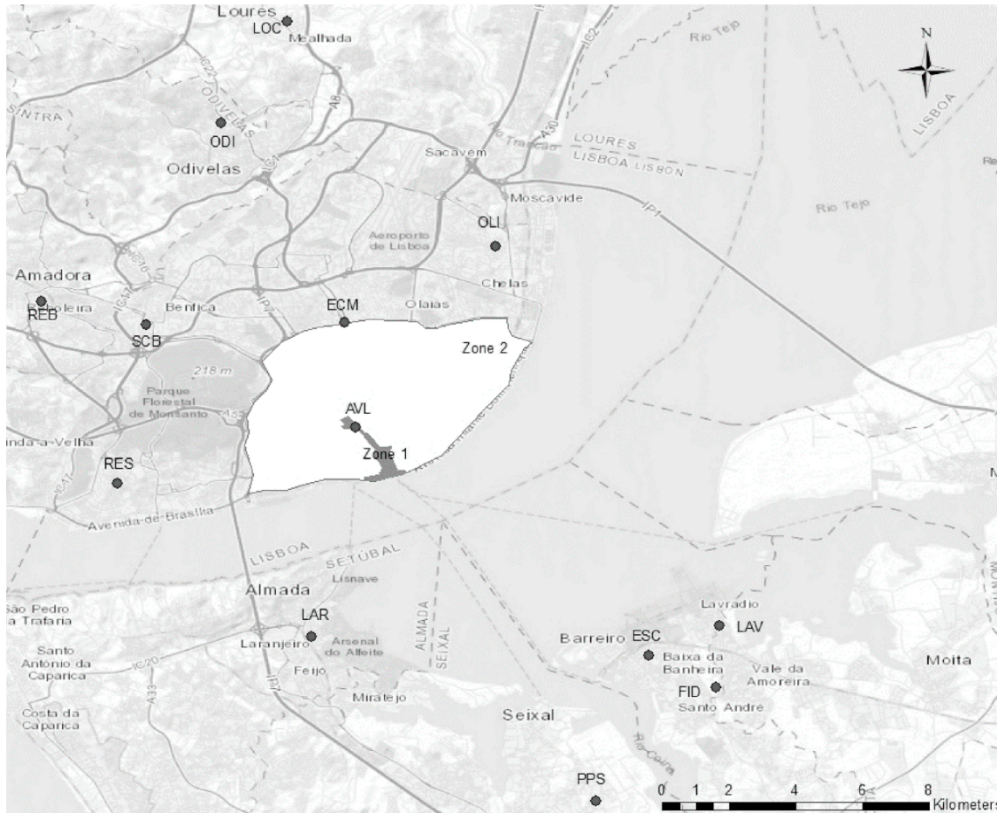


**Figure 5.1.** Low emission zone of Lisbon, Portugal (Santos, Gómez-Losada, & Pires, 2019).

The levels of  $PM_{10}$  concentration reduced by 14% and the levels of  $NO_2$  concentration reduced by 21% after the implementation of LEZ in Lisbon, Portugal.

The reduction of  $PM_{10}$  was lower due to the influence of regional background sources, while the reduction of  $NO_2$  concentration was higher due to the influence of local traffic (Monjardino et al., 2018). The analysis from 2009 to 2016 showed that the annual average level of  $PM_{10}$  concentration has reduced by 29% and 23% in Zone 1 and 2 respectively, and the annual average level of  $NO_2$  concentration has reduced



12% and 22% in Zone 1 and 2 respectively, after the implementation of LEZ to improve air quality in Lisbon (Santos et al., 2019).

Another study utilized the measurement of black carbon in LEZ to evaluate the effectiveness of LEZ in Milan, as black carbon is emitted primarily in traffic sources (Invernizzi et al. 2011). There were three zones being considered in this study, with fixed monitoring stations, including an outer zone with no traffic restriction, an intermediate zone which required vehicles with Euro 4 emission standards to pay a traffic congestion charge (Ecopass), and a pedestrian zone without cars in the city center. The results showed that there was a sharp decline in black carbon levels from the outer zone to the pedestrian zone, while the PM concentration showed no significant differences amongst the different zone. In addition, the ratio of black carbon to PM<sub>10</sub> showed a decrease of 47% and 62% in the Ecopass and pedestrian zones, respectively, in comparison to the outer zone. Therefore, these studies concluded that black carbon was an appropriate indicator to evaluate the improvement in air quality in LEZ (Holman et al., 2015; Invernizzi et al., 2011).

The implementation of LEZ has reduced the emission of PM<sub>10</sub> and diesel soot in German cities and there are currently 48 LEZ in operation across Germany (Cyrus et

al. 2014). The levels of  $PM_{10}$  concentrations has reduced by 10% after the implementation of LEZ in Cologne, Berlin, and Munich, while the levels of diesel soot concentrations have reduced by 52% in 2010 and by 63% in 2012 in comparison to the reference year of 2007 in Berlin and the levels of  $PM_{2.5}$  concentration has been reduced in Munich after the implementation of LEZ (Cyrus et al., 2014). The study of the concentration of air pollutants such as  $PM_{10}$ ,  $PM_{2.5}$ , NO,  $NO_2$ , and  $NO_x$  from 2002 to 2012 showed that the implementation of LEZ was positive on the improvement of air quality in Germany (Gehrsitz, 2017; Jiang et al., 2017; Malina & Scheffler, 2015).

In addition, studies showed elemental carbon (EC) to be a more appropriate indicator than  $PM_{10}$  and  $PM_{2.5}$  to evaluate the impact of traffic measures, such as LEZ, on air quality and human health in Amsterdam, Netherlands. The LEZ in Amsterdam restricted heavy-duty vehicles with Euro 0 to 2 emission standard and vehicles that are older than eight years with Euro 3 emission standard is successful at reducing air pollution in this area (Keuken et al., 2012). A study of five Dutch cities before (2008) and after (2010) the implementation of LEZ showed that the concentration of air pollutants such as  $PM_{10}$ ,  $PM_{2.5}$ ,  $NO_2$ ,  $NO_x$  and soot have been reduced after the implementation of the LEZ (Boogaard et al., 2012).

A study conducted in the city of Munich collected PM<sub>2.5</sub> samples before (2006 and 2007) and after (2009 and 2010) the implementation of a LEZ to analyze for elemental carbon (EC) and particle organic compounds (POC), which showed that there was a significant lower EC and POC concentration after LEZ implementation, with average EC concentration reduced from 1.1 to 0.5 µg/m<sup>3</sup> (Qadir et al., 2013).

Also, the ultrafine particles at two London sites and a Birmingham site in late 2007 showed a reduction between 30% to 59% after the introduction of sulphur-free diesel fuel and the implementation of LEZ in London for heavy-duty vehicles (Jones et al., 2012).

## **5.2 License Plate Restriction Policy**

In Asian cities, the majority has adopted a license restriction and a vehicle license lottery policy, which has been successful to reduce vehicle emission and promote the use of green and public transportation in city center. There are two types of license plate restrictions in China, which are either based on One-Day-Per-Week (ODPW) or Odd-And-Even (OAE) license plate restriction (Liu et al., 2018).

Nevertheless, there is still a serious air pollution problem in Beijing, in particular related with high concentrations of PM<sub>10</sub>, PM<sub>2.5</sub>, SO<sub>2</sub>, NO<sub>2</sub>, CO, and O<sub>3</sub>. Therefore,

the Chinese government has implemented the license plate restriction policy as a measure to improve the air quality in major cities such as Beijing, Hangzhou, Lanzhou, Langfang, and Tianjin (Chen et al., 2018; Huang et al., 2017; Jia et al., 2017; Liu et al., 2018; Pu et al., 2015; Sun et al., 2014; Xie et al., 2017; Xu et al., 2015).

The Chinese Capitol of Beijing has also adopted a vehicle license lottery policy to reduce the growth of cars in 2011 and this policy has reduced the total number of cars by 14% (Liu et al., 2018; Yang et al., 2020; Yang et al., 2014). The government's policy and attitude towards license plate lottery policy for electric vehicles played an important role in the adoption of electric vehicles in Beijing (Zhuge et al., 2020). The license plate restriction policy was first introduced during the Beijing Olympic Games in 2008 to reduce air pollution and traffic congestion and this measure has continued to be implemented in the current days (Lu, 2016).

The license plate restriction policy is based on the last digit of the vehicle license plate, and the Chinese people tend to prefer even numbers due to traditional superstition, which restricted the circulation of cars on the road during a specific day of the week (Liu et al., 2017). On certain days of the week, there are 7.5% fewer cars

being banned from driving on dates when number 4 is specified on the license plate restriction, because number 4 is associated with bad fortune and death in Chinese traditions (Gu et al., 2017; Yang et al., 2018).

The Chinese megacity of Shanghai has a different approach to limit the growth of car ownership, achieved by implementing a monthly car license auction policy (Chen & Zhao, 2013; Zhang et al., 2020). In addition, the implementation of license plate restriction showed that the total vehicle kilometer traveled and total emissions have been reduced by 9.6% and 6.9%, respectively, which demonstrates the effectiveness of emission reduction in Hangzhou, a close-by city from Shanghai (Pu et al., 2015). The comparison of before and after the implementation of license plate restriction showed that the levels of CO, NO<sub>2</sub>, and PM<sub>2.5</sub> concentration have significantly decreased by 15% to 23%, while the levels of O<sub>3</sub> concentration remained unaffected in Lanzhou (Zhao et al., 2017).

In addition, the Indian government successfully implemented a similar Odd-Even license plate restriction to reduce traffic emission in the capital of Delhi, one of the most polluted cities in the world (Jayakumar, 2017; Tiwari et al., 2018).

### **5.3 Incentives on Electric Vehicles (EV)**

Despite the limited area of Macao, with only 32.8 km<sup>2</sup>, there are a total of 233,417 privately owned vehicles, in particular of 109,579 cars and 123,838 motorcycles. The statistics of the vehicles were obtained from Macao Statistics and Census Service (DSEC), and the number of charging stations for EV in public parking lots were obtained from the Office for the Development of the Energy Sector (GDSE).

The Macao government has developed a Five-year Development Plan (2016-2020) and Environmental Protection Planning of Macao (2010-2020), as a measure to improve the roadside air quality and protect the health of the population. In order to achieve the goals defined in the plan, the Macao government has imposed a strict emission standard on the imported new vehicles and vehicles fuels, and promotion of environmentally friendly vehicles through tax incentives. These measures included the regulation of exhaust emissions from registered and imported new vehicles, regulation of the vehicle fuel standards, promotion for the use of environmentally friendly vehicles, and a subsidy scheme to eliminate motorcycles with two-stroke engine.

According to the second paragraph of Article 6 of the Motor Vehicle Tax

Regulation of Macao, motor vehicles that only use an alternative energy source, apart from traditional fossil fuel, such as electricity are exempt of the vehicle tax, a measure that has been implemented since February 2012. In addition, the Environmental Protection Bureau (DSPA) has been promoting the adoption of electric vehicles (EV) as an alternative to traditional fossil fuel vehicles, with efforts to increase the number EV recharging stations and EV-only parking spot throughout Macao.

In order to increase the convenience of recharging for EV owners, the Macao government has introduced a Five-year Development Plan (2016-2020) for installing EV charging stations in public parking lots. As a result, there is currently a total of 170 electric cars and 2 electric motorcycles charging stations evenly distributed throughout the public parking lots in Macao, and the number of EV charging stations is expected to reach 200 by the end of 2020. Figure 5.2 shows the total proposed EV charging station in the public parking lots of Macao.

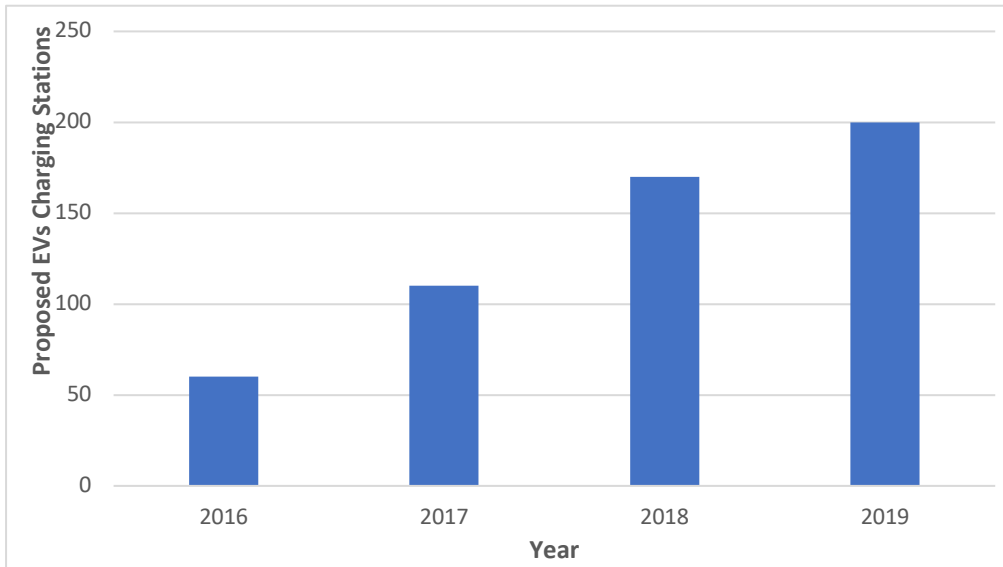


**Figure 5.2.** Total proposed EV charging stations in public parking lots of Macao.

The Traffic Bureau (DSAT) has implemented an exclusive corridor for public transportation, in particular for bus only, in certain stretches of the busiest road in Macao, from 7:30h to 9:00h and 16:30h to 19:00h, during every day of the week. The exclusive corridor is monitored by autonomous camera system and violators of exclusive corridor policy are subjected to a fine of MOP \$600 (an equivalent of USD \$75). This exclusive corridor for public transportation has been implemented since June 2016. The tax exemption on EV, increase of EV charging stations, and the exclusive corridors for public transportation are the most important measures adopted by the Macao government as an attempt to lower vehicle emissions and promote the use of green and public transportation in the city center.





## **Chapter 6: Conclusions and Future Development**

---

## 6.1 Air Quality Forecast Using Statistical Methods

For the Macao air quality forecast using statistical methods, a model was initially constructed using air quality and meteorological data from 2013 to 2016 data with multiple linear regression (MLR) and classification and regression tree (CART) analysis and validated with 2017 data. The 2013 to 2016 model was successful in the prediction of the 2017 data.

The development of statistical models to forecast the daily average concentration of NO<sub>2</sub>, PM<sub>10</sub>, PM<sub>2.5</sub>, and the maximum hourly average concentration of O<sub>3</sub> for the next day, in Macao region, was successfully accomplished for five locations, recurring to MLR analysis. In the case of O<sub>3</sub> predictions, CART analysis showed better results, specially improving high concentration levels predictions, assuring a more accurate prediction of critical pollution episodes. The pollutants for which best results were obtained were PM<sub>10</sub>, followed by PM<sub>2.5</sub>, and NO<sub>2</sub>. The most challenging pollutant to forecast was the maximum hourly concentration of O<sub>3</sub>, scoring the lowest R<sup>2</sup> (0.78), due to its secondary nature as a pollutant, involved in several atmospheric reactions that depend on the concentrations of other compounds, and also key meteorological conditions, such as sunlight and temperature.

The variables that explained most of the variability, for all pollutants, were the concentration levels measured in the previous 24-hours to the operational forecast. For PM and NO<sub>2</sub> the indicator of synoptic-scale weather pattern (geopotential height at 850 hPa parameter), was also a relevant variable. This work shows that in areas such as Macao, where data may not be easily obtained with a high level of confidence (such as spatially resolved emissions and traffic related data), this kind of statistical approach is an adequate alternative to reliably forecast air quality with a clearer understanding of the main factors affecting it.

New models were developed with two additional years of data, in particular of 2017 and 2018. The 2013 to 2018 models were successful in the prediction of the 2019 data. The additional data improved the air quality forecast for Macao. Despite the R<sup>2</sup> being identical between the 2013 to 2016 and the 2013 to 2018 model, validation of 2019 data had a lower root mean square error (RMSE), mean absolute error (MAE), and biases for the 2013 to 2018 model, which makes it the best forecast model, with the highest accuracy and stability in the prediction of the next day levels of pollutant concentrations in Macao. It is concluded that the additional two years of data helped to improve the accuracy and stability of the forecast.

A forecast for two days ahead (D2) was also developed for one air quality monitoring station (Taipa Ambient) with a considerable decrease in the coefficient of determination ( $R^2$ ), and a substantial increase in root mean square (RMSE), mean absolute error (MAE) and biases. Nevertheless, the result shows that  $PM_{10}$  is more resilient, while the levels of  $PM_{2.5}$ ,  $NO_2$ , and  $O_3$  have a greater variation related to the weather change.

## **6.2 Air Quality Forecast Under High and Low Pollution Episodes**

The 2013 to 2018 models were able to successfully predict the high pollution episode during the Chinese National Holiday in late September and early October 2019 and the low pollution episode during the preventive measures period of COVID-19 pandemic in late January and early February 2020. This shows that the air quality forecast models can be reliably applied to predict next-day pollutants concentrations across different magnitude levels of air pollution, being a useful tool for mitigation of air pollution impacts.

In addition, this shows that an improvement of global air quality in the territory is possible, but it is tightly linked to the implementation of air pollution control measures in the industry and mobility sectors in Macao, in particular, in Guangdong

Province. As previously studied, the air pollution problem associated with  $PM_{2.5}$  and  $O_3_{MAX}$  is a regional problem that is not only limited to Macao, but also in the nearby regions of Hong Kong and Guangdong Province.

### **6.3 Answers to Research Questions**

This section presents more detailed conclusions, summarizing the answers to the research questions identified in the beginning of the research work.

#### **1. What is the trend of the different air pollutant concentrations measured in the Macao air quality monitoring stations and the reason for those variations in the recent years?**

There is a decreasing trend in the levels of  $NO_2$ ,  $PM_{10}$  and  $PM_{2.5}$  concentration, which may be due to the implementation of stricter emission standard for newly imported and existing vehicles, and the promotion for the use of electric vehicles in Macao. Also, the air pollution preventive measures in the nearby Guangdong province may also be contributing to this trend. In contrast, there is an increasing trend in the levels of  $O_3$  concentrations, which may be due to the complex nature of the  $O_3$  precursors and the chemistry behind its formation and consumption.

**2. Is it possible to develop a statistical model to accurately forecast the next day concentrations of air pollutant in the Macao region?**

Yes, it is possible to develop an air quality forecast using statistical methods to accurately predict the next day concentrations for NO<sub>2</sub>, PM<sub>10</sub>, PM<sub>2.5</sub> and O<sub>3</sub> MAX in the region of Macao, as shown in the result of this thesis.

**a. What are the key meteorological and air quality variables that are necessary to develop the statistical model?**

The key meteorological and air quality variables was listed in the Table 3-2, Variables considered as predictors in the multiple linear regression (MLR) and classification and regression tree (CART) models in all of the air quality forecast models. The key meteorological variables included the geopotential height at 850 hPa (H850), average relative humidity (HRMD), and minimum relative air humidity (HRMN). The key air quality variables included the average levels of pollutant concentrations from 16:00 of yesterday to 15:00 of today (16D1), and the average levels of pollutant concentrations from 00:00 to 23:00 of yesterday (23D1).

**b. How does additional years of meteorological and air quality historical data may affect the performance of the statistical forecast?**

The additional years of meteorological and air quality historical data has slightly improved the accuracy of the air quality forecast as shown in Table 4-4, Model performance indicators for the 2013 to 2016 model validation with 2019 data, and Table 4-5 Model performance indicators for the 2013 to 2018 model validation with 2019 data.

**c. How does the statistical forecast perform under the critical situations, such as a high pollution episode during Chinese National Holiday and a low pollution episode during COVID-19 pandemic?**

The air quality forecast using statistical methods performed well under high pollution episodes ( $R^2 = 0.88$  and  $0.83$ ) for  $PM_{2.5}$  and  $O_3_{MAX}$  respectively, as shown in Figure 4.10, Observed and predicted  $PM_{2.5}$  concentrations for Taipa Ambient during Chinese National Holiday (from September to November 2019), and Figure 4.11, Observed and predicted  $O_3_{MAX}$  concentrations for Taipa Ambient during Chinese National Holiday (from September to November 2019).



In addition, the air quality forecast performed well under low pollution episodes ( $R^2 = 0.82$  and  $0.75$ ) for  $PM_{2.5}$  and  $O_3_{MAX}$  respectively, as shown in Figure 4.12, Observed and predicted  $PM_{2.5}$  concentrations for Taipa Ambient during preventive measures of COVID-19 pandemic (from January to March 2020), and Figure 4.13, Observed and predicted  $O_3_{MAX}$  concentrations for Taipa Ambient during preventive measures of COVID-19 pandemic (from January to March 2020).

#### **6.4 Main Constraints and Suggestions to Future Works**

Despite all the time and effort put in this work, there were several limitations and constraints identified, which include the following:

- The Macao Meteorological and Geophysical Bureau (SMG) does not release a weather balloon to collect the upper sounding data, so the closest station of Hong Kong King' Park (Station number 45004) was identified to collect the upper air observation, which is one of the key meteorological variables for the development of the air quality forecast model.
- The Ka-Ho air quality monitoring station has only become operational in the recent years and so there was not sufficient data available to perform the air

quality forecast for this station, which requires at least five years of historical data. However, the surrounding area of this air quality monitoring station is known to have a serious air pollution problem, so an air quality forecast is essential and necessary for the health and well-being of the nearby residents.

- The use of machine learning techniques may help to improve the air quality forecast for the next day levels of pollutant concentration as suggested by some of the literature. However, since it would require the necessary knowledge and testing of different specific algorithms and because the developed models were quite successful, the need to develop and implement such an approach was not considered as necessary in the case of the air quality forecast for Macao.



## Chapter 7: References

---

- Abdullah, A. M., Ismail, M., Yuen, F. S., Abdullah, S., & Elhadi, R. E. (2017). The relationship between daily maximum temperature and daily maximum ground level ozone concentration. *Polish Journal of Environmental Studies*, 26(2), 517–523.  
<https://doi.org/10.15244/pjoes/65366>
- Ahmad, M., Alam, K., Tariq, S., Anwar, S., Nasir, J., & Mansha, M. (2019). Estimating fine particulate concentration using a combined approach of linear regression and artificial neural network. *Atmospheric Environment*, 219(October), 117050.  
<https://doi.org/10.1016/j.atmosenv.2019.117050>
- Ai, Z. T., Mak, C. M., & Lee, H. C. (2016). Roadside air quality and implications for control measures: A case study of Hong Kong. *Atmospheric Environment*, 137, 6–16.  
<https://doi.org/10.1016/j.atmosenv.2016.04.033>
- Bao, R., & Zhang, A. (2020). Does lockdown reduce air pollution? Evidence from 44 cities in northern China. *Science of the Total Environment*, 731(1954), 139052.  
<https://doi.org/10.1016/j.scitotenv.2020.139052>
- Bhalgat, P., Pitale, S., & Bhoite, S. (2019). Air Quality Prediction using Machine Learning Algorithms. *International Journal of Computer Applications Technology and Research*, 8(9), 367–370. <https://doi.org/10.7753/ijcatr0809.1006>
- Boogaard, H., Janssen, N. A. H., Fischer, P. H., Kos, G. P. A., Weijers, E. P., Cassee, F. R., ... Hoek, G. (2012). Impact of low emission zones and local traffic policies on ambient air pollution concentrations. *Science of the Total Environment*, 435–436, 132–140.  
<https://doi.org/10.1016/j.scitotenv.2012.06.089>
- Brauer, M., Freedman, G., Frostad, J., Van Donkelaar, A., Martin, R. V., Dentener, F., ... Cohen, A. (2016). Ambient Air Pollution Exposure Estimation for the Global Burden of Disease 2013. *Environmental Science and Technology*, 50(1), 79–88.  
<https://doi.org/10.1021/acs.est.5b03709>

- Cassmassi, J. C. (1997). Objective Ozone Forecasting in South Coast Air Basin: Updating the Objective Prediction Models for the Late 1990's and Southern California Ozone Study (SCOS97-NARSTO) Applications.
- Catalano, M., & Galatioto, F. (2017). Enhanced transport-related air pollution prediction through a novel metamodel approach. *Transportation Research Part D: Transport and Environment*, 55, 262–276. <https://doi.org/10.1016/j.trd.2017.07.009>
- Chaplain, I. (2002). Urban regeneration and the sustainability of colonial built heritage: A case study of Macau, China. *Advances in Architecture Series*, 14, 367–376. Retrieved from <http://www.scopus.com/inward/record.url?eid=2-s2.0-3342946030&partnerID=40&md5=5b014839bf05fe3882af429b87620d47>
- Choi, W., Paulson, S. E., Cassmassi, J., & Winer, A. M. (2013). Evaluating meteorological comparability in air quality studies: Classification and regression trees for primary pollutants in California's South Coast Air Basin. *Atmospheric Environment*, 64(x), 150–159. <https://doi.org/10.1016/j.atmosenv.2012.09.049>
- Clapp, L. J., & Jenkin, M. E. (2001). Analysis of the relationship between ambient levels of O<sub>3</sub>, NO<sub>2</sub> and NO as a function of NO<sub>x</sub> in the UK. *Atmospheric Environment*, 35(36), 6391–6405. [https://doi.org/10.1016/S1352-2310\(01\)00378-8](https://doi.org/10.1016/S1352-2310(01)00378-8)
- Chen, J., Chen, H., Wu, Z., Hu, D., & Pan, J. Z. (2017). Forecasting smog-related health hazard based on social media and physical sensor. *Information Systems*, 64, 281–291. <https://doi.org/10.1016/j.is.2016.03.011>
- Chen, J., & Wang, J. (2019). Prediction of PM<sub>2.5</sub> concentration based on multiple linear regression. *Proceedings - 2019 International Conference on Smart Grid and Electrical Automation, ICSGEA 2019*, 457–460. <https://doi.org/10.1109/ICSGEA.2019.00109>

- Chen, W., Li, A., & Zhang, F. (2018). Roadside atmospheric pollution: still a serious environmental problem in Beijing, China. *Air Quality, Atmosphere and Health*, 11(10), 1203–1216. <https://doi.org/10.1007/s11869-018-0620-2>
- Chen, X., & Zhao, J. (2013). Bidding to drive: Car license auction policy in Shanghai and its public acceptance. *Transport Policy*, 27, 39–52. <https://doi.org/10.1016/j.tranpol.2012.11.016>
- Cyrus, J., Peters, A., Soentgen, J., & Wichmann, H. E. (2014). Low emission zones reduce PM10 mass concentrations and diesel soot in German cities. *Journal of the Air and Waste Management Association*, 64(4), 481–487. <https://doi.org/10.1080/10962247.2013.868380>
- Delavar, M. R., Gholami, A., Shiran, G. R., Rashidi, Y., Nakhaeizadeh, G. R., Fedra, K., & Afshar, S. H. (2019). A novel method for improving air pollution prediction based on machine learning approaches: A case study applied to the capital city of Tehran. *ISPRS International Journal of Geo-Information*, 8(2). <https://doi.org/10.3390/ijgi8020099>
- Deng, T., Chen, Y., Wan, Q., Zhang, Y., Deng, X., Huang, Y., ... Li, F. (2018). Comparative evaluation of the impact of GRAPES and MM5 meteorology on CMAQ prediction over Pearl River Delta, China. *Particuology*, 40, 88–97. <https://doi.org/10.1016/j.partic.2017.10.005>
- DSAT. (2018). Dados estatísticos da DSAT. Retrieved from <http://www.dsat.gov.mo/dsat/statistic.aspx#>
- DSEC. (2018). Macao in Figures. Retrieved from <http://www.dsec.gov.mo/Statistic.aspx?NodeGuid=ba1a4eab-213a-48a3-8fbb-962d15dc6f87>
- DSEC. (2020). Transport and Communications Statistics.

- Durão, R. M., Mendes, M. T., & Pereira, M. J. (2016). Forecasting O<sub>3</sub> levels in industrial area surroundings up to 24 h in advance , combining classification trees and MLP models. *Atmospheric Pollution Research*, 7, 961–970.
- EEA. (2014). *Air quality in Europe — 2014 report*. Copenhagen, Denmark.  
<https://doi.org/10.2800/22775>
- EEA. (2016). *Explaining Road Transport Emissions*. Copenhagen, Denmark.  
<https://doi.org/10.2800/71804>
- EEA. (2018). *Electric vehicles from life cycle and circular economy perspectives*. Copenhagen, Denmark. <http://doi:10.2800/77428>
- EEA. (2019). *Air quality in Europe — 2019 report — EEA Report No 10/2019*. Copenhagen, Denmark. <https://doi.org/10.2800/822355>
- EEA. (2020). *Health Impacts of Air Pollution*. Retrieved from  
<https://www.eea.europa.eu/themes/signals/signals-2013/infographics/health-impacts-of-air-pollution/view>
- Entwistle, M. R., Gharibi, H., Tavallali, P., Cisneros, R., Schweizer, D., Brown, P., & Ha, S. (2019). Ozone pollution and asthma emergency department visits in Fresno, CA, USA, during the warm season (June–September) of the years 2005 to 2015: a time-stratified case-crossover analysis. *Air Quality, Atmosphere and Health*, 661–672.  
<https://doi.org/10.1007/s11869-019-00685-w>
- EPA (2020). *Particulate Matter (PM) Basics*. United States Environmental Protection Agency.  
<https://www.epa.gov/pm-pollution/particulate-matter-pm-basics>
- Feng, C., Wang, H., & Rao, X. (2012). The Morphological Evolution of Macau. In *Eighth International Space Syntax Symposium*.



- Ferreira, F., Gomes, P., Tente, H., Carvalho, A. C., Pereira, P., & Monjardino, J. (2015). Air quality improvements following implementation of Lisbon's Low Emission Zone. *Atmospheric Environment*, 122, 373–381.  
<https://doi.org/10.1016/j.atmosenv.2015.09.064>
- Fu, S., & Gu, Y. (2017). Highway toll and air pollution: Evidence from Chinese cities. *Journal of Environmental Economics and Management*, 83, 32–49.  
<https://doi.org/10.1016/j.jeem.2016.11.007>
- García Nieto, P. J., Sánchez Lasheras, F., García-Gonzalo, E., & de Cos Juez, F. J. (2018). Estimation of PM10 concentration from air quality data in the vicinity of a major steelworks site in the metropolitan area of Avilés (Northern Spain) using machine learning techniques. *Stochastic Environmental Research and Risk Assessment*, 32(11), 3287–3298. <https://doi.org/10.1007/s00477-018-1565-6>
- GBD 2015 Risk Factors Collaborators. (2016). Global, regional, and national comparative risk assessment of 79 behavioural, environmental and occupational, and metabolic risks or clusters of risks, 1990–2015: a systematic analysis for the Global Burden of Disease Study 2015. *The Lancet*, 388(10053), 1659–1724.  
[https://doi.org/10.1016/S0140-6736\(16\)31679-8](https://doi.org/10.1016/S0140-6736(16)31679-8)
- Gehrsitz, M. (2017). The effect of low emission zones on air pollution and infant health. *Journal of Environmental Economics and Management*, 83, 121–144.  
<https://doi.org/10.1016/j.jeem.2017.02.003>
- Ghazali, N. A., Ramli, N. A., Yahaya, A. S., Yusof, N. F. F. M., Sansuddin, N., & Al Madhoun, W. A. (2010). Transformation of nitrogen dioxide into ozone and prediction of ozone concentrations using multiple linear regression techniques. *Environmental Monitoring and Assessment*, 165(1–4), 475–489. <https://doi.org/10.1007/s10661-009-0960-3>

- Gu, Y., Deakin, E., & Long, Y. (2017). The effects of driving restrictions on travel behavior evidence from Beijing. *Journal of Urban Economics*, 102(February 2009), 106–122. <https://doi.org/10.1016/j.jue.2017.03.001>
- Guttikunda, S., Calori, G., Velay-Lasry, F., & Ngo, R. (2011). Air Quality Forecasting System for Cities: Modeling Architecture for Delhi. *SIM-Air Working Paper Series*, 36. <https://doi.org/10.13140/RG.2.2.20285.92648>
- He, D., Zhou, Z., He, K., Hao, J., Liu, Y., Wang, Z., & Deng, Y. (2000). Assessment of traffic related air pollution in urban areas of Macao. *Journal of Environmental Sciences*, 12(1), 39–46.
- HKEPD. (2020). Hong Kong Air Pollutant Emission Inventory – Road Transport. Retrieved from [https://www.epd.gov.hk/epd/english/environmentinhk/air/data/emission\\_inve\\_transport.html#:~:text=Road%20transport%20was%20a%20major,19%25%20during%20the%20same%20period.](https://www.epd.gov.hk/epd/english/environmentinhk/air/data/emission_inve_transport.html#:~:text=Road%20transport%20was%20a%20major,19%25%20during%20the%20same%20period.)
- HKO. (2018). King's Park Meteorological Station. Retrieved from <http://www.hko.gov.hk/wxinfo/aws/kpinfo.htm>
- HKO. (2020). Weather Chart. Retrieved from <https://www.hko.gov.hk/en/wxinfo/currwx/wxcht.htm>
- Holman, C., Harrison, R., & Querol, X. (2015). Review of the efficacy of low emission zones to improve urban air quality in European cities. *Atmospheric Environment*, 111, 161–169. <https://doi.org/10.1016/j.atmosenv.2015.04.009>
- Huang, H., Fu, D., & Qi, W. (2017). Effect of driving restrictions on air quality in Lanzhou, China: Analysis integrated with internet data source. *Journal of Cleaner Production*, 142, 1013–1020. <https://doi.org/10.1016/j.jclepro.2016.09.082>

- Invernizzi, G., Ruprecht, A., Mazza, R., De Marco, C., Močnik, G., Sioutas, C., & Westerdahl, D. (2011). Measurement of black carbon concentration as an indicator of air quality benefits of traffic restriction policies within the ecopass zone in Milan, Italy. *Atmospheric Environment*, 45(21), 3522–3527.  
<https://doi.org/10.1016/j.atmosenv.2011.04.008>
- Jayakumar, T. (2017). Odds of Success of the Odd-Even Rule †. *South Asian Journal of Management*, 24(2), 169–198.
- Jevtić, M., Dragić, N., Bijelović, S., & Popović, M. (2014). Cardiovascular diseases and air pollution in Novi Sad, Serbia. *International Journal of Occupational Medicine and Environmental Health*, 27(2), 153–164. <https://doi.org/10.2478/s13382-014-0239-y>
- Jia, N., Zhang, Y., He, Z., & Li, G. (2017). Commuters' acceptance of and behavior reactions to license plate restriction policy: A case study of Tianjin, China. *Transportation Research Part D: Transport and Environment*, 52, 428–440.  
<https://doi.org/10.1016/j.trd.2016.10.035>
- Jiang, W., Boltze, M., Groer, S., & Scheuven, D. (2017). Impacts of low emission zones in Germany on air pollution levels. *Transportation Research Procedia*, 25, 3370–3382.  
<https://doi.org/10.1016/j.trpro.2017.05.217>
- Jones, A. M., Harrison, R. M., Barratt, B., & Fuller, G. (2012). A large reduction in airborne particle number concentrations at the time of the introduction of “ sulphur free” diesel and the London Low Emission Zone. *Atmospheric Environment*, 50, 129–138.  
<https://doi.org/10.1016/j.atmosenv.2011.12.050>
- Kang, G. K., Gao, J. Z., Chiao, S., Lu, S., & Xie, G. (2018). Air Quality Prediction: Big Data and Machine Learning Approaches. *International Journal of Environmental Science and Development*, 9(1), 8–16. <https://doi.org/10.18178/ijesd.2018.9.1.1066>

- Keuken, M. P., Jonkers, S., Zandveld, P., Voogt, M., & Elshout van den, S. (2012). Elemental carbon as an indicator for evaluating the impact of traffic measures on air quality and health. *Atmospheric Environment*, 61, 1–8.  
<https://doi.org/10.1016/j.atmosenv.2012.07.009>
- Kocijan, J., Gradišar, D., Stepančič, M., Božnar, M. Z., Grašič, B., & Mlakar, P. (2018). Selection of the data time interval for the prediction of maximum ozone concentrations. *Stochastic Environmental Research and Risk Assessment*, 32(6), 1759–1770. <https://doi.org/10.1007/s00477-017-1468-y>
- Krzyzanowski, M., & Cohen, A. (2008). Update of WHO air quality guidelines, 7–13.  
<https://doi.org/10.1007/s11869-008-0008-9>
- Kukkonen, J., Partanen, L., Karppinen, A., Ruuskanen, J., Junninen, H., Kolehmainen, M., ... Cawley, G. (2003). Extensive evaluation of neural network models for the prediction of NO<sub>2</sub> and PM<sub>10</sub> concentrations, compared with a deterministic modelling system and measurements in central Helsinki. *Atmospheric Environment*, 37(32), 4539–4550.  
[https://doi.org/10.1016/S1352-2310\(03\)00583-1](https://doi.org/10.1016/S1352-2310(03)00583-1)
- Kumar, R., Barth, M. C., Pfister, G. G., Delle Monache, L., Lamarque, J. F., Archer-Nicholls, S., ... Walters, S. (2018). How Will Air Quality Change in South Asia by 2050? *Journal of Geophysical Research: Atmospheres*, 123(3), 1840–1864.  
<https://doi.org/10.1002/2017JD027357>
- Lee, M., Brauer, M., Wong, P., Tang, R., Tsui, T. H., Choi, C., ... Barratt, B. (2017). Land use regression modelling of air pollution in high density high rise cities: A case study in Hong Kong. *Science of the Total Environment*, 592, 306–315.  
<https://doi.org/10.1016/j.scitotenv.2017.03.094>

- Lei, M. T., Monjardino, J., Mendes, L., Gonçalves, D., & Ferreira, F. (2019). Macao air quality forecast using statistical methods. *Air Quality, Atmosphere and Health*, 12(9), 1049–1057. <https://doi.org/10.1007/s11869-019-00721-9>
- Li, L., Li, Q., Huang, L., Wang, Q., Zhu, A., Xu, J., ... Chan, A. (2020). Air quality changes during the COVID-19 lockdown over the Yangtze River Delta Region: An insight into the impact of human activity pattern changes on air pollution variation. *Science of the Total Environment*, 732. <https://doi.org/10.1016/j.scitotenv.2020.139282>
- Li, X., Lopes, D., Mok, K. M., & Miranda, A. I. (2019). Development of a road traffic emission inventory with high spatial – temporal resolution in the world ’ s most densely populated region — Macau.
- Lin, H. X., Jin, J., & Van Den Herik, J. (2019). Air quality forecast through integrated data assimilation and machine learning. *ICAART 2019 - Proceedings of the 11th International Conference on Agents and Artificial Intelligence*, 2(Icaart), 787–793. <https://doi.org/10.5220/0007555207870793>
- Liu, A. A., Linn, J., Qin, P., & Yang, J. (2018). Vehicle ownership restrictions and fertility in Beijing. *Journal of Development Economics*, 135(January), 85–96. <https://doi.org/10.1016/j.jdeveco.2018.07.005>
- Liu, B. C., Binaykia, A., Chang, P. C., Tiwari, M. K., & Tsao, C. C. (2017). Urban air quality forecasting based on multidimensional collaborative Support Vector Regression (SVR): A case study of Beijing-Tianjin-Shijiazhuang. *PLoS ONE*, 12(7), 1–17. <https://doi.org/10.1371/journal.pone.0179763>
- Liu, J. C., & Peng, R. D. (2018). Health effect of mixtures of ozone, nitrogen dioxide, and fine particulates in 85 US counties. *Air Quality, Atmosphere & Health*, 11(3), 311–324. <https://doi.org/10.1007/s11869-017-0544-2>

- Liu, Y., Yan, Z., Liu, S., Wu, Y., Gan, Q., & Dong, C. (2017). The effect of the driving restriction policy on public health in Beijing. *Natural Hazards*, 85(2), 751–762. <https://doi.org/10.1007/s11069-016-2602-8>
- Liu, Z., Li, R., Wang, X., & Shang, P. (2018). Effects of vehicle restriction policies: Analysis using license plate recognition data in Langfang, China. *Transportation Research Part A: Policy and Practice*, 118(December 2017), 89–103. <https://doi.org/10.1016/j.tra.2018.09.001>
- Lopes, D., Ferreira, J., Hoi, K. I., Miranda, A. I., Yuen, K. V., & Mok, K. M. (2018). Weather research and forecasting model simulations over the Pearl River Delta Region. *Air Quality, Atmosphere and Health*, 115–125. <https://doi.org/10.1007/s11869-018-0636-7>
- Lopes, D., Hoi, K. I., Mok, K. M., Miranda, A. I., Yuen, K. V., & Borrego, C. (2016). Air quality in the main cities of the pearl river delta region. *Global Nest Journal*, 18(4), 794–802.
- Lu, X. (2016). Effectiveness of government enforcement in driving restrictions: a case in Beijing, China. *Environmental Economics and Policy Studies*, 18(1), 63–92. <https://doi.org/10.1007/s10018-015-0112-7>
- Ma, J., Cheng, J. C. P., Lin, C., Tan, Y., & Zhang, J. (2019). Improving air quality prediction accuracy at larger temporal resolutions using deep learning and transfer learning techniques. *Atmospheric Environment*, 214(August), 116885. <https://doi.org/10.1016/j.atmosenv.2019.116885>
- Malina, C., & Scheffler, F. (2015). The impact of Low Emission Zones on particulate matter concentration and public health. *Transportation Research Part A: Policy and Practice*, 77, 372–385. <https://doi.org/10.1016/j.tra.2015.04.029>

- Martinez, N. M., Montes, L. M., Mura, I., & Franco, J. F. (2018). Machine Learning Techniques for PM 10 Levels Forecast in Bogotá. In 2018 ICAI Workshops (ICAIW) (pp. 1–7). IEEE. <https://doi.org/10.1109/ICAIW.2018.8554995>
- Masih, A. (2019). Machine learning algorithms in air quality modeling. *Global Journal of Environmental Science and Management*, 5(4), 515–534. <https://doi.org/10.22034/gjesm.2019.04.10>
- MEE. (2012). Ambient Air Quality Standards. Retrieved from <http://210.72.1.216:8080/gzaqi/Document/gjzlbz.pdf>
- Monjardino, J., Barros, N., Ferreira, F., Tente, H., Fontes, T., Pereira, P., & Manso, C. (2018). Improving Air Quality in Lisbon: modelling emission abatement scenarios. *IFAC-PapersOnLine*, 51(5), 61–66. <https://doi.org/10.1016/j.ifacol.2018.06.211>
- Neto, J., Torres, P., Ferreira, F., & Boavida, F. (2009). Lisbon air quality forecast using statistical methods. *International Journal of Environment and Pollution*, 39(3/4), 333. <https://doi.org/10.1504/IJEP.2009.028695>
- Nhung, N. T. T., Amini, H., Schindler, C., Kutlar Joss, M., Dien, T. M., Probst-Hensch, N., ... Künzli, N. (2017). Short-term association between ambient air pollution and pneumonia in children: A systematic review and meta-analysis of time-series and case-crossover studies. *Environmental Pollution*, 230, 1000–1008. <https://doi.org/10.1016/j.envpol.2017.07.063>
- Oduro, S. D., Ha, Q. P., & Duc, H. (2016). Vehicular emissions prediction with CART-BMARS hybrid models. *Transportation Research Part D: Transport and Environment*, 49, 188–202. <https://doi.org/10.1016/j.trd.2016.09.012>

- Pagowski, M., Grell, G. A., Devenyi, D., Peckham, S. E., McKeen, S. A., Gong, W., ... Lee, P. (2006). Application of dynamic linear regression to improve the skill of ensemble-based deterministic ozone forecasts. *Atmospheric Environment*, 40(18), 3240–3250. <https://doi.org/10.1016/j.atmosenv.2006.02.006>
- Pope, C. A., & Dockery, D. W. (2006). Health effects of fine particulate air pollution: Lines that connect. *Journal of the Air and Waste Management Association*, 56(6), 709–742. <https://doi.org/10.1080/10473289.2006.10464485>
- Pu, Y., Yang, C., Liu, H., Chen, Z., & Chen, A. (2015). Impact of license plate restriction policy on emission reduction in Hangzhou using a bottom-up approach. *Transportation Research Part D: Transport and Environment*, 34, 281–292. <https://doi.org/10.1016/j.trd.2014.11.007>
- Qadir, R. M., Abbaszade, G., Schnelle-Kreis, J., Chow, J. C., & Zimmermann, R. (2013). Concentrations and source contributions of particulate organic matter before and after implementation of a low emission zone in Munich, Germany. *Environmental Pollution*, 175(2), 158–167. <https://doi.org/10.1016/j.envpol.2013.01.002>
- Qi, J., Ruan, Z., Qian, Z. M., Yin, P., Yang, Y., Acharya, B. K., ... Lin, H. (2020). Potential gains in life expectancy by attaining daily ambient fine particulate matter pollution standards in mainland China: A modeling study based on nationwide data. *PLoS Medicine*, 17(1), e1003027. <https://doi.org/10.1371/journal.pmed.1003027>
- RCP. (2016). Report of a working party February 2016. London, UK. Retrieved from <https://www.rcplondon.ac.uk/projects/outputs/every-breath-we-take-lifelong-impact-air-pollution>
- Reid, N., Yap, D., & Bloxam, R. (2008). The potential role of background ozone on current and emerging air issues: An overview. *Air Quality, Atmosphere & Health*, 1(1), 19–29. <https://doi.org/10.1007/s11869-008-0005-z>



- Ritter, M., Müller, M. D., Tsai, M. Y., & Parlow, E. (2013). Air pollution modeling over very complex terrain: An evaluation of WRF-Chem over Switzerland for two 1-year periods. *Atmospheric Research*, 132–133, 209–222.  
<https://doi.org/10.1016/j.atmosres.2013.05.021>
- Sahanavin, N., Prueksasit, T., & Tantrakarnapa, K. (2018). Relationship between PM10 and PM2.5 levels in high-traffic area determined using path analysis and linear regression. *Journal of Environmental Sciences (China)*, 69, 105–114.  
<https://doi.org/10.1016/j.jes.2017.01.017>
- Saide, P. E., Carmichael, G. R., Spak, S. N., Gallardo, L., Osses, A. E., Mena-Carrasco, M. A., & Pagowski, M. (2011). Forecasting urban PM10 and PM2.5 pollution episodes in very stable nocturnal conditions and complex terrain using WRF-Chem CO tracer model. *Atmospheric Environment*, 45(16), 2769–2780.  
<https://doi.org/10.1016/j.atmosenv.2011.02.001>
- Samadianfard, S., Delirhasannia, R., Kişi, Ö., & Agirre-Basurko, E. (2013). Comparative analysis of ozone level prediction models using gene expression programming and multiple linear regression. *Geofizika*, 30(1), 43–74.
- Santos, F. M., Gómez-Losada, Á., & Pires, J. C. M. (2019). Impact of the implementation of Lisbon low emission zone on air quality. *Journal of Hazardous Materials*, 365(November 2018), 632–641. <https://doi.org/10.1016/j.jhazmat.2018.11.061>
- Sheng, N., & Tang, U. W. (2013). Risk assessment of traffic-related air pollution in a world heritage city. *International Journal of Environmental Science and Technology*, 10(1), 11–18. <https://doi.org/10.1007/s13762-012-0030-1>
- Shi, X., & Brasseur, G. P. (2020). The Response in Air Quality to the Reduction of Chinese Economic Activities During the COVID-19 Outbreak. *Geophysical Research Letters*, 47(11), 1–8. <https://doi.org/10.1029/2020GL088070>

- Shimadera, H., Kojima, T., & Kondo, A. (2016). Evaluation of Air Quality Model Performance for Simulating Long-Range Transport and Local Pollution of PM<sub>2.5</sub> in Japan. *Advances in Meteorology*, 2016. <https://doi.org/10.1155/2016/5694251>
- SMG. (2014). Climate in Macao. Macao. Retrieved from [http://www.smg.gov.mo/smg/climate/e\\_climaintro.htm](http://www.smg.gov.mo/smg/climate/e_climaintro.htm)
- SMG. (2019). Resumo anual sobre qualidade do ar em Macau - 2019. Retrieved from [https://cms.smg.gov.mo/uploads/sync/pdf/AIR\\_report/p\\_IQA\\_annual\\_report/IQA\\_2019.pdf](https://cms.smg.gov.mo/uploads/sync/pdf/AIR_report/p_IQA_annual_report/IQA_2019.pdf)
- SMG (2020). Daily Index and Forecast. Macao Meteorological and Geophysical Bureau. <https://www.smg.gov.mo/en/subpage/65/iqa-report>
- Song, J., Liu, Y., Lu, M., An, Z., Lu, J., Chao, L., ... Xu, D. (2019). Short-term exposure to nitrogen dioxide pollution and the risk of eye and adnexa diseases in Xinxiang, China. *Atmospheric Environment*, 218(March), 117001. <https://doi.org/10.1016/j.atmosenv.2019.117001>
- Stern, R., Builtjes, P., Schaap, M., Timmermans, R., Vautard, R., Hodzic, A., ... Kerschbaumer, A. (2008). A model inter-comparison study focussing on episodes with elevated PM<sub>10</sub> concentrations. *Atmospheric Environment*, 42(19), 4567–4588. <https://doi.org/10.1016/j.atmosenv.2008.01.068>
- Suleiman, A., Tight, M. R., & Quinn, A. D. (2019). Applying machine learning methods in managing urban concentrations of traffic-related particulate matter (PM<sub>10</sub> and PM<sub>2.5</sub>). *Atmospheric Pollution Research*, 10(1), 134–144. <https://doi.org/10.1016/j.apr.2018.07.001>
- Sun, C., Zheng, S., & Wang, R. (2014). Restricting driving for better traffic and clearer skies: Did it work in Beijing? *Transport Policy*, 32, 34–41. <https://doi.org/10.1016/j.tranpol.2013.12.010>

- Tao, Q., Liu, F., Li, Y., & Sidorov, D. (2019). Air Pollution Forecasting Using a Deep Learning Model Based on 1D Convnets and Bidirectional GRU. *IEEE Access*, 7, 76690–76698. <https://doi.org/10.1109/ACCESS.2019.2921578>
- Tiwari, S., Thomas, A., Rao, P., Chate, D. M., Soni, V. K., Singh, S., ... Hopke, P. K. (2018). Pollution concentrations in Delhi India during winter 2015–16: A case study of an odd-even vehicle strategy. *Atmospheric Pollution Research*, 9(6), 1137–1145. <https://doi.org/10.1016/j.apr.2018.04.008>
- Tong, C. H. M., Yim, S. H. L., Rothenberg, D., Wang, C., Lin, C.-Y., Chen, Y. D., & Lau, N. C. (2018a). Assessing the impacts of seasonal and vertical atmospheric conditions on air quality over the Pearl River Delta region. *Atmospheric Environment*, 180, 69–78. <https://doi.org/10.1016/j.atmosenv.2018.02.039>
- Tong, C. H. M., Yim, S. H. L., Rothenberg, D., Wang, C., Lin, C. Y., Chen, Y. D., & Lau, N. C. (2018b). Projecting the impacts of atmospheric conditions under climate change on air quality over the Pearl River Delta region. *Atmospheric Environment*, 193(April), 79–87. <https://doi.org/10.1016/j.atmosenv.2018.08.053>
- Tsai, W. Y., Chan, L. Y., Blake, D. R., & Chu, K. W. (2006). Vehicular fuel composition and atmospheric emissions in South China: Hong Kong, Macau, Guangzhou, and Zhuhai. *Atmospheric Chemistry and Physics*, 6(11), 3281–3288. <https://doi.org/10.5194/acp-6-3281-2006>
- US EPA. (2003). Guidelines for Developing an Air Quality (Ozone and PM2.5) Forecasting Program. <https://doi.org/EPA-456/R-03-002>
- US EPA. (2003). Particle Pollution and Your Health. Retrieved from <https://nepis.epa.gov/Exe/ZyPDF.cgi?Dockey=P1001EX6.txt>
- US EPA. (2009). Ozone and Your Health. Retrieved from <https://www3.epa.gov/airnow/ozone-c.pdf>

- US EPA. (2011). Air Quality Guide for Nitrogen Dioxide. Retrieved from <https://www3.epa.gov/airnow/no2.pdf>
- Wang, P., Chen, K., Zhu, S., Wang, P., & Zhang, H. (2020). Severe air pollution events not avoided by reduced anthropogenic activities during COVID-19 outbreak. *Resources, Conservation and Recycling*, 158. <https://doi.org/https://doi.org/10.1016/j.resconrec.2020.104814>
- Wang, W., Lu, W., Wang, X., & Leung, A. Y. T. (2003). Prediction of maximum daily ozone level using combined neural network and statistical characteristics. *Environment International*, 29(5), 555–562. [https://doi.org/10.1016/S0160-4120\(03\)00013-8](https://doi.org/10.1016/S0160-4120(03)00013-8)
- Wang, Y., Yuan, Y., Wang, Q., Liu, C. G., Zhi, Q., & Cao, J. (2020). Changes in air quality related to the control of coronavirus in China: Implications for traffic and industrial emissions. *The Science of the Total Environment*, 731(December 2019), 139133. <https://doi.org/10.1016/j.scitotenv.2020.139133>
- Wang, Z., Maeda, T., Hayashi, M., Hsiao, L. F., & Liu, K. Y. (2001). A Nested Air Quality Prediction Modeling System for Urban and Regional Scales: Application for High-Ozone Episode in Taiwan. *Water, Air, and Soil Pollution*, 130, 391–396.
- Wendt, E. A., Quinn, C. W., Miller-Lionberg, D. D., Tryner, J., L'Orange, C., Ford, B., ... Volckens, J. (2019). A low-cost monitor for simultaneous measurement of fine particulate matter and aerosol optical depth - Part 1: Specifications and testing. *Atmospheric Measurement Techniques*, 12(10), 5431–5441. <https://doi.org/10.5194/amt-12-5431-2019>
- WHO. (2003). Health Aspects of Air Pollution with Particulate Matter, Ozone and Nitrogen Dioxide. *Health Aspects of Air Pollution with Particulate Matter, Ozone and Nitrogen Dioxide*, (January), 98. <https://doi.org/10.2105/AJPH.48.7.913>

- WHO. (2018). Ambient ( outdoor ) air quality and health. Retrieved July 2, 2019, from [https://www.who.int/news-room/fact-sheets/detail/ambient-\(outdoor\)-air-quality-and-health](https://www.who.int/news-room/fact-sheets/detail/ambient-(outdoor)-air-quality-and-health)
- WHO. (2019). Air pollution and health : Summary. Retrieved July 2, 2019, from <https://www.who.int/airpollution/ambient/about/en/>
- WHO. (2020). Air Pollution - The Silent Killer. Retrieved from <https://www.who.int/airpollution/infographics/en/>
- WHO Europe. (2006). Air Quality Guidelines. Retrieved from [http://202.171.253.71/www.euro.who.int/\\_\\_data/assets/pdf\\_file/0005/78638/E90038.pdf](http://202.171.253.71/www.euro.who.int/__data/assets/pdf_file/0005/78638/E90038.pdf)
- WHO Europe. (2008). Health risks of ozone from long-range transboundary air pollution. Retrieved from [https://www.euro.who.int/\\_\\_data/assets/pdf\\_file/0005/78647/E91843.pdf](https://www.euro.who.int/__data/assets/pdf_file/0005/78647/E91843.pdf)
- Wiśniewska, K., Lewandowska, A. U., & Staniszewska, M. (2019). Air quality at two stations (Gdynia and Rumia) located in the region of Gulf of Gdansk during periods of intensive smog in Poland. *Air Quality, Atmosphere & Health*, 12(7), 879–890. <https://doi.org/10.1007/s11869-019-00708-6>
- Xie, J., Liao, Z., Fang, X., Xu, X., Wang, Y., Zhang, Y., ... Wang, B. (2019). The characteristics of hourly wind field and its impacts on air quality in the Pearl River Delta region during 2013–2017. *Atmospheric Research*, 227, 112–124. <https://doi.org/10.1016/j.atmosres.2019.04.023>
- Xie, X., Tou, X., & Zhang, L. (2017). Effect analysis of air pollution control in Beijing based on an odd-and-even license plate model. *Journal of Cleaner Production*, 142, 936–945. <https://doi.org/10.1016/j.jclepro.2016.09.117>

- Xu, M., Grant-Muller, S., Huang, H. J., & Gao, Z. (2015). Transport management measures in the post-Olympic Games period: Supporting sustainable urban mobility for Beijing? *International Journal of Sustainable Development and World Ecology*, 22(1), 50–63. <https://doi.org/10.1080/13504509.2014.990542>
- Yang, J., Liu, A. A., Qin, P., & Linn, J. (2020). The effect of vehicle ownership restrictions on travel behavior: Evidence from the Beijing license plate lottery. *Journal of Environmental Economics and Management*, 99, 102269. <https://doi.org/10.1016/j.jeem.2019.102269>
- Yang, J., Liu, Y., Qin, P., & Liu, A. A. (2014). A review of Beijing's vehicle registration lottery: Short-term effects on vehicle growth and fuel consumption. *Energy Policy*, 75, 157–166. <https://doi.org/10.1016/j.enpol.2014.05.055>
- Yang, J., Lu, F., Liu, Y., & Guo, J. (2018). How does a driving restriction affect transportation patterns? The medium-run evidence from Beijing. *Journal of Cleaner Production*, 204, 270–281. <https://doi.org/10.1016/j.jclepro.2018.08.069>
- Zafra, C., Ángel, Y., & Torres, E. (2017). ARIMA analysis of the effect of land surface coverage on PM10 concentrations in a high-altitude megacity. *Atmospheric Pollution Research*, 8(4), 660–668. <https://doi.org/10.1016/j.apr.2017.01.002>
- Zaheer, J., Jeon, J., Lee, S.-B., & Kim, J. S. (2018). Effect of Particulate Matter on Human Health, Prevention, and Imaging Using PET or SPECT. *Progress in Medical Physics*, 29(3), 81. <https://doi.org/10.14316/pmp.2018.29.3.81>
- Zhang, B., Chen, H., Du, Z., & Wang, Z. (2020). Does license plate rule induce low-carbon choices in residents' daily travels: Motivation and impacts. *Renewable and Sustainable Energy Reviews*, 124(February). <https://doi.org/10.1016/j.rser.2020.109780>

- Zhang, J., & Ding, W. (2017). Prediction of air pollutants concentration based on an extreme learning machine: The case of Hong Kong. *International Journal of Environmental Research and Public Health*, 14(2), 1–19. <https://doi.org/10.3390/ijerph14020114>
- Zhang, Y., Bocquet, M., Mallet, V., Seigneur, C., & Baklanov, A. (2012a). Real-time air quality forecasting, part I: History, techniques, and current status. *Atmospheric Environment*, 60, 632–655. <https://doi.org/10.1016/j.atmosenv.2012.06.031>
- Zhang, Y., Bocquet, M., Mallet, V., Seigneur, C., & Baklanov, A. (2012b). Real-time air quality forecasting, Part II: State of the science, current research needs, and future prospects. *Atmospheric Environment*, 60, 656–676. <https://doi.org/10.1016/j.atmosenv.2012.02.041>
- Zhao, R., Gu, X., Xue, B., Zhang, J., & Ren, W. (2018). Short period PM<sub>2.5</sub> prediction based on multivariate linear regression model. *PLoS ONE*, 13(7), 1–16. <https://doi.org/10.1371/journal.pone.0201011>
- Zhao, S., Yu, Y., Qin, D., Yin, D., & He, J. (2017). Assessment of long-term and large-scale even-odd license plate controlled plan effects on urban air quality and its implication. *Atmospheric Environment*, 170, 82–95. <https://doi.org/10.1016/j.atmosenv.2017.09.041>
- Zheng, Y., Che, H., Zhao, T., Zhao, H., Gui, K., Sun, T., ... Zhang, X. (2017). Aerosol optical properties observation and its relationship to meteorological conditions and emission during the Chinese National Day and Spring Festival holiday in Beijing. *Atmospheric Research*, 197(July), 188–200. <https://doi.org/10.1016/j.atmosres.2017.07.003>
- Zheng, J., Zhang, L., Che, W., Zheng, Z., & Yin, S. (2009). A highly resolved temporal and spatial air pollutant emission inventory for the Pearl River Delta region, China and its uncertainty assessment. *Atmospheric Environment*, 43(32), 5112–5122. <https://doi.org/10.1016/j.atmosenv.2009.04.060>

Zhou, Y., Shan, Y., Liu, G., & Guan, D. (2018). Emissions and low-carbon development in Guangdong-Hong Kong-Macao Greater Bay Area cities and their surroundings.

*Applied Energy*, 228(July), 1683–1692.

<https://doi.org/10.1016/j.apenergy.2018.07.038>

Zhuge, C., Wei, B., Shao, C., Shan, Y., & Dong, C. (2020). The role of the license plate lottery policy in the adoption of Electric Vehicles: A case study of Beijing. *Energy Policy*, 139(February), 111328.

<https://doi.org/10.1016/j.enpol.2020.111328>